P-92

DEVELOPMENT OF HIGH Tc (>110K) Bi, Tl and Y-BASED MATERIALS AS SUPERCONDUCTING CIRCUIT ELEMENTS

ANNUAL REPORT

to

National Aeronautics and Space Administration
Langley Research Center
Hampton, VA 23665-5225

Period: February, 1991 - February, 1992

Principal Investigator:

Gene Haertling

Supporting Investigators:

Gregory Grabert
Phillip Gilmour

Contract No. NAG-1-1108

May 12, 1992

Department of Ceramic Engineering
College of Engineering

CLEMSON UNIVERSITY

DEVELOPMENT OF HIGH Tc (>110K) Bi, Tl and Y-BASED MATERIALS AS SUPERCONDUCTING CIRCUIT ELEMENTS

ANNUAL REPORT

to

National Aeronautics and Space Administration
Langley Research Center
Hampton, VA 23665-5225

Period: February, 1991 - February, 1992

Principal Investigator:
Gene Haertling

Supporting Investigators:
Gregory Grabert
Phillip Gilmour

Contract No. NAG-1-1108

May 12, 1992

CLEMSON
UNIVERSITY

Department of Ceramic Engineering
College of Engineering

Summary

Experimental work has continued on the development and characterization of bulk and hot pressed powders and tapecast materials in the Bi-Sr-Ca-Cu-O and Tl-Ba-Ca-Cu-O systems. A process for producing warp-free, sintered, superconducting tapes of Bi composition $Bi_2Sr_2Ca_2Cu_3O_x$ with a mixed oxide process was established. This procedure required a triple calcination at 830°C for 24 hours and sintering at 845°C from 20 to 200 hours. Hot pressing the triple calcined powder at 845°C for 6 hours at 5000 psi yielded a dense material which on further heat treatment at 845°C for 24 hours exhibited a Tc of 108.2K.

A further improvement in the processing of the bismuth materials was achieved via a chemical coprecipitation process wherein the starting nitrate materials were coprecipitated with oxalic acid, thus yielding a more chemically homogeneous, more reactive powder. With the coprecipitated powders, only one calcine at 830°C for 12 hours and a final sinter at 845°C for 30 hours was sufficient to produce a bulk superconducting material with a Tc of 108.4K. SAFIRE-type grounding links have been successfully fabricated from sintered, tapecast, coprecipitated BSCCO 2223 powders.

As anticipated, the Bi compositions were found to be much less oxygen sensitive than the Y (123) compositions. This was especially noted in the case of the hot pressed materials which were superconducting (Tc = 82K) as hot pressed - a condition which could not be achieved in the Y compositions.

Compositional and processing investigations were continued on the Tl-based superconductors. Manganese and lithium additions and sintering temperature and time were examined to determine their influence on superconducting properties. It was found that lithium substitutions for copper enhance the transition temperatures while manganese additions produced deleterious effects on the superconducting properties.

A suitable procedure for producing reproducible bulk and tapecast material of Tl composition $Tl_2Ba_2Ca_2Cu_3O_x$ was developed. In this method, a prereacted Tl-Ba-Ca-Cu-O material was sintered at 775°C for 48 hours in a silver foil enclosure. Parameters such as initial particle size, sintering time and temperature and burnout rate were found to be crucial to developing a uniform superconducting tape. The highest transition temperature for Tl-based tapes was measured at 110.2K. Thallium superconducting SAFIRE-type grounding links were fabricated from the tapes.

I. Introduction

This report details work that was carried out over the period from February, 1991 thru February, 1992, in the Ceramic Engineering Department of Clemson University under NASA contract No. NAG-1-1108. The work described in this report covers the second year of a program involving the development of high Tc superconducting circuit elements in the Bi-Sr-Ca-Cu-O and Tl-Ba-Ca-Cu-O compositional systems. This effort is intended to build on the results of the previous contract (NAG-1-820) which involved the development of the $YBa_2Cu_3O_{7-x}$ (123) material in circuit elements; and more specifically, a superconducting grounding link for the SAFIRE (Spectroscopy of the Atmosphere using Far Infra-Red Emission) program.

The technology developed for the SAFIRE grounding link involves a rigid-structure approach to superconducting elements rather than the flexible-wire idea promoted by most other institutions. In principle, the rigid-structure concept is quite simple and is tailor-made to take advantage of the inherent desirable properties of the superconducting ceramics while at the same time recognizing the low strength and basic brittleness of these materials. This is accomplished by pre-forming, sintering and testing the ceramic superconductor prior to bonding it to a rigid supporting substrate which is then totally encapsulated for further support and environmental protection. This approach has the advantages of (1) pre-testing of the superconducting material separate from the substrate, (2) optimization of the development of superconductivity in the ceramic without temperature limitations imposed by the substrate, (3) wider selection of substrate materials since the high temperature processing step precedes mounting of the superconductor to the printed circuit board, (4) freedom from firing shrinkage and other material compatibility problems and (5) high anticipated reliability because of its simplicity, rigid design and total encapsulation from the environment.

The report is presented in two parts; i.e., Part I dealing with the Bi-based materials and Part II covering work on the Tl-based materials.

Development of High T_c (>110 K) Bi, Tl and Y-Based Materials as Superconducting Circuit Elements

Annual Report
Part I: Bi-Based Materials

Submitted to

National Aeronautics and Space Administration
Langley Research Center

Submitted by
Gregory Grabert

Principal Investigator
Gene H. Haertling

Department of Ceramic Engineering
Clemson University
Contract No. NAG-1-1108
April 1992

I. Introduction

Since the discovery of a High T_c superconducting phase in the Bi-Sr-Ca-Cu-O (BSCCO) system by Maeda and his coworkers[1], extensive work has been done to fabricate devices out of these materials. Ceramic superconducting devices in the Y-Ba-Cu-O system have been fabricated at Clemson University using the rigid conductor process (RCP)[2,3] for the SAFIRE (Spectroscopy of the Atmosphere using Far Infra-Red Emission) program. This process is currently being applied to the bismuth-based materials because the bismuth-based materials have several advantages over the yttrium-based materials. Besides having a critical temperature (T_c) of 110 K as compared to that of 92 K for the yttrium-based material, the bismuth-based material (1) is less oxygen stiochiometry sensitive than the yttrium-based material, (2) is much more resistant to moisture degradation than the yttrium or thallium-based materials and (3) has a higher intrinsic critical current density (J_c) than the yttrium-based material and with better grain alignment could possibly have higher extrinsic J_c.

The BSCCO compound consists of an oxygen deficient perovskite layer containing copper oxide planes sandwiched between bismuth oxide layers. The highest T_c material is very difficult to synthesize in phase-pure form because separation of the 110 K phase from the 80 K phase is near impossible in bulk form. The 110 K phase has a very small sintering temperature range and long sintering times are required to obtain bulk material which is almost phase-pure. Many investigators worked on doping the BSCCO material with lead. They showed that the lead increased the percentage of the 110 K phase and decreased the sintering temperature and time[4, 5]. The lead has also been shown to act as a flux and promote crystallization. Another reason for lead doping is to increase the apparent valence of copper. As with the lanthanum-based system, the copper valence should be greater than 2+. By replacing some of the Bi^{3+} with Pb^{2+}, the apparent valence of copper is increased. Other phases that were present in other investigators' work were Ca_2PbO_4, Ca_2CuO_3, a

semiconducting phase, $(Sr, Ca)_xCu_yO_z$ and excess CuO. Some of these investigators believe that the Ca_2PbO_4 phase, the CuO and the 80 K phase interact with one another in some way to form the 110 K phase. The amount of strontium in these superconductors has also been investigated. It was shown that as the amount of strontium in the superconductor was increased, the 80 K phase tends to form instead of the 110 K phase[6, 7]. The reason for this is that the 80 K phase is strontium-rich and leaves the leftover calcium in the Ca_2PbO_4 form. The optimum amount of strontium was found to be somewhere between 1.6 and 1.95 moles. As a result of these ideas the composition decided upon for this investigation was $Bi_{1.6}Pb_{0.4}Sr_{1.9}Ca_{2.05}Cu_{3.05}O_x$.

In exploring other techniques used to synthesize superconductors and the bismuth-based materials, two were chosen for further work. Melt quenching was chosen because of the ease of processing and the possibility of obtaining a sample with a much higher J_c[8,9]. Since, the formation of the higher T_c phase is achieved through partial melting or liquid phase sintering, it was thought that the BSCCO material could be synthesized, in primarily the high T_c phase form, with a better grain alignment and possibly a higher J_c. Chemical coprecipitation was chosen because of the ability to make very homogeneous and uniform powder. Powder prepared by the mixed oxide process must be ground and calcined several times in order to obtain a powder which gives reliable and reproducible results. However, each time the material is ground or ball milled, impurities are introduced, thus lowering the quality of the powder produced. Coprecipitated powder, on the other hand, because of fine particle size, less than 1 μm, and high purity, is more reactive and may not need to be calcined at all[10]. The $YBa_2Cu_3O_x$ material had been coprecipitated at Clemson University using the oxalate route with both the acetates and nitrates. The nitrates were chosen over the acetates for the bismuth- based material because copper acetate is soluble only in a basic solution and bismuth acetate only in an acidic solution. The only problem with the nitrates is the solubility of bismuth nitrate[10-12]. Actually, the bismuth nitrate powder was found to dissolve in a dilute nitric acid solution quite easily.

This report contains the sample preparation procedure for the bismuth-based materials synthesized in bulk form by the mixed oxide process, the coprecipitation process and the melt-quench process and in tapecast form by the mixed oxide and coprecipitation processes. It also contains data on the bismuth-based superconducting grounding link and material results obtained since June, 1991.

II. Experimental Procedure

As previously stated, the composition decided upon for this investigation was $Bi_{1.6}Pb_{0.4}Sr_{1.9}Ca_{2.05}Cu_{3.05}O_x$. All of the materials were first tested for the Meissner effect. The critical temperature and critical current density for both the bulk and the tapecast materials were evaluated using a standard four point method. The resistance was measured by a Keithley, Model 580, micro-ohmmeter with a sensitivity of $10^{-6}\,\Omega$. The critical currents were measured using a 1 μV per cm standard by a Keithley, Model 197, Autoranging MicroVolt DMM. In addition, the structures of the samples were examined by powder X-ray diffraction (XRD) using Cu K_α radiation. Scanning electron microscopy (SEM) was used to observe the homogeneity and surface morphology of the materials. The electrodes for all materials were applied using a commercial silver paste, C8710 from Heraeus Inc., Cermalloy Division, and fired at 845 °C for eighteen minutes.

1. Mixed Oxide Process

Figure 1 shows the preparation process for the uniaxial and hot pressed bulk bismuth-based material. Figure 2 shows the preparation process for the tapecast bismuth- based material. In all cases, the starting materials were Bi_2O_3, PbO, $SrCO_3$, $CaCO_3$ and CuO. The powders were weighed out and ball milled with distilled water for one hour and dried at 100 °C for eighteen hours. The dried powder was then pressed into pellets and calcined at 810 °C for twelve hours and one or three times at 830 °C for twenty-four hours depending on the process. The calcined powder was

then ground with a mortar and pestle for processing into the bulk and tapecast material. For the uniaxially pressed material, the calcined powder was pressed into one square inch pellets and sintered at 845 °C for twenty to two hundred hours in air. For the hot pressed material, the calcined powder was hot pressed at 5000 psi for six hours at 845 °C in oxygen. This material was then tested or subjected to an additional heat treatment of twenty-four hours at 845 °C in air. The furnace schedule for the bulk material can be seen in Figure 3. For the tapecast material, the calcined powder was ball milled with trichloroethylene for one hour and dried at 100 °C for eighteen hours. The dried powder was then mixed with a commercial binder, B73305 from Metoramic Sciences, Inc., in the ratio of 150 grams of powder to 80 grams of binder and ball milled for one hour. The mixture was deaired for ten minutes and tapecast by a conventional tapecasting processes[13]. The tape was cut into strips with the dimensions 25.4 mm x 2.0 mm x 0.5 mm. The strips were sintered by a single and double ramp process. In the single ramp process the tapes were sintered at 845 °C for twenty-eight to forty-eight hours in air using the furnace schedule seen in Figure 3. In the double ramp process, the tapes were covered and sintered at 500°C to 800°C for two hours, cooled down to room temperature, uncovered and sintered at 845 °C for thirty hours in air. Tapes were also sintered covered at 845 °C for thirty hours using the double ramp process. The furnace schedule for the double ramp process can be seen in Figure 4.

2. Melt Quench Process

Figure 5 shows the preparation process for the melt quenched bulk bismuth-based material. The starting materials were oxides prepared via the mixed oxide route. The material was calcined three times, once at 810 °C for twelve hours in air and twice at 830 °C for twenty-four hours in air. The three times calcined material was then melted in an alumina crucible at 1150 °C for forty minutes in air. The crucible was removed from the furnace and the BSCCO melt was quenched in a stainless steel pan. When the material cooled to room temperature, it was cut and tested or subjected to an additional heat treatment at 845 °C for thirty hours in air.

The sample was then electroded and tested. The furnace schedule is the same as that for the bulk material and can be seen in Figure 3.

3. Coprecipitation Process

Figure 6 shows the preparation process for the coprecipitated bulk bismuth-based material and Figure 7 shows the process for the tapecast bismuth- based material. In both cases the starting materials were $Bi(NO_3)_3$,in a dilute nitric acid solution , $Pb(NO_3)_2$, $Sr(NO_3)_2$, $Ca(NO_3)_2 \cdot 4H_2O$ and $Cu(NO_3)_2 \cdot 2.5H_2O$. The materials were weighed out according to the batch information sheet shown in Table 1. The bismuth nitrate solution was put into a beaker and the other constituents were added one at a time, until each dissolved in the dilute nitric acid solution. Distilled water was added periodically to aid in the process. The solution was constantly stirred by a magnetic stirrer. Once all the constituents were dissolved, a twenty percent excess aqueous solution of oxalic acid was added and stirred for twenty minutes. The pH was adjusted to approximately 3.5 with ammonium hydroxide and the solution dried in a vacuum oven for twelve hours. The powder is then heated to 600 °C for two hours in an alumina crucible to burn off all of the organic radicals. The precalcined powder was then ground and pressed into pellets and sintered at 845 °C for thirty hours in air or calcined at 830 °C for twelve hours in air. The calcined powder was then ground with a mortar and pestle for processing into bulk and tapecast material. For the bulk material, the calcined and precalcined was sintered at 845 °C for thirty hours in air. These materials were then electroded and tested. For the tapecast material, only calcined material was used to cast tape. The tapecast procedure for the coprecipitated powder was the same as for the mixed oxide powder, with the exception of the ratio of powder to binder was 100 to 45. The tape was cut into strips and sintered covered using the single ramp process which can be seen in Figure 3.

III. Results and Discussion

1. BSCCO Bulk Material

Figure 8 shows the resistance versus temperature curve for the hot pressed compact which was prepared at 845 °C for six hours in oxygen at 5000 psi. The curve showed that the material had a sharp transition to the superconducting state at 83.3 K. Figure 9 shows the resistance versus temperature curve for the same compact with an additional twenty-four hour heat treatment at 845 °C in air. The curve showed that the material now has a sharp transition to the superconducting state at 108.2 K. This material is now less dense, the bulk density dropped from 6.18 to 6.01 g/cc, but the additional twenty-four hour heat treatment has increased the T_c by almost 25 K. From the SEM micrographs, shown in Figure 10, one can see that the compact with no additional heat treatment appears to be a very dense melt with no apparent grain structure, but the heat treated compact's structure now has grain growth and the grains exhibit the same plate like morphology seen before in the bulk uniaxially pressed material[14]. The bulk uniaxially pressed compact had to be sintered for two-hundred hours to reach the same T_c as the heat treated compact[14]. The reason the hot pressed compact can be converted to the higher Tc phase in a substantially shorter amount of time is due to the compact being much more dense and uniform than the uniaxially pressed pellet making the driving force for conversion much higher.

A preliminary study of the effect the number of calcinations had on the superconducting properties of the uniaxially and hot pressed material was preformed. In the uniaxially pressed material sintered for thirty hours at 845 °C in air, shown in Figure 11, the two times calcined material had a T_c of 99.1 K, whereas the three times calcined material had a T_c that was 3 K higher at 102.0 K. In the hot pressed material with no additional heat treatment, shown in Figure 12, the two times calcined material did not superconduct, while the three times calcined material had a T_c of 83.3 K. The same two compacts with an additional heat treatment of twenty-four hours at 845 °C in air, shown in Figure 13, the two times calcined material

had a T_c of 104.4 K, and the three times calcined material had a T_c that was 4 K higher at 108.2 K. When four times calcined powder was used to produce the uniaxially pressed bulk material, which was sintered for thirty hours at 845 °C in air, the material did not show a significant change in either critical temperature, critical current density or bulk density. Four times calcined powder has not yet been used to produce the hot pressed material.

2. BSCCO Tapecast Material

All of the powder used to make the tapecast material was calcined three times. There was a problem with the tapecast material, after thirty hours sintering, a percentage of the tapes started to curl and fracture. As the sintering time increased so did the percentage of unacceptable tapes. To alleviate the curling problem, the tapes were covered and sintered at 845 °C for thirty hours using the single ramp furnace schedule shown in Figure 3. These tapes did not curl but they did partially react with the setter plate. From information about the binder burnout rate and the Y-Ba-Cu-O system, it was decided that the tapes were to be covered and sintered at 500 to 800 °C for two hours using the double ramp furnace schedule shown in Figure 4, then uncovered and sintered for thirty hours at 845 °C. These results are shown in Table 2. The best results came from the tapes which were covered and sintered at 845 °C, but these tapes partially reacted with the setter plate.

A sintering time versus critical temperature curve in the twenty-eight to forty-eight hour single ramp sintering time range with a dot for the double ramp process of 700 °C is shown in Figure 14. The curve shows just how much higher the T_c of the double ramp process is over the single ramp process. The J_c's of the double ramp process are twice that of the single ramp process.

3. BSCCO Melt Quenched Material

Figure 15 shows the resistance versus temperature curve for the melt quenched compact with no additional heat treatment. The curve showed that the material, originally in the semiconducting state, did show

superconducting behavior with an onset temperature of approximately 100 K. However, the material did not superconduct at 77.3 K. Figure 16 shows the resistance versus temperature curves for the melt quenched compacts with additional heat treatment. Curve (a) shows a compact with thirty hours of additional heat treatment at 845 °C and curve (b) shows a compact with sixty hours of additional heat treatment at 845 °C. Both curves showed metallic behavior, the thirty hour compact had an onset temperature of about 110 K and the sixty hour compact had an onset temperature of about 120 K. Neither of the compacts superconducted at 77.3 K and both curves showed double hump transistions, indicating the presence of a large amount of low T_c second phase material. The room temperature resistance of the sixty hour compact was about half that of the thirty hour compact. The microstructure of the melt quenched material looks very inhomogeneous, there are areas of solid melt and areas of very porous material. Figure 17 shows the microstructure of the two different areas of a melt quenched sample with sixty hours of additional heat treament. If these micrographs are compared with those of the hot pressed material in Figure 10, similarities can be detected. One possible conclusion would be that these are regions of high T_c phase, the porous grain growth region, and low T_c phase, the solid melt region.

4. BSCCO Coprecipitated Material

The coprecipitated powder was much easier to process and the time required to obtain a workable material was much less. Figure 18 shows the resistance versus temperature curve for the coprecipitated material which was sintered, uncalcined, at 845 °C for thirty hours in air. The curve showed that the material had a transition to the superconducting state at 99.1 K. Figure 19 shows the resistance versus temperature curve for the coprecipitated material which was calcined at 830 °C for twelve hours and sintered at 845 °C for thirty hours in air. The curve showed that the material had a transition to the superconducting state at 104.8 K. The Tc increased about five degrees with the addition of the twelve hour calcine. Calcining the material for twenty-four hours, instead of twelve, did not seem to affect the results. Again from the microstructure, shown in

Figure 20, one can see that the grains of the coprecipitated compact exhibit the same plate like morphology as those of the uniaxial and hot pressed mixed oxide compacts. A preliminary study on the effect pressing pressure has on the superconducting properties was performed on the coprecipitated powder in the same manner as it was on the mixed oxide powder[10]. Figure 21 shows the resistance versus temperature curve for the two compacts which were calcined at 830 °C for twelve hours and sintered at 845 °C for thirty hours in air. The compact that was pressed at 3200 psi had a T_c of 104.8 K, while the compact pressed at 20,120 psi had a T_c of 108.4 K. This 3.6 degree increase was due to an increase in densification and reactivity of the higher pressed compact. The bulk density increased from 4.4 g/cc to 5.1 g/cc. Comparing the SEM micrograph shown in Figure 22 (a) to that of Figure 20, one can see that the compact is more dense. In fact, a closer look, Figure 22 (b), at the same micrograph at a higher magnification shows that there is actually some partial melting which contributes to the increase in density and T_c. This again reinforces the idea that liquid phase sintering contributes to the formation of the high T_c phase. Since partial melting has occurred more and more in the higher Tc/Jc samples, a Differential Thermal Analysis (DTA) curve was run for the coprecipitated powder to determine the melting point of the high Tc phase. Figure 23 shows the DTA curve, and the melting point was determined to be about 865 °C. From this information, work done by other investigators[15-17], and work currently going on at Clemson University in the area of thick films, a compact was sintered at 845 °C for thirty hours after the powder had been calcined at 860 °C for twelve hours in air. Figure 24 shows the resistance versus temperature curve for the two compacts which were calcined at 830 °C and 860 °C for twelve hours and sintered at 845 °C for thirty hours in air. As one can see, the Tc curves are very similar and the other properties tested were also very close to identical, but more work needs to be done to determine what, if any the calcination temperature has on the final properties.

The coprecipitated tapecast material, like the bulk material, was much easier to process. Figure 25 shows the resistance versus temperature curve for coprecipitated tapecast material which was sintered

for thirty hours. For all the tapecasting, the powder used was calcined at 830 °C for twelve hours. The curve, like those for the bulk material, showed that the material had a sharp transition to the superconducting state and the Tc was 102.4 K. Comparing the microstructure of the coprecipitated tapecast material to that of the mixed oxide tapecast material, one can see, from Figure 26, that the coprecipitated tape is much more uniform and seems to have a better alignment than the mixed oxide tape. Also, the curling problem experienced with the mixed oxide tape, has not seemed to be a problem with the coprecipitated tape.

5. BSCCO Grounding Links

Superconducting grounding links were made from the coprecipitated tapecast material and can be seen, along with the resistance versus temperature curve, in Figure 27. The critical temperature of the links were approximately 96 K. The resistance at liquid nitrogen temperature due to the solder and the gold pins was 0.9 mΩ. The thermal expansion of the material was determined to see if the links could be made from the same materials as the YBCO links were made from. The thermal expansion was determined to be approximately 12×10^{-6} in/in °C from the thermal expansion curve shown in Figure 28. The thermal expansion of the printed circuit board was determined to be 16×10^{-6} in/in °C and for the epoxy resin was 50×10^{-6} in/in °C [2]. From this information, the materials used for the YBCO links should work fine for the BSCCO material.

IV. Conclusions

In conclusion, the coprecipitated process has been determined to be the best method of those investigated to synthesize the BSCCO material with the best electrical properties. The coprecipitated material has the best properties when calcined for twelve hours at 830 °C. While the tapes produced by the mixed oxide process need to be covered and the double ramp method used to prevent cracking and curling, the coprecipitated tapes need

only to be covered to produce a good product. To produce the uniaxially and hot pressed bulk material, made from mixed oxide powders, with the best properties the starting material should be calcined three times. Higher pressing pressures have shown to produce powders which have better electical properties than those produced from the lower pressing pressures. Furthermore, hot pressing the bulk material before sintering allows the high Tc phase to be developed in significantly shorter time. Superconducting grounding links have been made with the best properties using tapes made from coprecipitated powder.

References

1. Maeda, H., Y. Tanaka, M. Fukutomi and T. Asano, (1988). "A New high-T_c Oxide Superconductor Without a Rare Earth Element," *Jap. J. Appl. Phys.*, vol. 27, No. 2, February, pp. L209-L210.

2. Haertling, G. H., (1990). "Development and Evaluation of Superconducting Circuit Elements," NASA Final Report, Contract No. NAG-1-820, October.

3. Haertling, G. H., (1991). "Ceramic Superconducting Components," *Ceramic Transaction*, Vol. 18

4. Sunshine, S. A., T. Siegrist, L. F. Schneemeyer, D. W. Murphy, R. J. Cava, B. Batlogg, R. B. Van Dover, R. M. Fleming, S. H. Glarum, S. Nakahara, R. Farrow, J. J. Krajewski, S. M. Zahurak, J. V. Waszczak, J. H. Marshall, P. Marsh, L. W. Rupp and W. F. Peck, (1988). "Structure and Physical Properties of Single Crystals of the 84-K Superconductor $Bi_{2.2}Sr_2Ca_{0.8}Cu_2O_{8+\partial}$," *Phys. Rev. B*, vol. 38, pg. 893.

5. Takano M., J. Takada, K. Oda, H. Kitaguchi, Y. Miura, Y. Ikeda, Y. Tomii and H. Mazaki, (1988). "High-T_c Phase Promoted and Stabilized in the Bi, Pb-Sr-Ca-Cu-O System," *Jap. J. Appl. Phys.*, vol. 27, No. 2, February, pg. L1041.

6. Endo, U., S. Koyama and T. Kawai, (1989). "Composition Dependence on the Superconducting Properties of Bi-Sr-Ca-Cu-O," *Jap. J. Appl. Phys.*, vol. 28, No. 2, February, pp. L190-L192.

7. Huang, Y. T., R. G. Liu, S. W. Lu, P. T. Wu and W. N. Wang, (1990). Accelerated Formation of 110 K High T_c Phase in the Ca- and Cu-rich Bi-Pb-Sr-Ca-Cu-O System," *Appl. Phys. Lett.*, 56 (8), 19 February, pp. 779-781.

8. Komatsu, T., K. Imai, R. Sato, K. Matusita and T. Yamashita, (1988). "Preparation of High-T_c Superconducting Bi-Sr-Ca-Cu-O Ceramics by the Melt Qunching Method," *Jap. J. Appl. Phys.*, vol. 27, No. 4, April, pp. L533-L535.

9. Ibara, Y., H. Nasu, T. Imura and Y. Osaka, (1988). "Preparation and Crystallization Process of the High-T_c Superconducting Phase (Tc(end)>100 K) in Bi, Pb-Sr-Ca-Cu-O Glass-Ceramics," *Jap. J. Appl. Phys.*, vol. 28, No. 1, January, pp. L37-L40.

10. Hagberg, J., A. Uusimaki, J. Levoska and S. Leppavuori, (1989). "Preparation of Bi-Pb-Sr-Ca-Cu-O High-T_c Superconducting Material via oxalate route at Various pH Values," *Physica C*, vol. 160, pp. 369-374.

11. Weast, R. C., (1987). *CRC Handbook of Chemistry and Physics*, CRC Press Inc., Boca Raton, Florida

12. Shei, C. Y., R. S. Liu, C. T. Chang and P. T. Wu, (1990). "Preparation and Characterization of Superconducting (Bi, Pb)$_2$Sr$_2$Ca$_2$Cu$_3$ Oxides with T_c above 110 K by Coprecipitation in Triethylamine Media," *Inorg. Chem.*, vol. 29, pp. 3117-3119.

13. Reed, J. S., (1988). *Introduction to the Principles of Ceramic Processing*, John Wiley & Sons, New York.

14. Haertling, G. H., (1991). " Development of High Tc (>110 K) Bi, Tl and Y-Based Materials as Superconducting Circuit Elements," NASA Annual Report, Contract No. NAG-1-1108, June.

15. Seshu Bai, V., S. Ravi, T. Rajasekharan and R. Gopalan, (1991). "On the composition of 110 K superconductor in a (Bi, Pb)-Sr-Ca-Cu-O system," *J. Appl. Phys.*, vol. 70, No. 8, October, pp. 4378-4382.

16. Strobel, P., and T. Fournier, (1990). Phase Diagram in the Bi (Pb)-Sr-Ca-Cu-O system," *J. of Less Common Metals*, I64 & I65, pp. 519-525.

17. Briggs, A., B. A. Bellamy, I. E. Denton and J. M. Perks, (1990). Preparation of Single Phase Bismuth-Based 2212 and 2223 Superconducting Oxides, and Quantitative X-Ray Diffraction Analysis of 2212 and 2223 Mixtures," *J. of Less Common Metals*, I64 & I65, pp. 559-567.

18. Sax, N. I., and R. J. Lewis Sr., (1988). *Hawley's Condensed Chemical Dictionary*, 11 th ed., Van Nostrand Reinhold Co., New York.

Batch Information Sheet

Composition # 1 **Batch #** 1

Formula $Bi_{1.6}Pb_{0.4}Sr_{1.9}Ca_{2.05}Cu_{3.05}O_x$

Batch Size 100 gms. **Date** January 21, 1992

Raw Materials and Source

$Bi(NO_3)_3$ Mallinckrodt **$Pb(NO_3)_2$** Fisher **$Sr(NO_3)_2$** Mallinckrodt

$Ca(NO_3)_2 \cdot 4H_2O$ Mallinckrodt **HNO_3** Mallinckrodt

$Cu(NO_3)_2 \cdot 2.5H_2O$ Mallinckrodt **NH_4OH** Fisher

Batching

Oxide	Mole Wt	Moles	Formula Wt	Wt %	% Oxide	Batch Wt
Bi2O3	465.96	0.80	372.768	36.672	11.098	330.436
SrO	103.62	1.90	196.878	19.369	48.963	39.558
CaO	56.08	2.05	114.964	11.310	23.748	47.626
CuO	79.54	3.05	242.597	23.866	34.198	69.790
PbO	223.19	0.40	89.276	8.783	67.388	13.033
			1016.483	100		500.442

Table 1 The batch information for the materials in the BSCCO coprecipitation process, showing the raw materials used, their source, and the amounts of each needed to achieve the required batch size.

Table 2 The firing schedule, process, the Tc, and the Jc of the tapecast material using the two stage ramp firing process. All of the tapes were firing at 845 °C for thirty hours.

Temp	Firing	T_c (K)	J_c (A/cm^2)
845	Single	101.5	80.8
800	Double	99.0	46.6
700	Double	101.3	50.9
650	Double	90.8	20.1
500	Double	NS	NS

NS - Non Superconducting

Table 3 The results of the bismuth base material to date. The table contains information on the material, the process used, the Tc, the Jc, the bulk density and any special procedures used in synthesizing the material.

Material	Process	Special	T_c (K)	J_c (A/cm^2)	Bulk Density (gms/cc)
Mixed oxide	Bulk	200 hr Sintering	108.1	80	4.5
		High pressure (125 hr)	107.3	78	4.8
		Low pressure (125 hr)	106.8	75	4.4
		20 hr Sintering	98.9	50	4.1
		2 Calcines (30 hr)	99.1	50	4.1
		3 Calcines (30 hr)	102.0	50	4.2
	Hot pressed	2 Calcines	NS	NS	NS
		3 Calcines	83.3		6.2
		2 Calcines (24 hr)	104.4	100	5.7
		3 Calcines (24 hr)	108.2	140	6.0
	Tapecast	Single ramp	99.5	20	3.3
		Single ramp (covered)	101.5	81	3.5
		Double ramp (covered)	99.0	47	3.3
Melt Quenched	Bulk		NS		
		30 hr Sintering	NS		
		60 hr Sintering	NS		
Coprecipitated	Bulk	No Calcine	99.1		4.0
		1 Calcine	104.8	100	4.4
		High pressure (830 °C)	108.4		5.1
		High pressure (860 °C)	108.8		5.2
	Tapecast		102.4	120	3.9
		Link	96.0		

NS - Non Superconducting

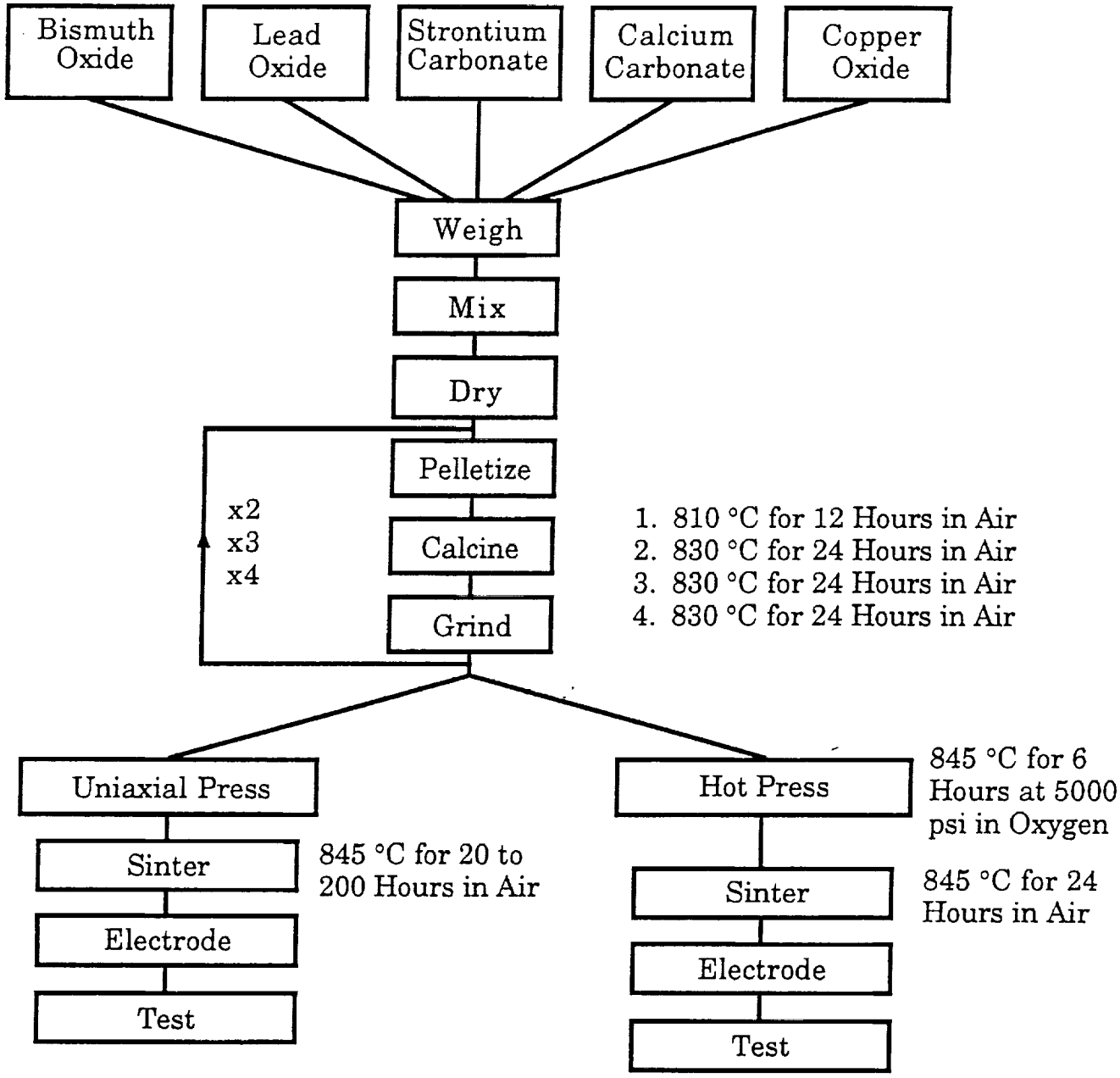

Figure 1 Flow chart for the uniaxially and hot pressed bismuth-based materials showing the procedures used to synthesize these materials. These materials were sythesized using both two, three and four times calcined powder.

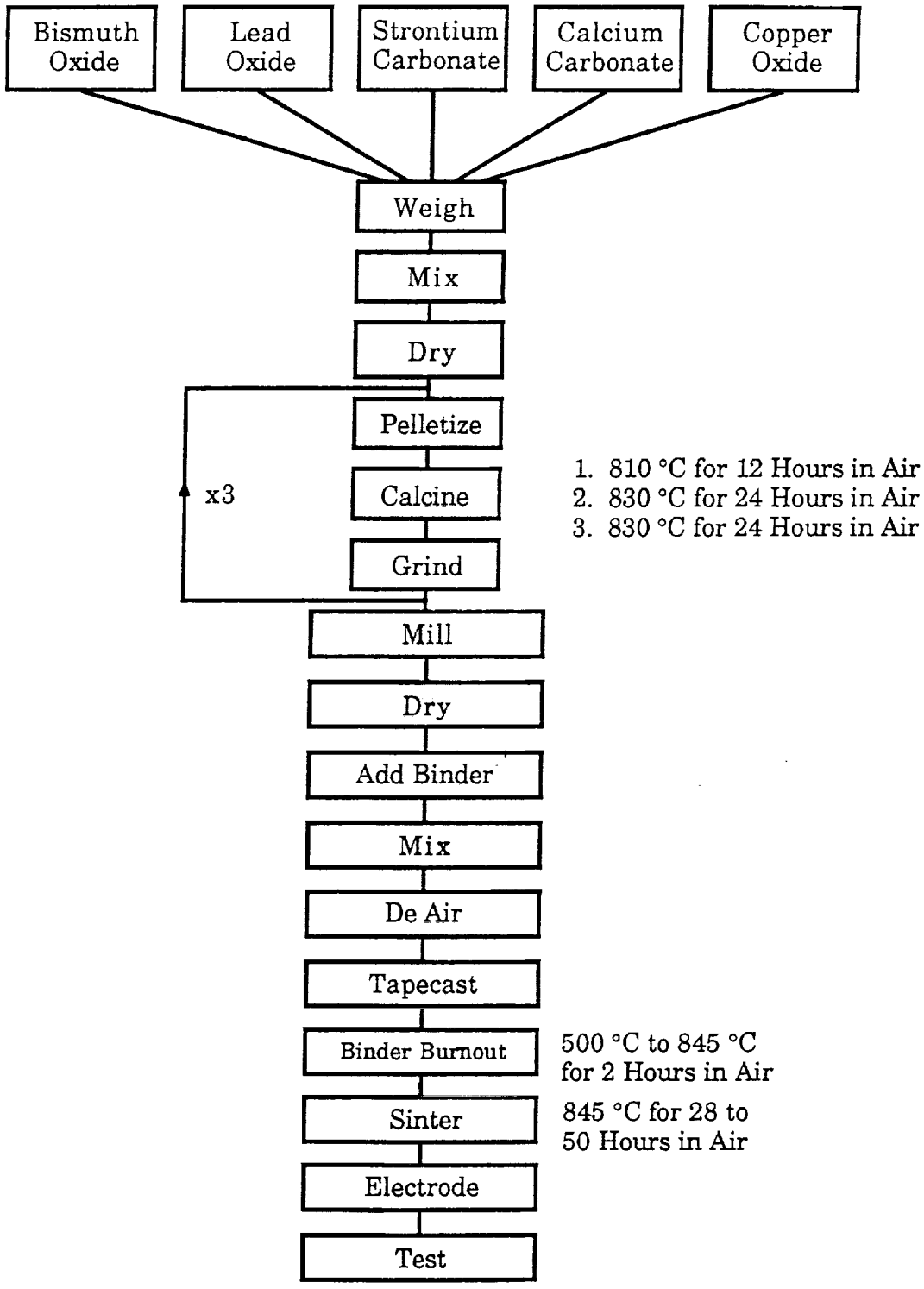

Figure 2 Flow chart for the tapecast bismuth-based materials showing the procedures used to synthesize these materials. These materials were sythesized using three time calcined powder.

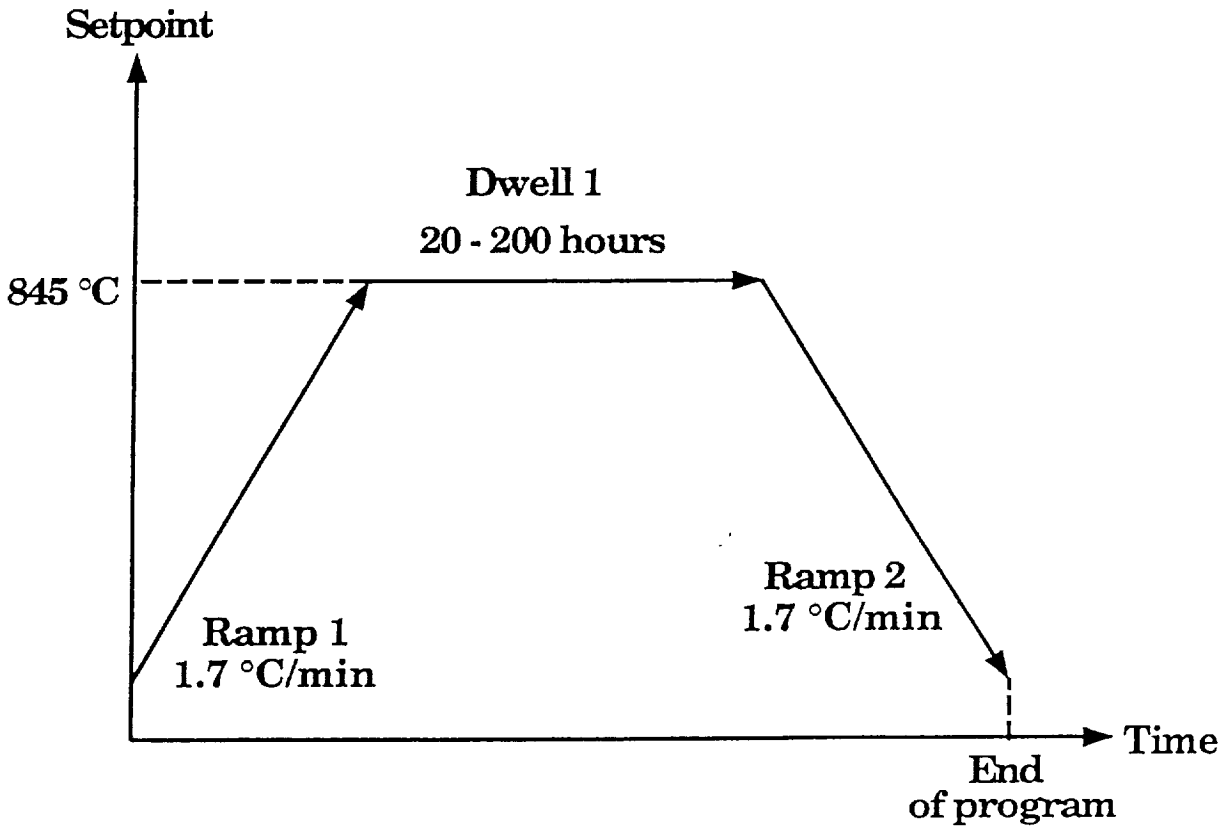

Figure 3 The furnace schedule and operation for the bulk, melt quench, and single ramp tapecast bismuth-based materials.

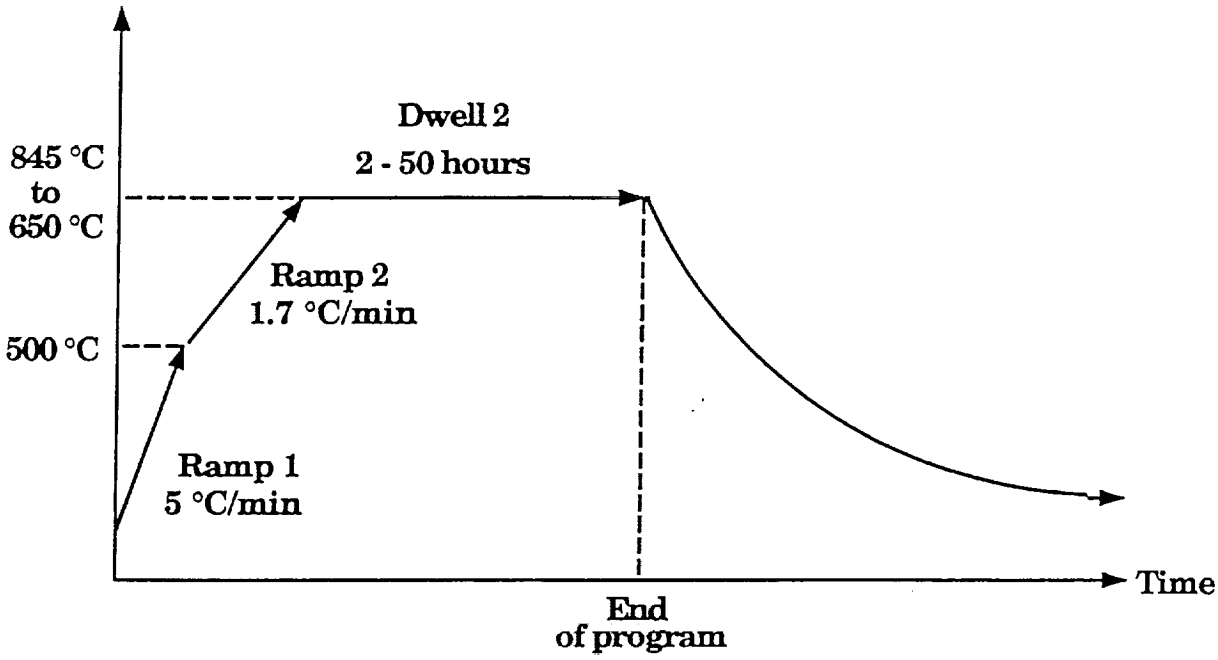

Figure 4 The furnace schedule and operation for the double ramp tapecast bismuth-based materials.

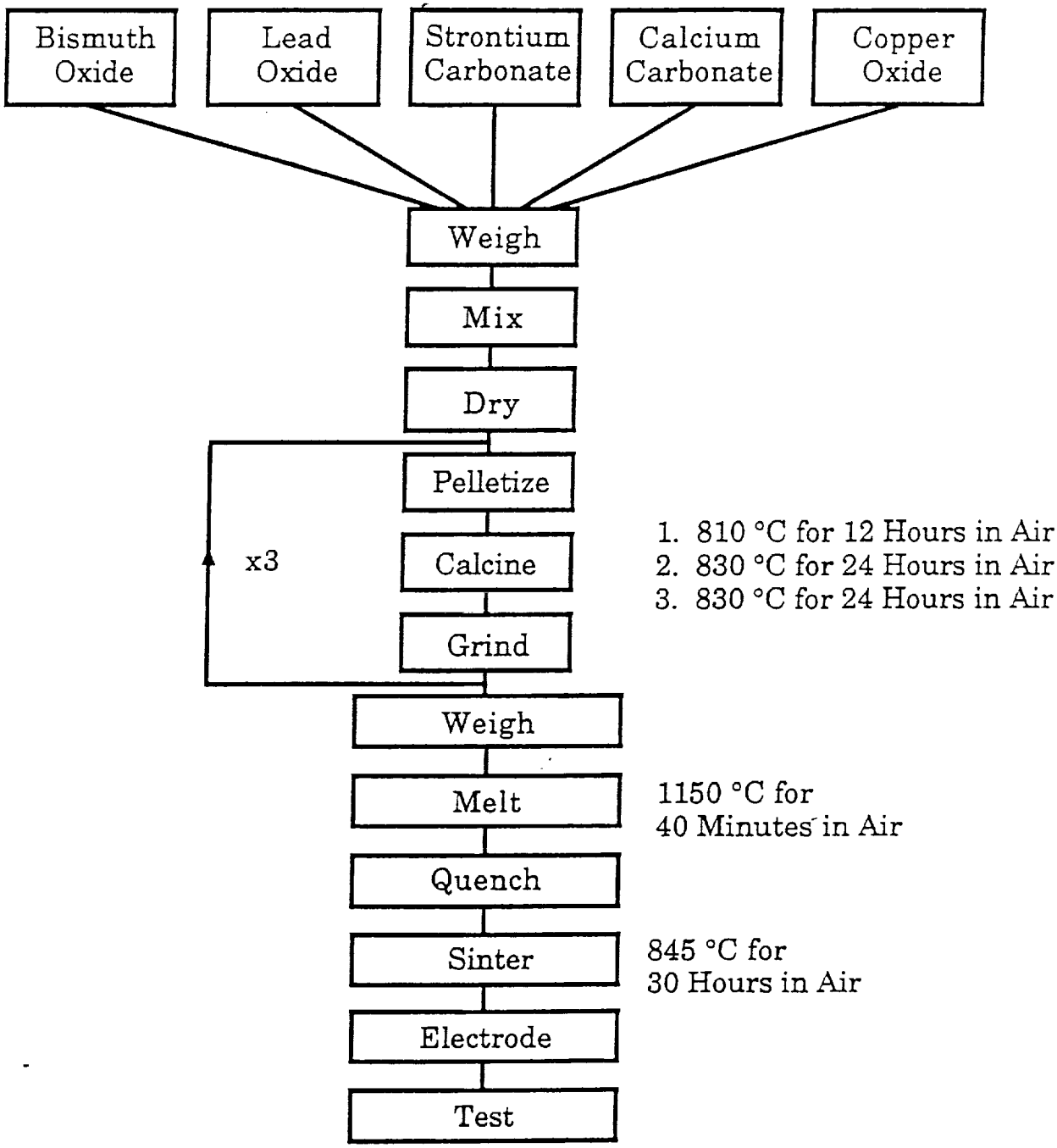

Figure 5 Flow chart for the melt quenched bismuth-based materials showing the procedures used to synthesize these materials. These materials were synthesized using three times calcined, mixed oxide powder.

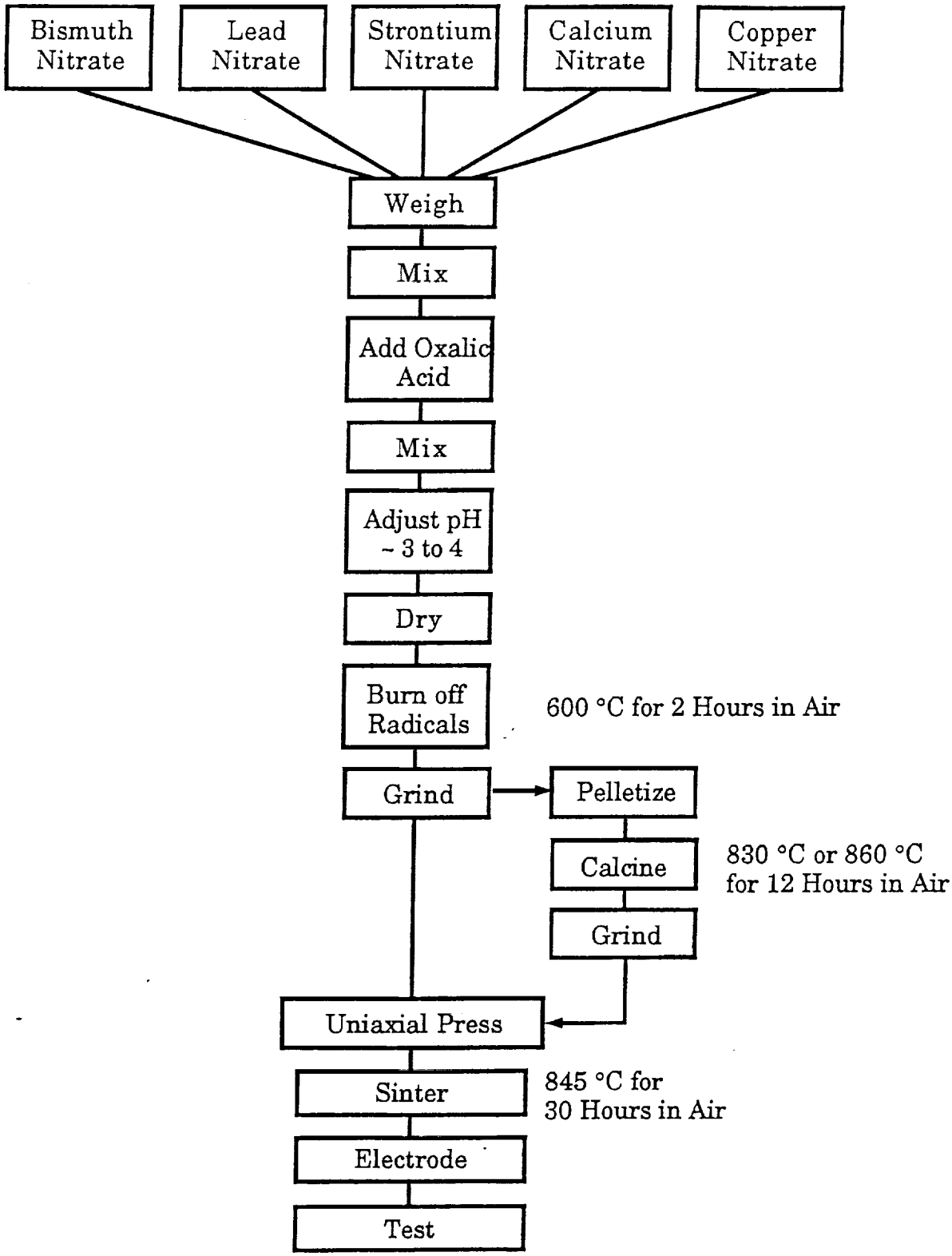

Figure 6 Flow chart for the coprecipitated bismuth-based materials showing the procedures used to synthesize these materials. These materials were synthesized using both calcined and uncalcined powder.

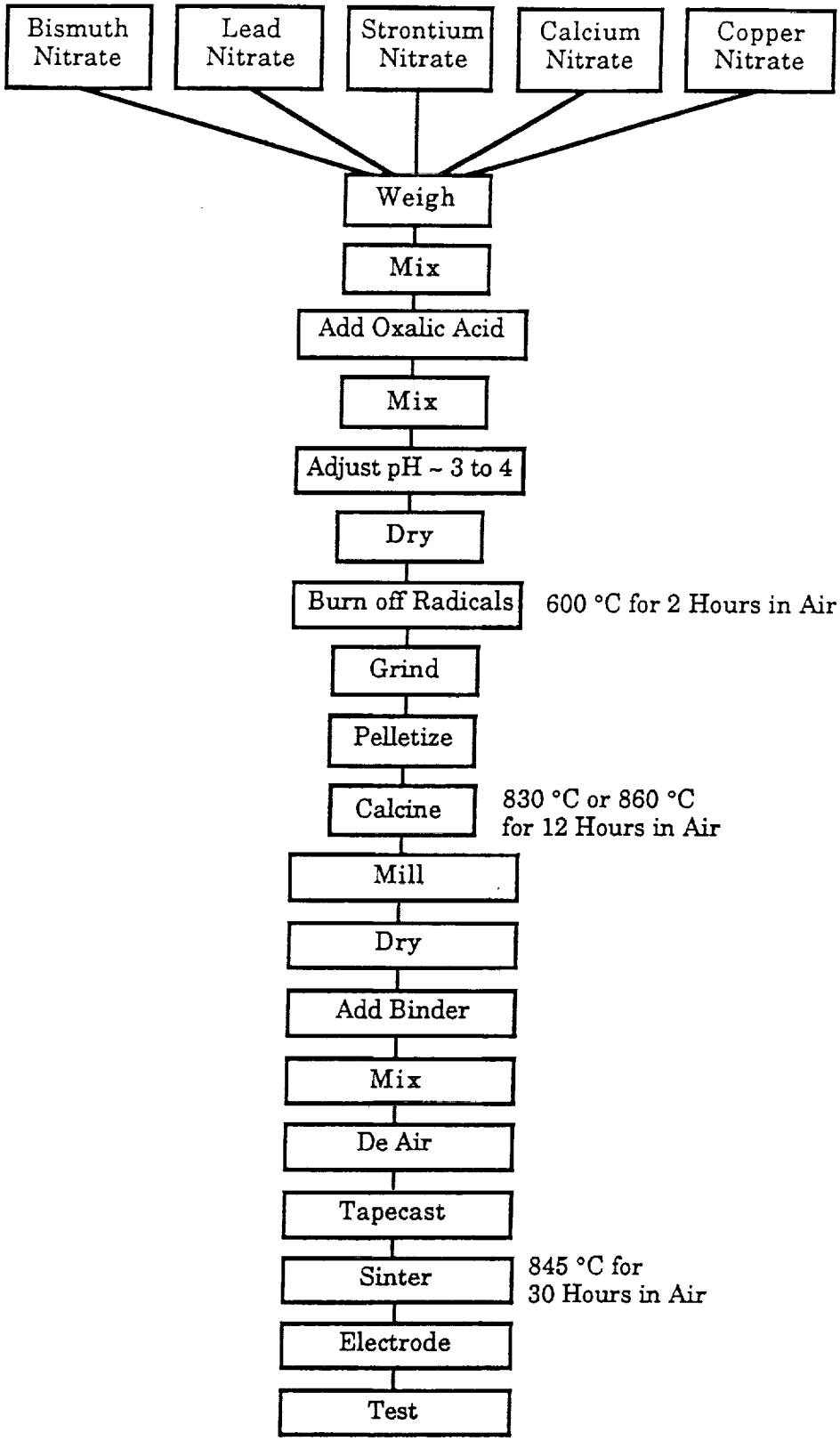

Figure 7 Flow chart for the tapecast bismuth-based materials, made by the coprecipitation process, showing the procedures used to synthesize these materials. These materials were synthesized using one time calcined powder.

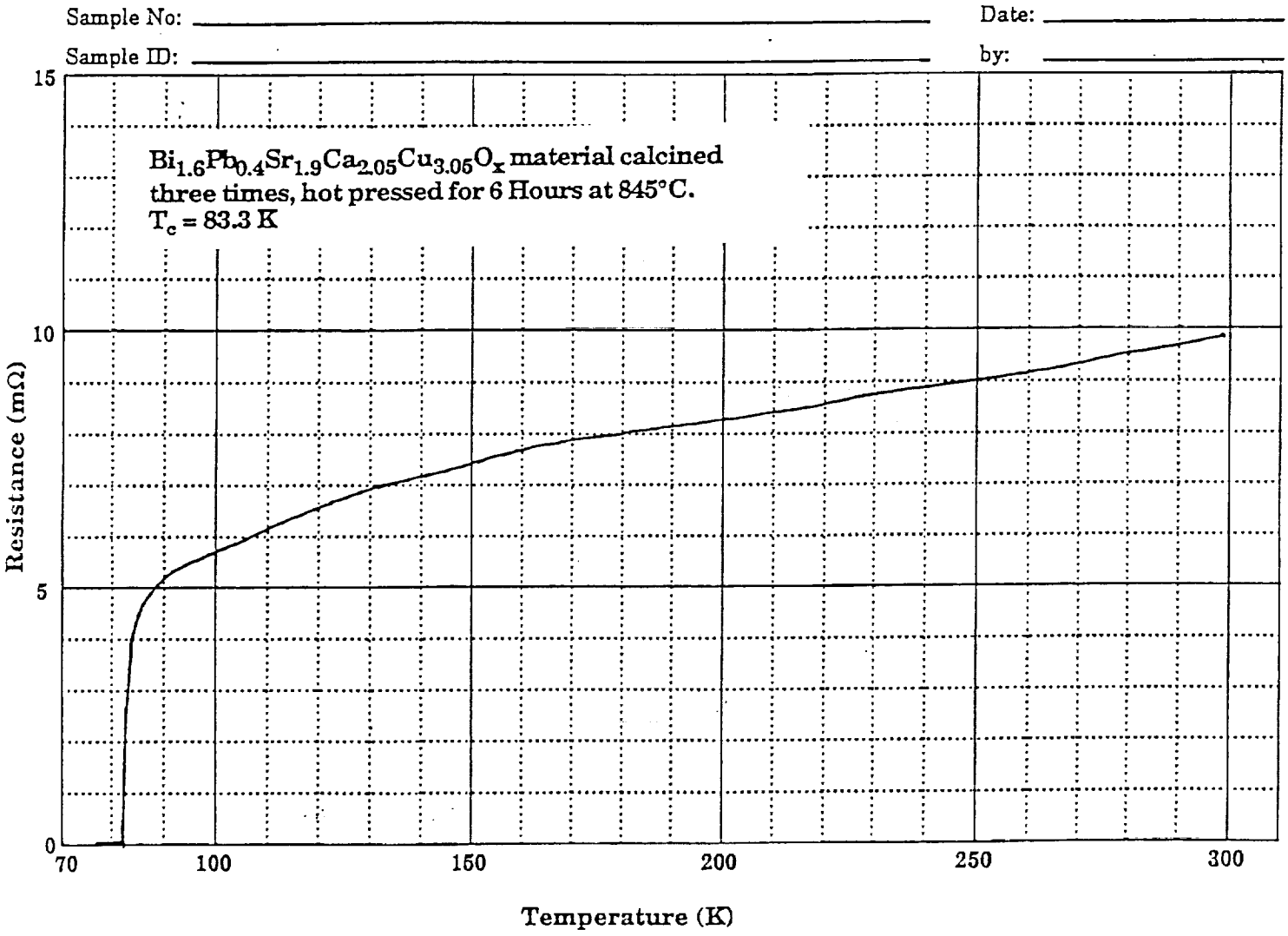

Figure 8 Resistance versus Temperature curve for a bulk hot pressed sample with no additional heat treatment.

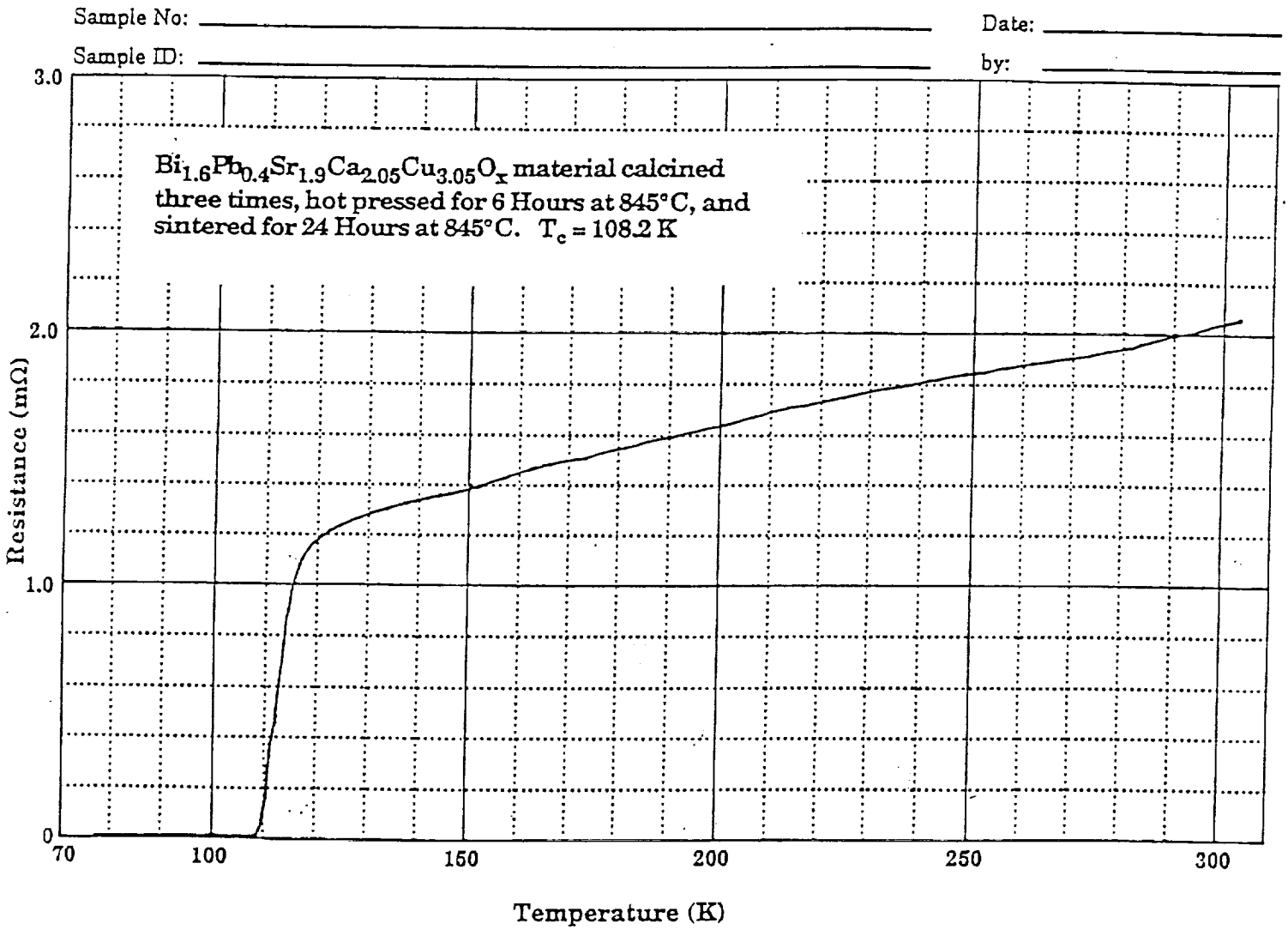

Figure 9 Resistance versus Temperature curve for a bulk hot pressed sample with twenty-four hours additional heat treatment at 845 °C.

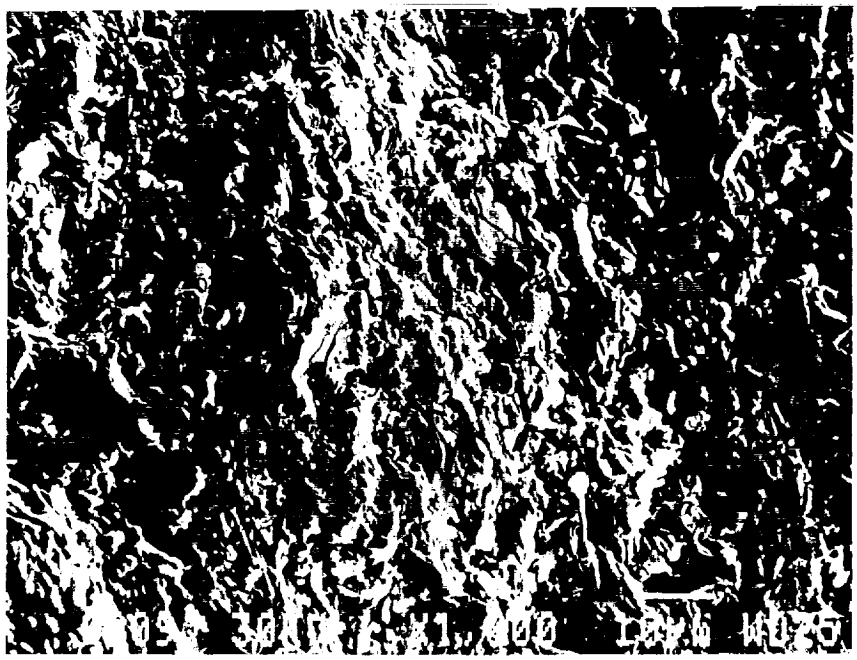

a) Hot pressed pellet with no additional heat treatment.

b) Hot pressed pellet sintered for an additional twenty-four hours in air.

Figure 10 SEM micrographs for bulk hot pressed pellets pressed at 5000 psi for six hours at 845 ° C in oxygen.

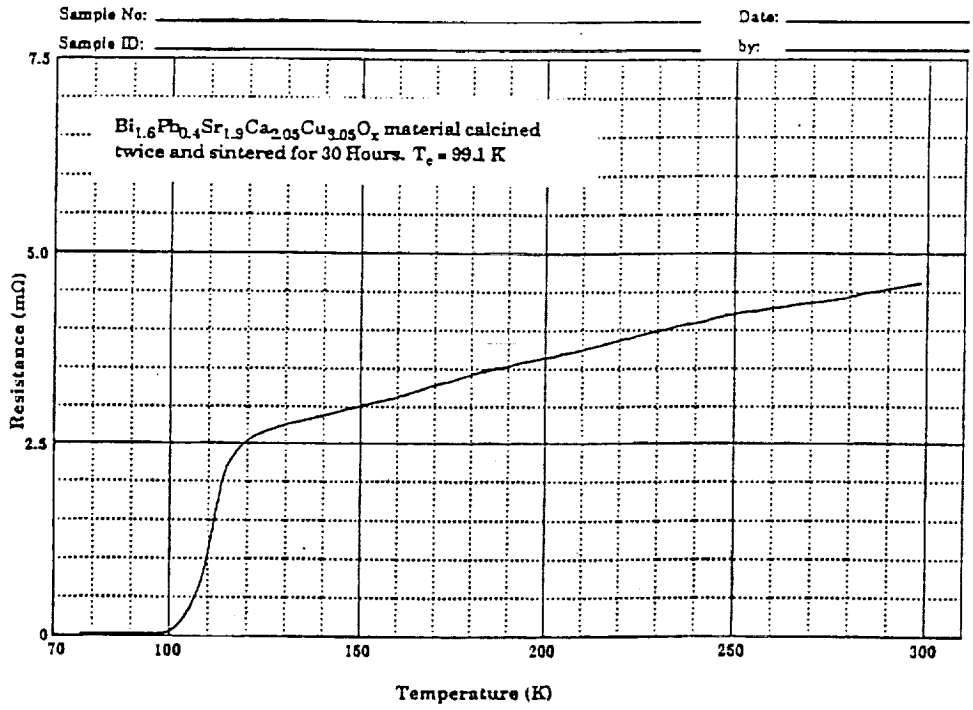

a) Uniaxially pressed pellet calcined twice. The Tc is 99.1 K

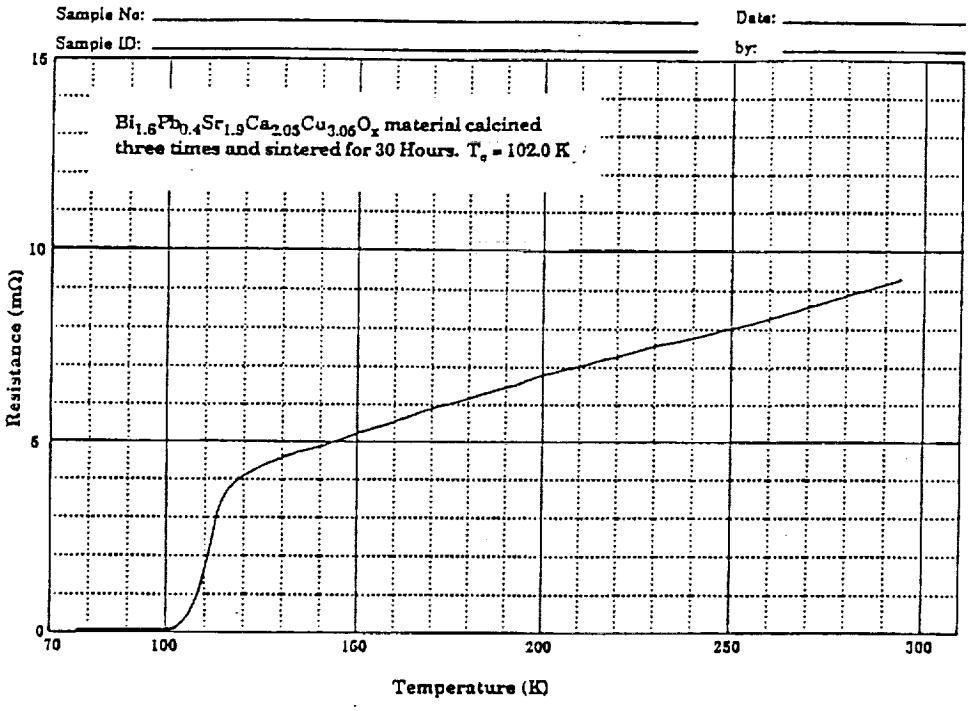

b) Uniaxially pressed pellet calcined three times. The Tc is 102.0 K

Figure 11 Resistance versus Temperature curves for a bulk samples sintered for thirty hours in air at 845 °C. They varied in number of times the material was calcined.

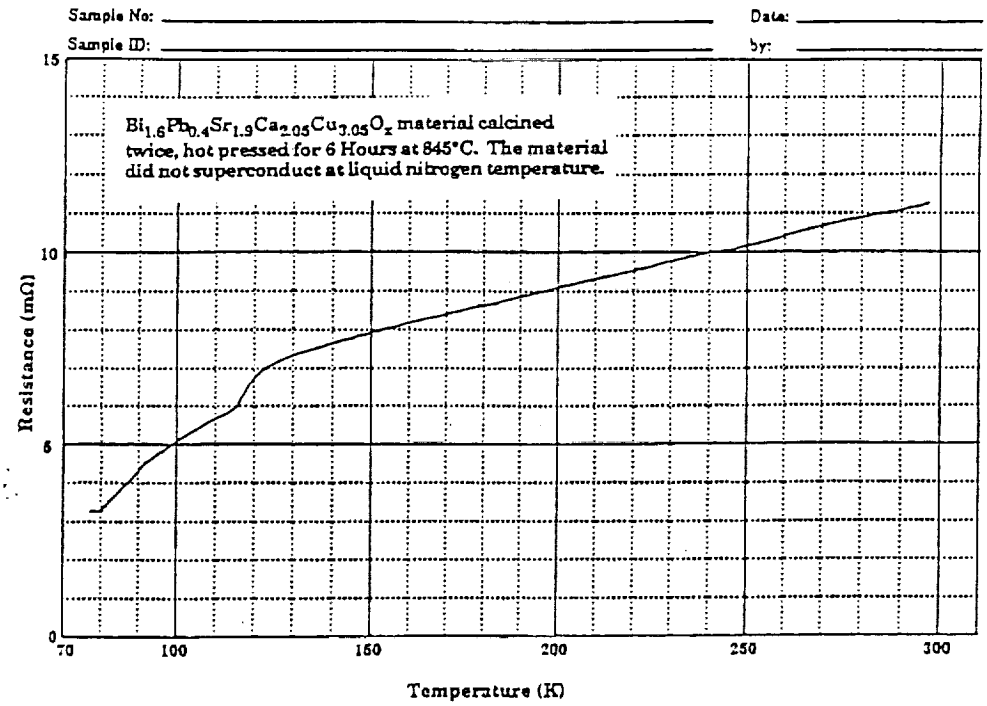

a) Hot pressed pellet with no additional heat treatment, calcined twice. The material did not superconduct.

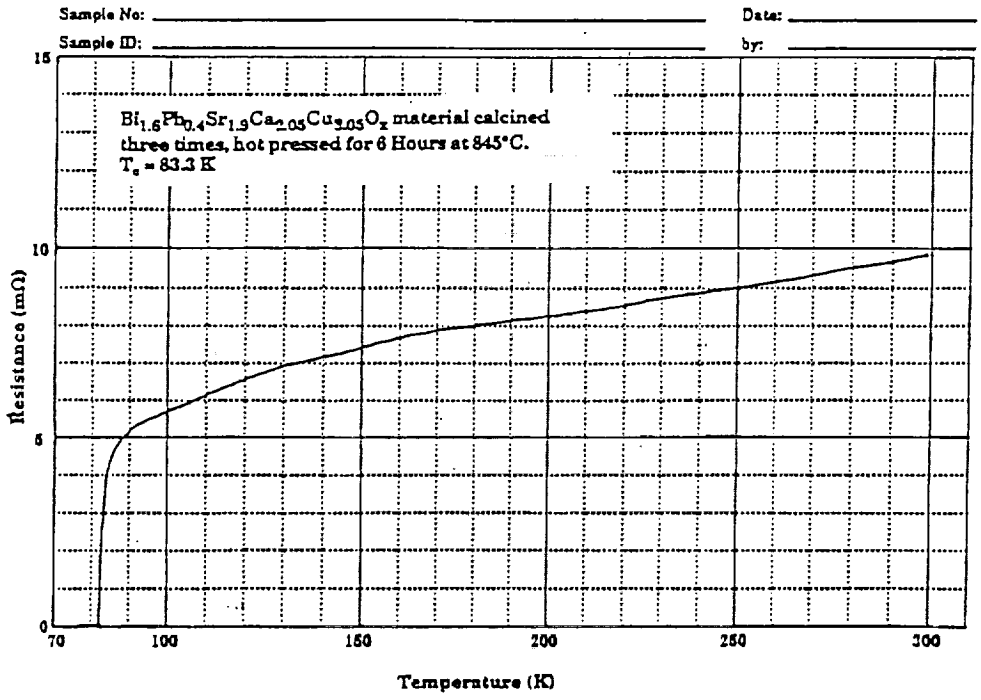

b) Hot pressed pellet with no additional heat treatment, calcined three times. The Tc was 83.3 K

Figure 12 Resistance versus Temperature curves for bulk hot pressed samples with no additional heat treatment. They varied in number of times the material was calcined.

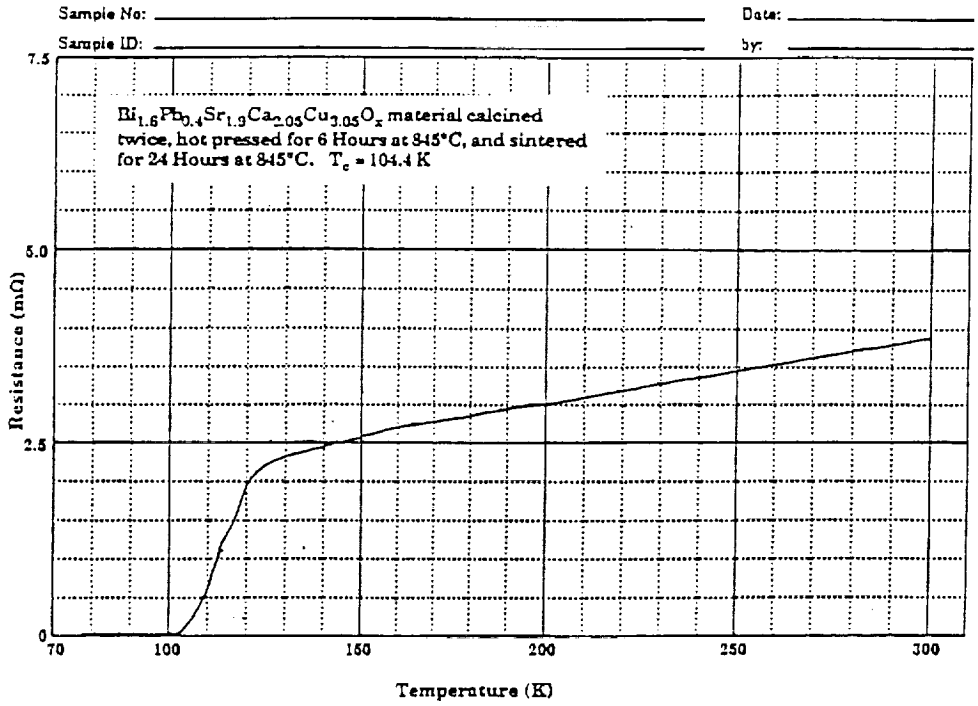

a) Hot pressed pellet with additional heat treatment calcined twice. The Tc was 104.4 K

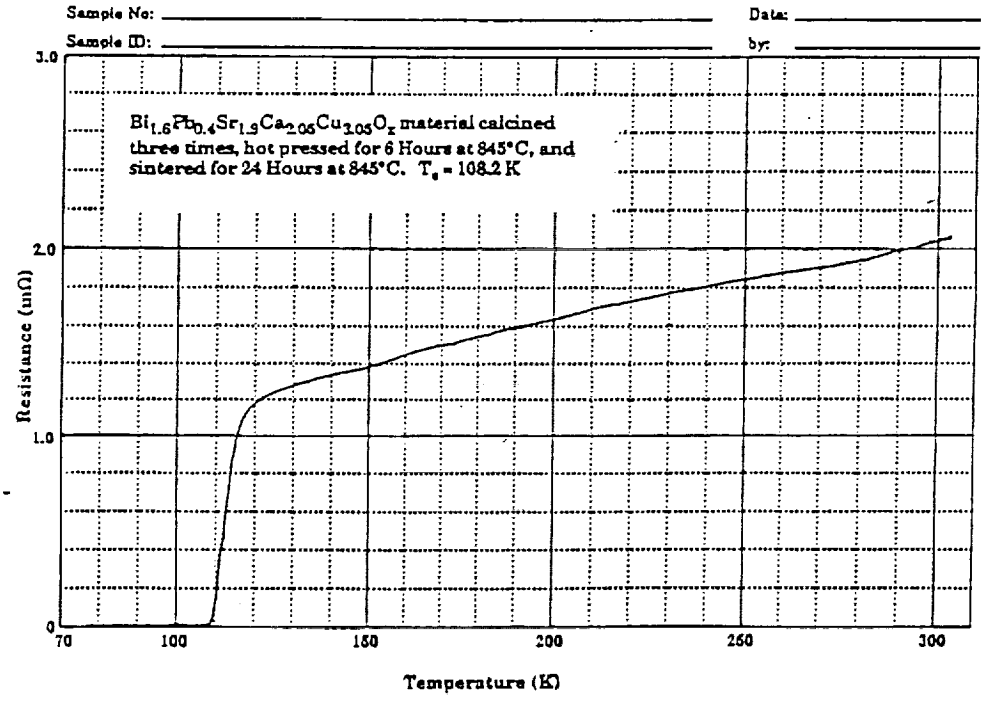

b) Hot pressed pellet with additional heat treatment calcined three times. The Tc was 108.2 K

Figure 13 Resistance versus Temperature curves for bulk hot pressed samples with twenty-four hours additional heat treatment at 845 °C. They varied in number of times the material was calcined.

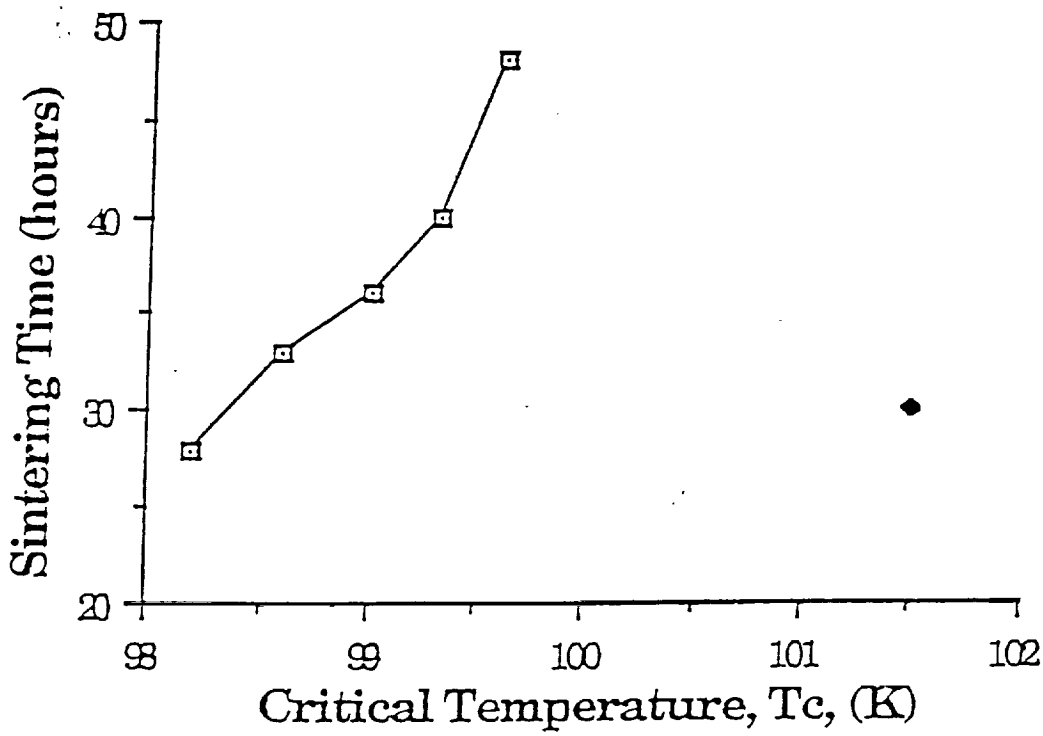

Figure 14 Sintering Time versus Critical Temperature curve for the single ramp tapecast material with a dot for the double ramp tapecast material, showing why the double ramp process is preferred.

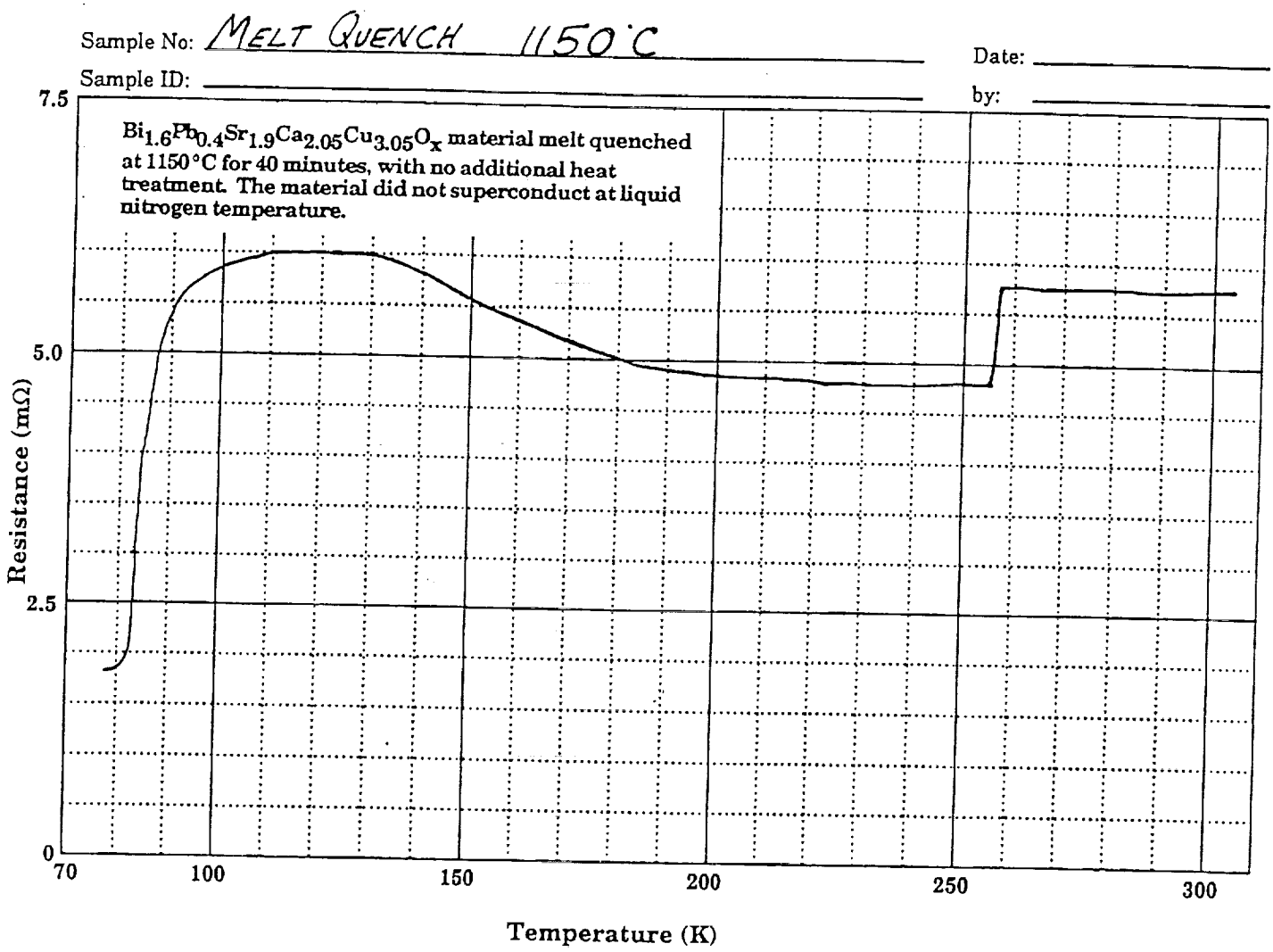

Figure 15 Resistance versus temperature curve for a melt quenched sample with no additional heat treatment. This material did not superconduct at 77.3 K.

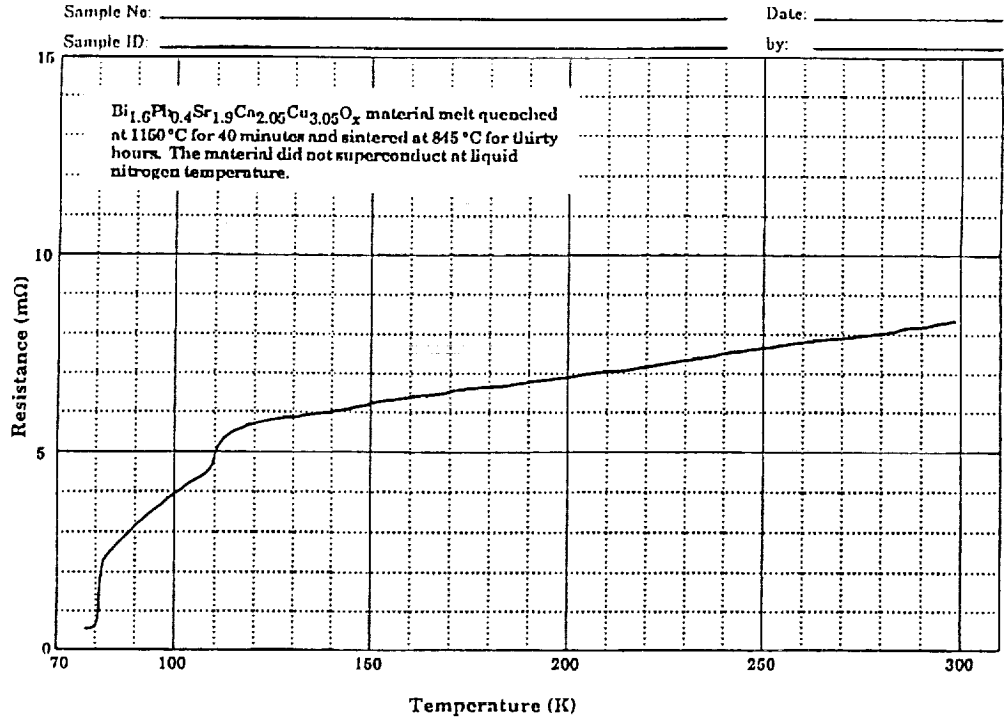

a) Melt quenched sample with thirty hours of additional heat treatment. The material did not superconduct at 77.3 K.

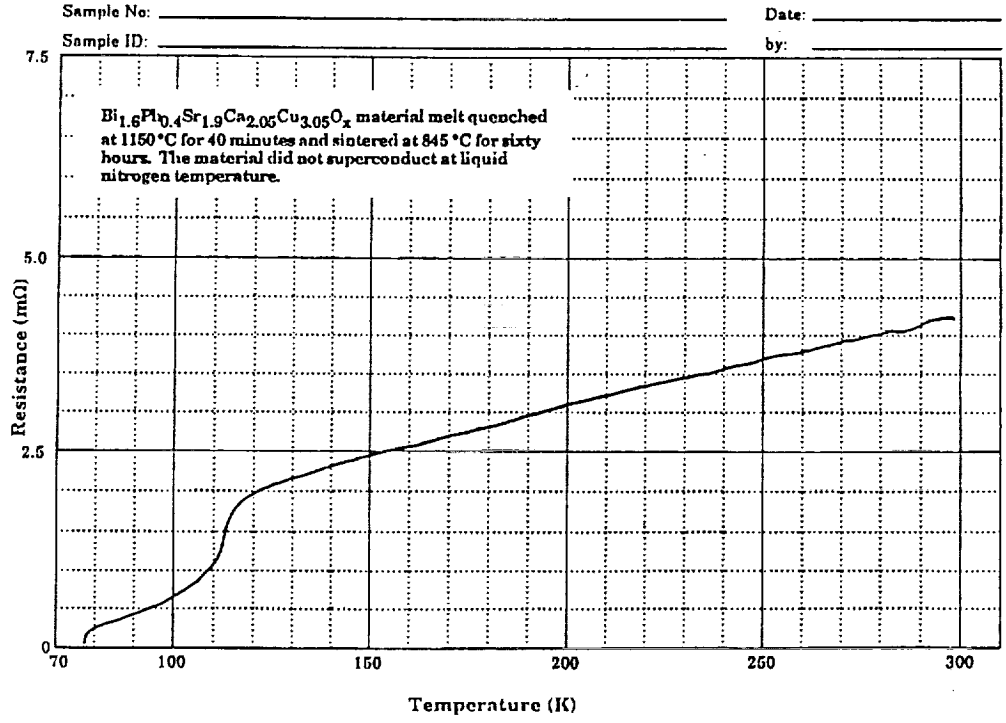

b) Melt quenched sample with sixty hours of additional heat treatment. The material did not superconduct at 77.3 K.

Figure 16 Resistance versus temperature curves for melt quenched samples with additional heat treatment. They varied in the amount of additional heat treatment time at 845 °C.

a) An area of a melt quenched sample which shows the solid melt behavior of the sample.

b) An area of a melt quenched sample which shows the porous behavior of the sample. This region appears to be exhibiting grain growth.

Figure 17 SEM micrographs for melt quenched samples with sixty hours of additional heat treatment at 845 °C in air. These micrographs show the inhomogeneities in the melt quenched material.

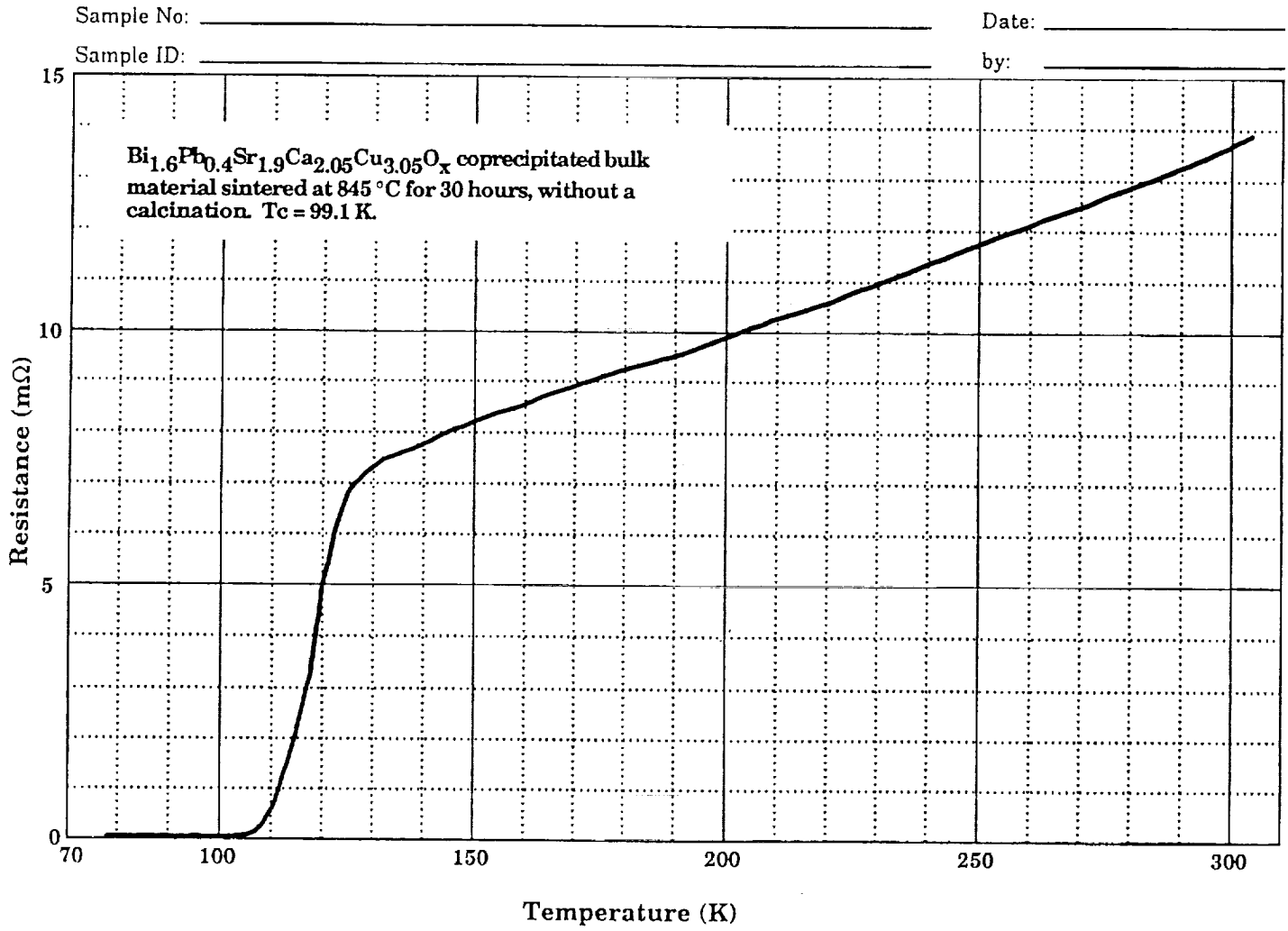

Figure 18 Resistance versus temperature curve for a bulk coprecipitated sample which was sintered, uncalcined, at 845 °C for thirty hours. T_c = 99.1 K

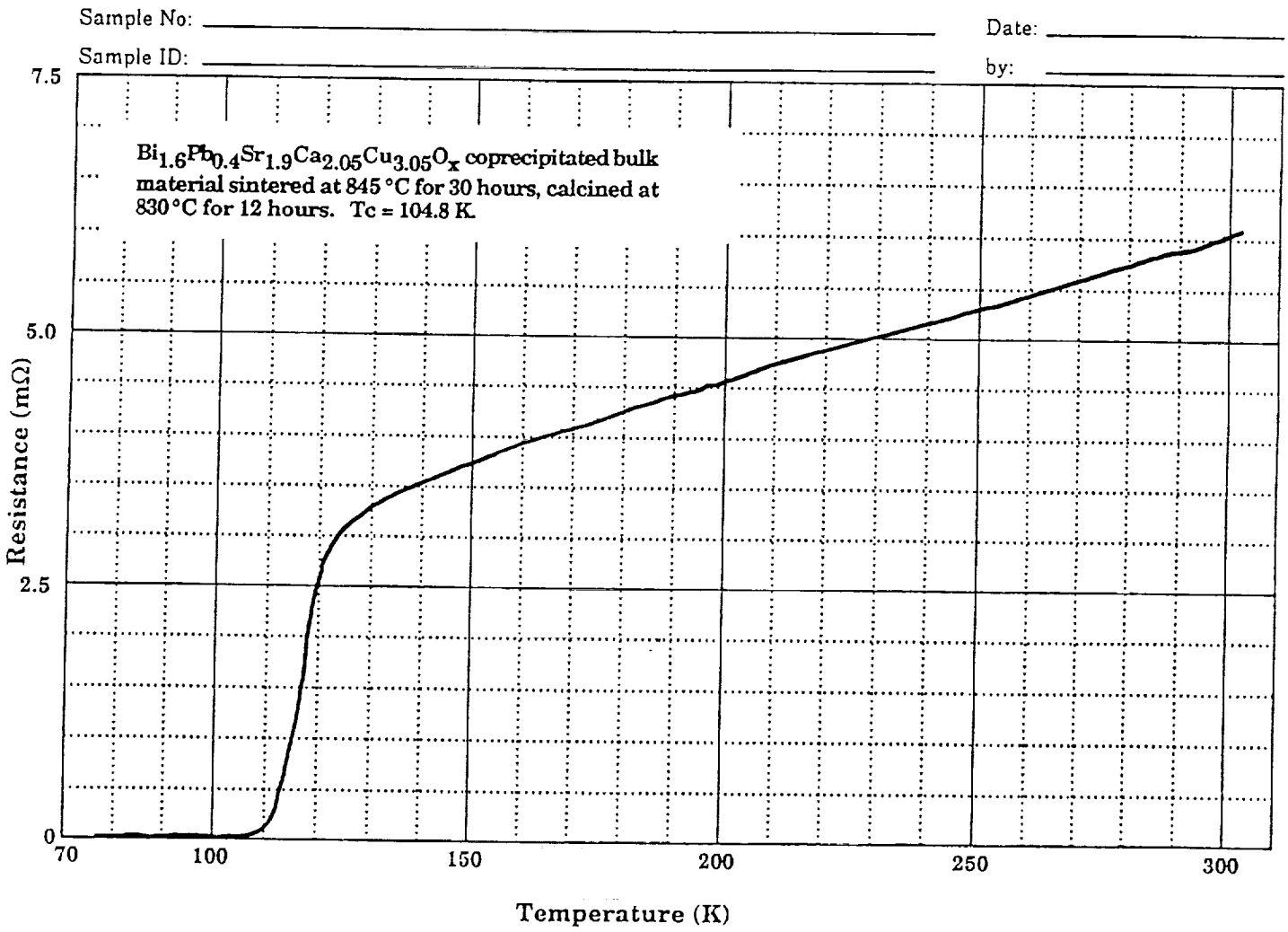

Figure 19 Resistance versus temperature curve for a bulk coprecipitated sample which was calcined at 830 °C for twelve hours and sintered at 845 °C for thirty hours. $T_c = 104.8$ K

Figure 20 SEM Micrograph for bulk coprecipitated sample which was calcined at 830 °C for twelve hours and sintered at 845 °C for thirty hours.

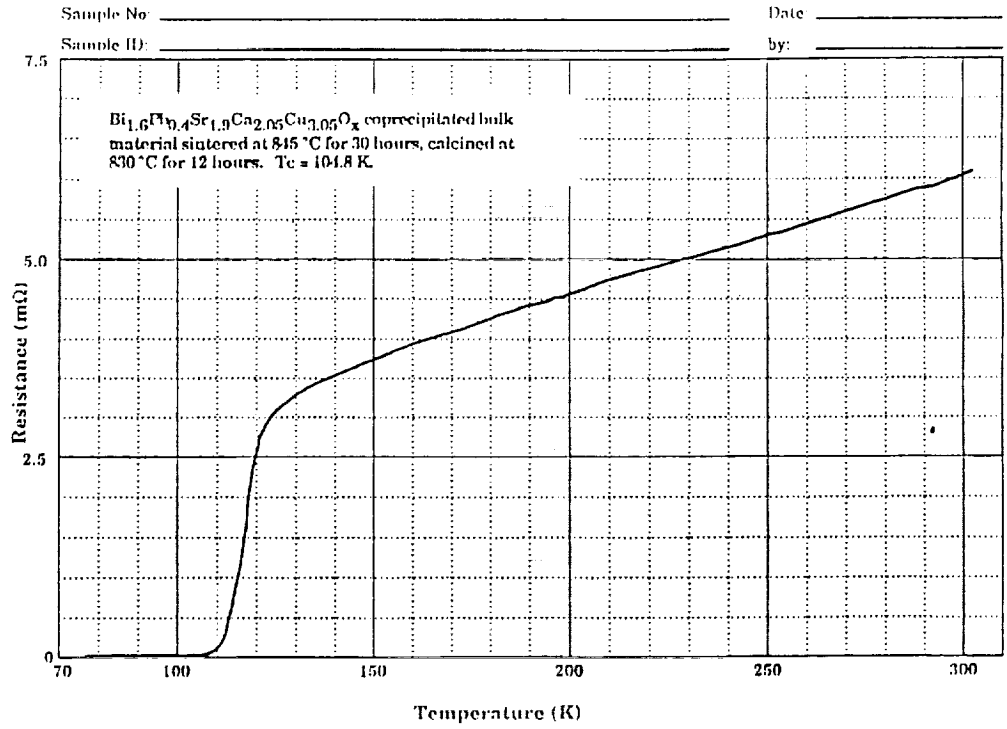

a) Coprecipitated compact which was pressed at 3200 psi. Tc = 104.8 K

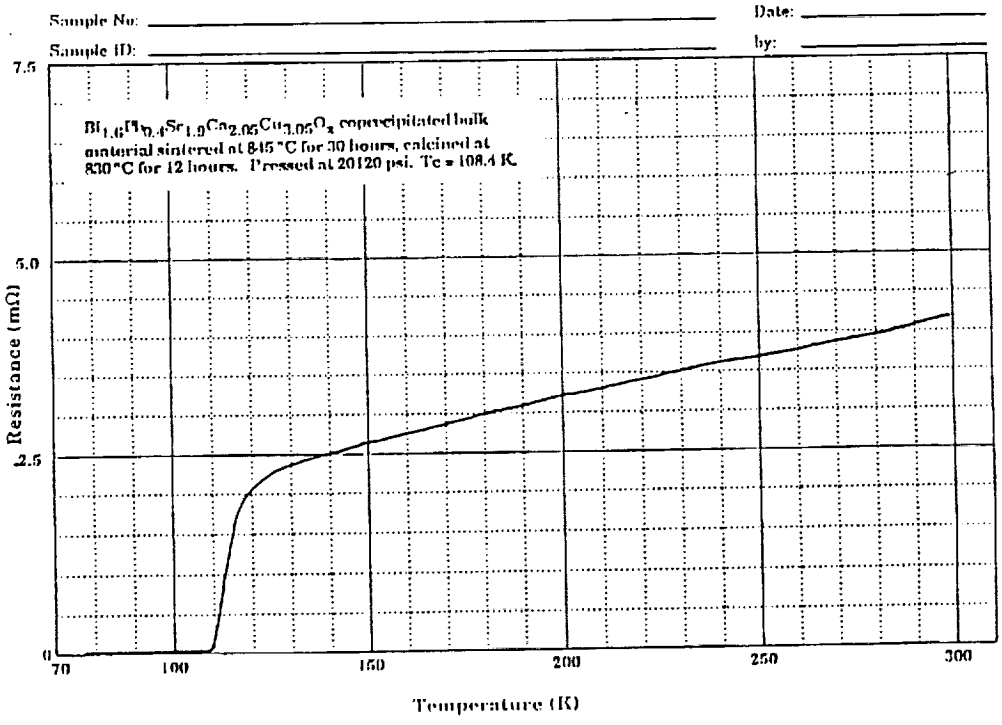

b) Coprecipitated compact which was pressed at 20120 psi. Tc = 108.4 K

Figure 21 Resistance versus temperature curves for bulk coprecipitated samples which were calcined at 830 °C for twelve hours and sintered at 845 °C for thirty hours.

a) High pressure compact at 1000 magnification.

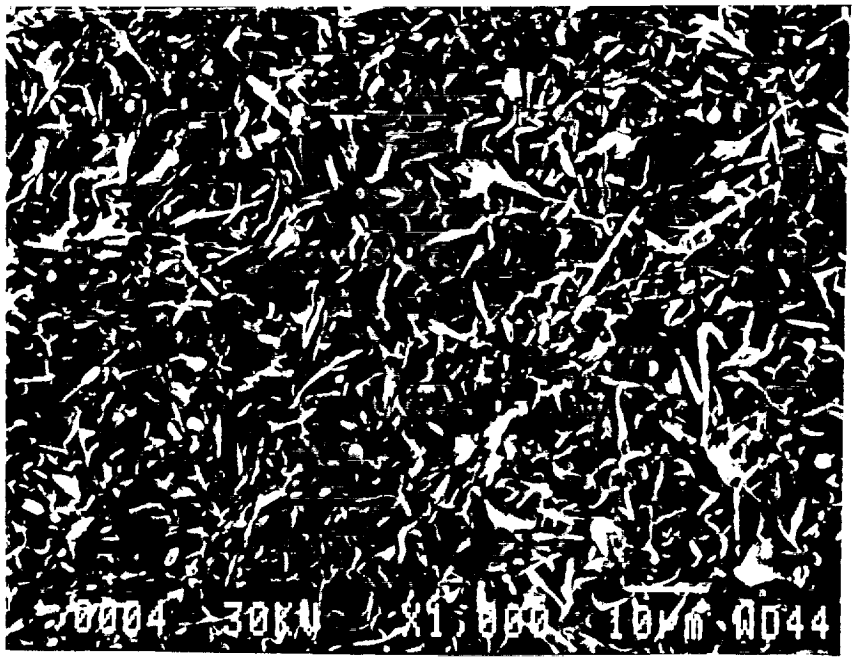

b) High pressure compact at 4000 magnification.

Figure 22 SEM micrographs of coprecipitated samples which were calcined at 830 °C for twelve hours and sintered at 845 °C for thirty hours.

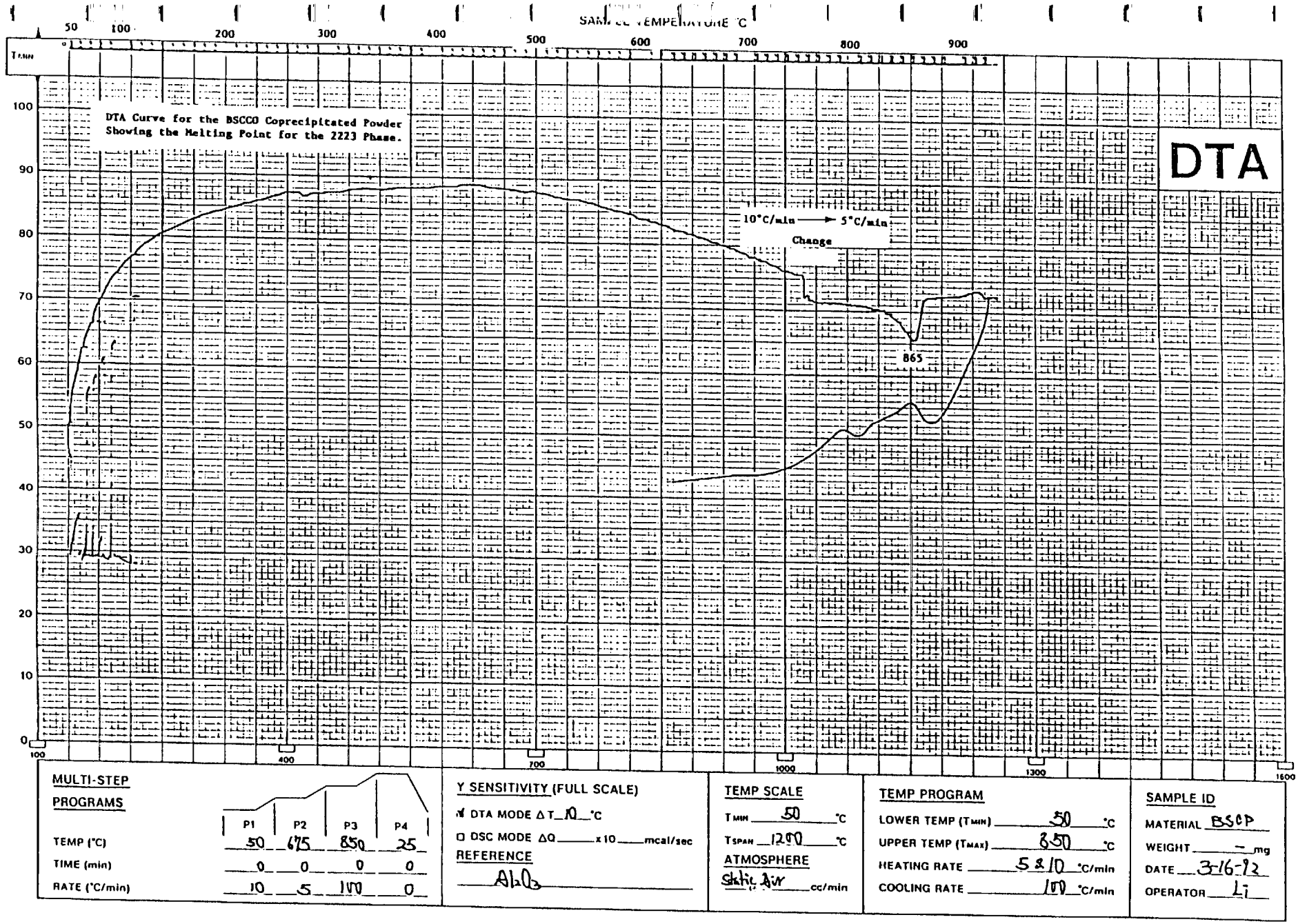

Figure 23 Differential Thermal Analysis curve for the BSCCO coprecipitated material showing the melting point of the 2223 phase at 865 °C.

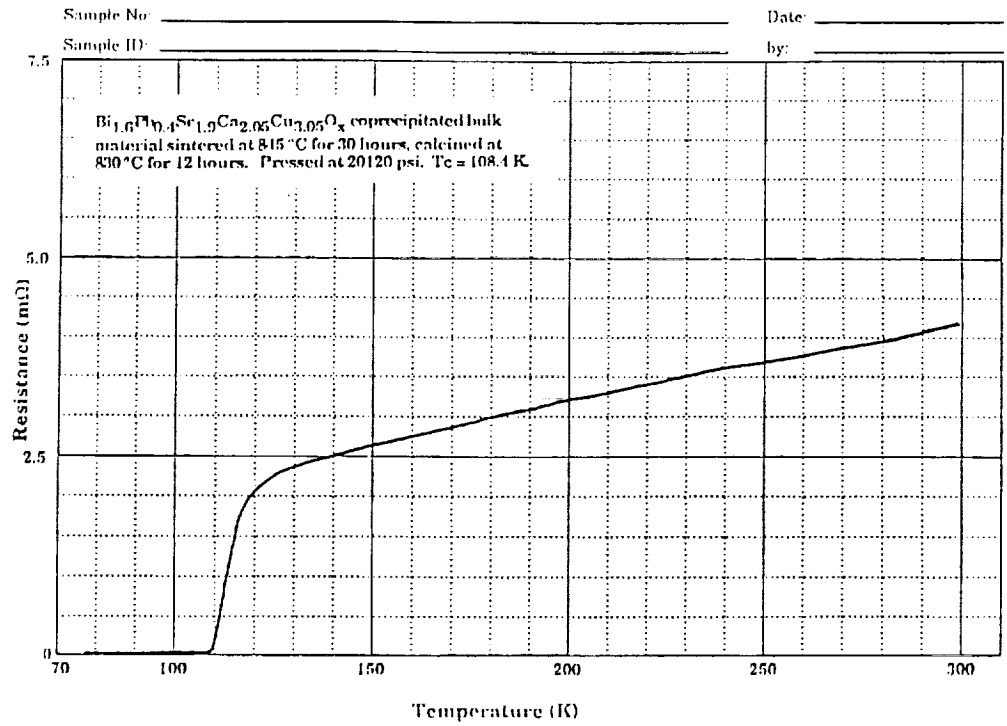

a) Coprecipitated compact which was calcined at 830 °C. Tc = 108.4 K

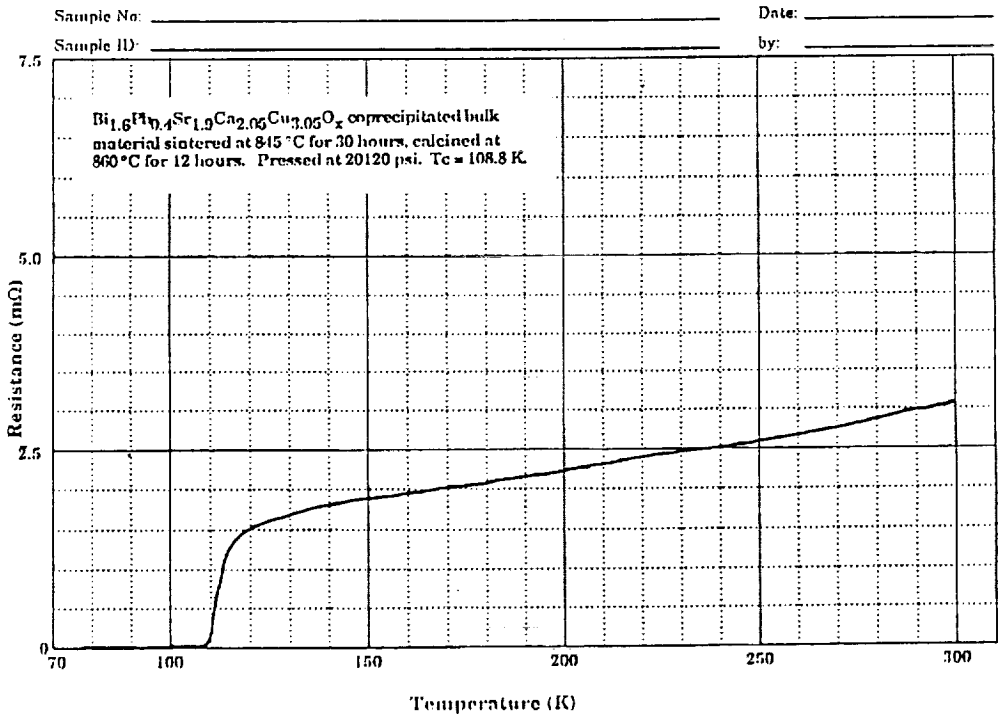

b) Coprecipitated compact which was calcined at 860 °C. Tc = 108.8 K

Figure 24 Resistance versus temperature curves for bulk coprecipitated samples which were calcined at different temperature for twelve hours and sintered at 845 °C for thirty hours.

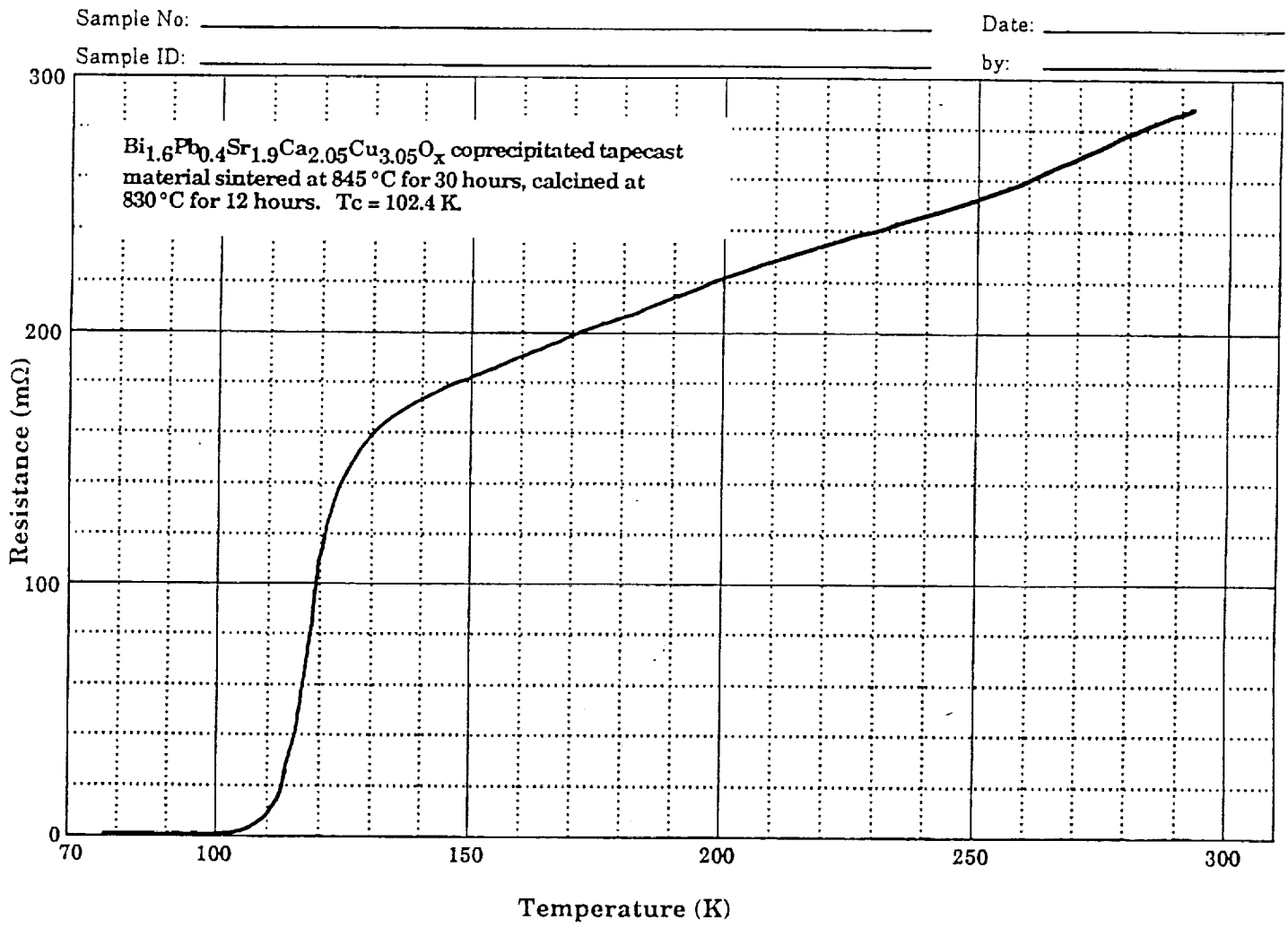

Figure 25 Resistance versus temperature curve for a tapecast coprecipitated sample which was sintered at 845 °C for thirty hours. $T_c = 102.4$ K

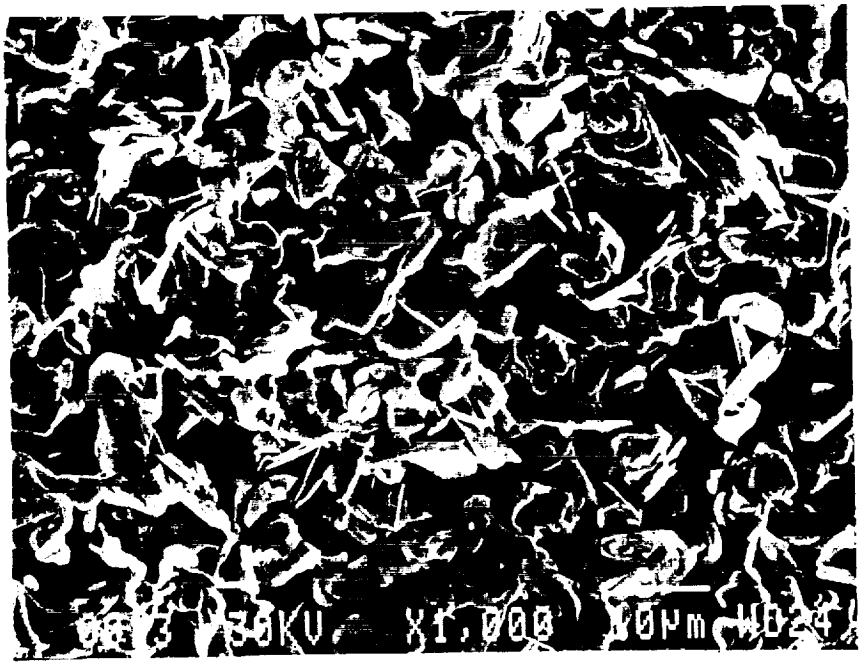

a) Tape that was prepared by the mixed oxide process.

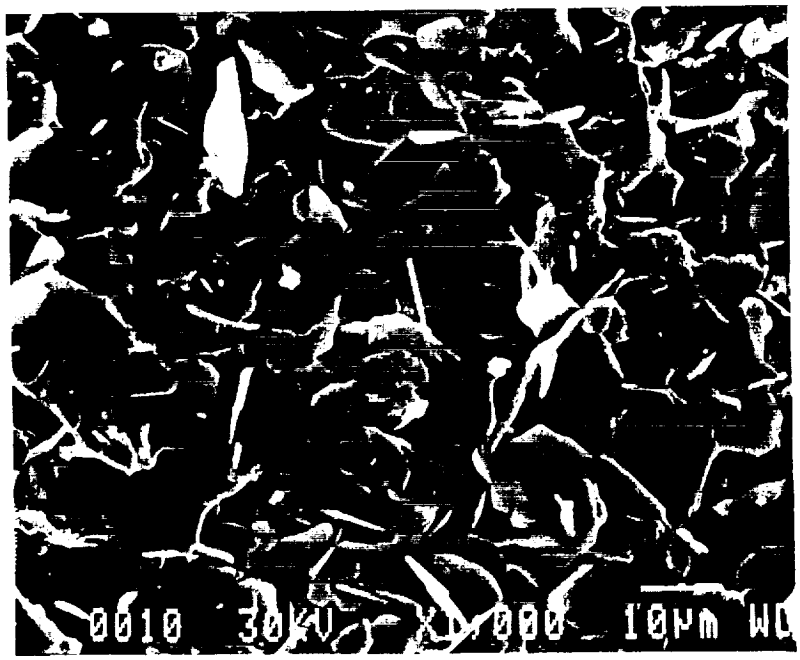

b) Tape that was prepared by the coprecipitation process.

Figure 26 SEM micrographs of tapecast samples which were sintered at 845 °C for thirty hours.

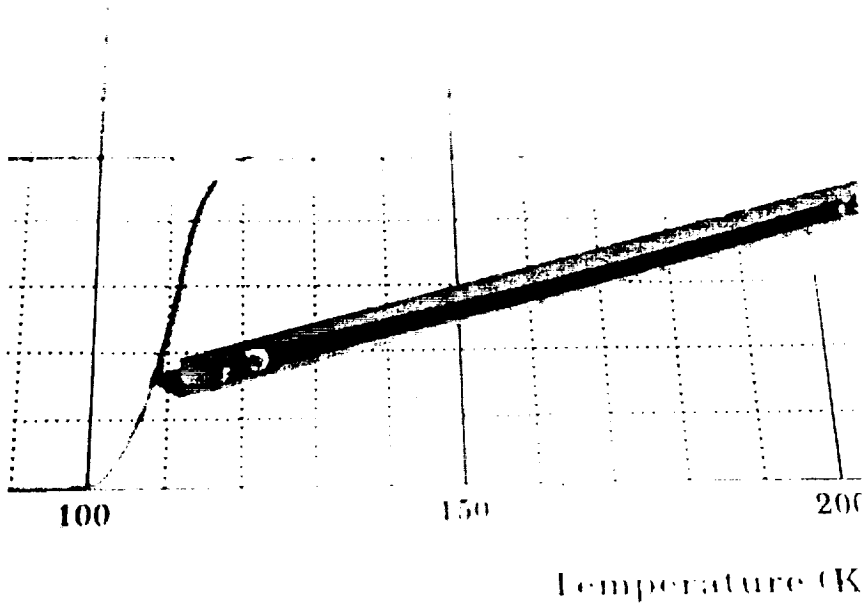

a) Superconducting grounding links were produced with bismuth-based coprecipitated tapecast material. $T_c = 100.5$ K.

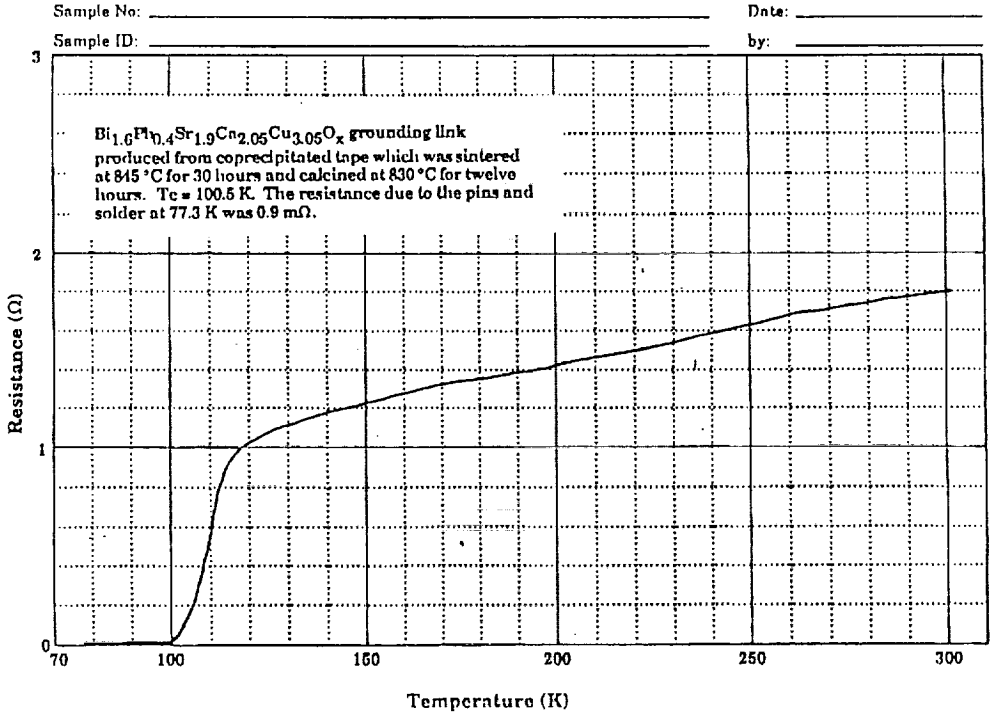

b) Resistance versus temperature curve for grounding links produced from coprecipitated tapecast material.

Figure 27 Superconducting grounding link property data.

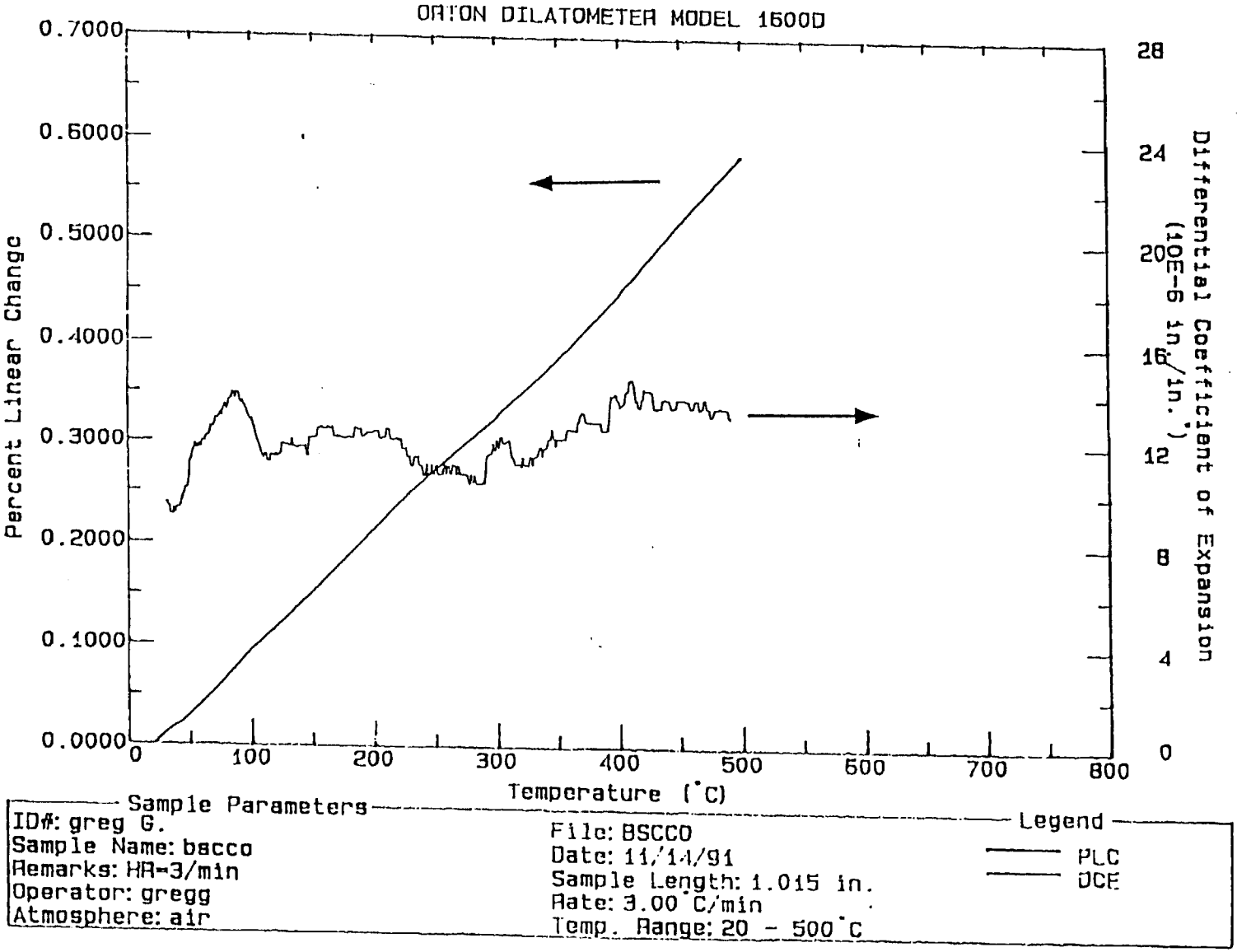

Figure 28 The thermal expansion curve of the coprecipitated bismuth-based material. The TE = 12 x 10^{-6} in/in °C

Annual Report

Part II

Development of Tl-Based Materials

submitted to

National Aeronautics and Space Administration
Langley Research Center

submitted by
Phillip Gilmour

Principal Investigator
Gene H. Haertling

Department of Ceramic Engineering
Clemson University
Contract No. NAG-1-1108
April 1992

Abstract

Work during this period has concentrated on developing thallium superconductor, tape-cast bulk materials as for grounding links for possible use in the NASA SAFIRE project. Also, continued investigations of bulk ceramics were performed in order to understand processing effects on these materials. The highest transition temperature for the bulk material was found to be 117.8K.

Manganese and lithium additions and sintering temperature and time were examined to determine influence on superconducting ceramic pellets. It was found that lithium substitutions for copper enhance transition temperatures while manganese produced deleterious effects on the superconducting properties.

Thallium superconducting tapes were fabricated via a novel thallium tape cast process. In this method a prereacted Tl-Ba-Ca-Cu-oxide material was tape-cast. Parameters such as initial particle size, sintering time and temperature, and burnout rate were found to be crucial parameters to develop a uniform superconducting tape. The highest transition temperature for Tl-tapes was measured at 110.2K--comparable to values reported in the literature. Thallium superconductor grounding links were fabricated from the tapes.

I. Introduction

Thallium-based superconductors are layered materials often described as intergrowths of perovskite and rocksalt layers. In general, with increased layering of copper oxygen planes there is a concomitant increase in transition temperature. The $Tl_2Ba_2Ca_2Cu_3O_{10}$ structure [the so called Tl-2223 phase] exhibits the highest reproducible superconducting transition temperatures to date, 120-125K.

There are several potential advantages of Tl-2223 compared to other high-temperature superconductors. Unlike $YBa_2Cu_3O_{7-\delta}$ (the 123 structure), there is no phase transition down to 1K;[2] therefore microcracking due to crystal structure changes cannot occur, although differential thermal expansion of different lattice directions could present a problem.[3] Complete phase formation of Tl-2223 is more easily attained than the bismuth analogue, $Bi_2Ca_2Cu_3O_{10}$. Also, the intrinsic critical current density, greater than $1x10^8$ A/cm^2, is believed to be at least an order of magnitude higher than the 123 system.[4]

However, there are important disadvantages of thallium superconductors; probably foremost among these are thallium toxicity and volatility. The highly volatile nature of thallium arises from the transition

$$Tl_2O_3 \text{ --> } Tl_2O + O_2 \quad 875°C.$$

Reduction of Tl_2O_3 close to sintering temperatures creates a low melting point compound. Thallous oxide also exhibits a low boiling point which creates significant thallium loss. To ameliorate this problem, oxygen sintering is often used to shift the above reaction to the left. Thallium loss is further reduced by complete encapsulation or wrapping the material in an inert metal foil. Yet, these steps usually do not yield consistent results. Loss of thallium and controlled melting to create the Tl-2223 phase presents a major problem for reliable fabrication of thallium superconductors.

Perusal of the thallium superconductor processing literature often presents a confusing and contradictory picture of how to attain the highest transition temperature and optimize the critical current density. As an example, some studies use stoichiometric mixtures of thallium, barium, calcium, and copper oxides to maximize the superconducting transition temperature.[5,6] Another study suggests reduced amounts of calcium will stabilize the highest transition temperatures;[7] while yet another investigation

shows increased calcium at the expense of thallium will yield high transition temperatures.[8] Part of the confusing state of thallium superconductor processing stems from the similar free energies of thallium layered structures; however, a large contribution to thallium superconductor fabrication variability arises from the volatility of thallium and attaining correct oxygen stoichiometry and distribution.[9,10,11]

The investigations described hereon are built upon initial studies, described in a previous annual report,[12] which studied fabrication of bulk thallium superconducting ceramics. Previous results have led to increased understanding of thallium processing and allowed the development of tape cast thallium superconductors for potential use as grounding straps in the NASA SAFIRE project.

II. Experimental Procedure

II. A Bulk Ceramic Formation from Oxide Precursors

To create bulk superconductors in this study, one method utilized mixed oxide precursors, BaO_2, CaO, and CuO, and calcined these at 925°C for 24 hours to form the low melting point compound $Ba_2Ca_2Cu_3O_7$. Sheng and Hermann[13] developed this technique to aid densification by liquid phase sintering. Prior to sintering, thallic oxide was mixed with the precursor to attain the nominal composition $Tl_2Ba_2Ca_2Cu_3O_{10}$.

The general ceramic processing scheme is shown in Figure 1. Stoichiometric amounts of the initial oxides were thoroughly mixed in a porcelain mortar and pestle. If the precursors were calcined, the powders were placed on an alumina setter and heated with the furnace to 925°C. After calcining for 8 hours, the material was allowed to cool with the furnace. The calcined material was ground and passed through a 100 mesh sieve. This process was performed three times for a total calcination time of 24 hours.

After the calcination step, Tl_2O_3 was added to the calcined material in stoichiometric proportions. (To reduce thallium loss, thallic oxide is usually added prior to sintering and not in the calcination step.) Green pellets, 13mm diameter by 3 mm thick, were formed by pressing 1.5g of material at a pressure of $2.7x10^3 Kg/cm^2$ ($1.3x10^4$ psi).

The green pellets were wrapped in silver foil and fast-fired in flowing oxygen. Oxygen was fed into the furnace to reduce thallium volatility. After the specified soak time, pellets were taken out of the furnace and air-quenched to room temperature.

Pellets were electroded by firing with silver paste at 600°C for 20 minutes and cooled with the furnace. Due to the low temperature (and consequently low thallium volatility), pellets were not wrapped in silver foil.

II. B Bulk Ceramic Formation from Coprecipitated Powders

In some studies precursor powders were synthesized through the oxalate coprecipitation technique. Figure 2 shows a schematic of the oxalate coprecipitation route for thallium superconductors. A few comments should be made on the processing steps. Thallium nitrate was not used since it is a relatively expensive compound and more toxic than

thallium oxide. Therefore, a precursor made from barium, calcium, and copper nitrates was coprecipitated, calcined, and then mixed with thallium oxide before the final sintering step. Oxalic acid was added to slightly warmed methanol to facilitate the dissolution process. The number of moles of oxalic acid added was 150% of the moles of metal ions in solution. If a molar equivalent of oxalic acid and metal ions were added, segregated regions of blue and white crystals appeared in the powder after drying; whereas, excess oxalic acid created a uniform mixture.

Calcination of coprecipitated powders were subjected to the same conditions as oxide precursors. Also, sintering was performed with the same heating schedule as the oxide precursor conditions described above.

II. C Ceramic Tape Formation

Ceramic superconducting tapes were formed by employing the same processing steps used to make Tl-superconductors by the oxide route. After forming the superconducting phase, the powder was passed through 400 mesh, mixed with a 30 weight percent total weight percent binder concentration. After defoaming the slurry, a 50 mil tape was cast with a single edge doctor-blade and allowed to dry. Tapes were cut and placed on a zirconia setter plate with the ends pinned down. Binder burnout was performed in an oxygen atmosphere with a final soak of 550°C for 90 minutes.

To contain thallium vapors during sintering, tapes were carefully wrapped in silver foil and sintered. Particulars of sintering schedules as well as binder burnout are discussed in the results section.

III. Results and Discussion

III A. Lithium Additions

In the previous annual report,[12] small amounts of lithium appeared to increase the superconducting transition temperatures of thallium superconductors in a pelletized form. More data is included in this report which supports this conclusion. Synthesis of superconductors containing lithium was accomplished via the mixed oxide process. Equimolar substitutions of lithium for copper were made by substituting Li_2O for CuO in the initial batching.

Figure 3 shows the change in superconducting transition temperature with increased lithium oxide additions for pellets sintered at 890°C for 30 minutes (pellets were batched to the nominal composition $Tl_2Ba_2Ca_2Cu_3O_{10}$). A maximum transition temperature of 108.3K occurs for 6.7 mole percent lithium substitution for copper, corresponding to the formula $Tl_2Ba_2Ca_2Cu_{2.8}Li_{0.2}O_{10}$. Higher lithium concentrations reduce the transition temperature. While it was hoped lithium would act as a flux and lower the sintering temperature, thereby reducing thallium volatility, results from the previous study suggest temperatures above 880°C must be attained to produce appreciable amounts of the Tl-2223 phase. However, lithium could be added in small amounts to slightly improve the superconducting transition temperature.

III.B Manganese Additions

In an attempt to further improve upon the processing procedure and superconducting properties of thallium superconductors--with the ultimate objective of developing a reliable process for fabricating good quality Tl-superconductor tapes--manganese substitutions for copper were investigated. It was hoped that manganese would increase oxygen diffusivity while sintering, yielding improved superconductor properties.

It is well-known in the capacitor industry that small additions of manganese to perovskite-based capacitor compositions can enhance densification and dramatically increase resistivity.[14,15,16] A complete understanding of the mechanism by which manganese accomplishes this effect is not yet known. Since manganese ions can easily undergo redox reactions, a partial explanation may be due to enhanced anion diffusivity stemming from

the ease in which manganese can change its oxidation state to accomodate oxygen/oxygen vacancy diffusion in the lattice while sintering.[17]

Optimizing anion distribution in the perovskite sublattice is critical in attaining good electrical properties for high temperature superconductors; this similarity suggests manganese substitutions for copper could improve superconducting properties. Previous papers found manganese substitutions for copper do not degrade or only slightly degrade the transition temperature.[18,19] However, manganese/copper substitutions in these studies were an order-of-magnitude higher than typical manganese/transition metal substitutions used in the capacitor industry.

Superconducting ceramic pellets containing manganese substitutions for copper were processed by the same procedure as lithium substituted superconductors. Substitutions of manganese, in the form of MnO_2, were added in concentrations of 0, 0.47, 0.93 and 1.87 mole percent of copper in the formula $Tl_2Ba_2Ca_2Cu_3O_{10}$. Figure 4 shows the dependence of the superconducting transition temperature on manganese concentration. These pellets, which were sintered at 885°C for 30 minutes, show a decrease in transition temperature with increasing manganese concentration. Similarly, Figure 5 shows pellets fired at 885°C for 120 minutes exhibit a decrease in transition temperature with increasing manganese substitutions. Hence, it appears manganese produces a deleterious effect on the transition temperature under the conditions investigated.

III.C Coprecipitation

Coprecipitation routes for superconductor synthesis has achieved much attention. Coprecipitation often yields a finer, more homogeneous powder which consequently yields improve superconducting properties. Energy dispersive x-ray analysis coupled with scanning electron photomicrographs, shown in Figure 6, show elemental distribution of a Tl-superconductor pellet is relatively uniform within the superconducting grains (shown as "blocky"grains); however, a small amount of copper segregation occurs outside of these grains. Also, inhomogeneities also occur, to a smaller extent, for barium and calcium. Coprecipitation was examined to determine if homogeneity can be improved in ceramic pellets.

Resistance as a function of temperature curves for coprecipitated thallium superconductor ceramic pellets for various soak times at 893°C are shown in Figure 7. All pellets did not show any traces of superconductivity. The result seemed surprising in light of the large number of studies which have shown coprecipited techniques to improve the final superconducting properties. Energy dispersive x-ray analysis and scanning electron micrographs of the surface of coprecipitated thallium-superconductor pellets is shown in Figure 8. The reason for nonzero resistance is evident upon examination of the figure: the surface growth is almost entirely composed of thallium. (A small region of copper is shown in the hole below the growth. Barium and calcium rich regions were also evident underneath Tl-needle growths in regions not pictured.) Apparently, encapsulation of pellets made via the coprecipitation route allows thallium to easily escape from the sample. A possible reason for the ease of thallium escaping is because coprecipitation often yields more homogeneous and finer grains. This may create a more reactive powder which would require a lower sintering temperature to prevent thallium from leaving. A future study to examine sintering temperature on coprecipitated thallium powders will be done.

III.D High Temperature Sintering of Superconductor Tapes

There is a paucity of fabrication techniques used to create $Tl_2Ba_2Ca_2Cu_3O_{10}$ or $Tl_2Ba_2CaCu_2O_8$ tapes. Previous investigations in the literature attempt to develop thallium superconductor tapes by placing a $Ba_2Ca_2Cu_3O_7$ precursor tape and Tl_2O_3 powder (or a mixture of Tl/Ba/Ca/Cu oxides) in a hermetically sealed container.[20,21] Upon heating above 720°C, thallium oxide gasifies and diffuses into the percursor while the sealed container prevents thallium from seeping into the outside environment. Sheng and Hermann developed this method to reduce thallium volatility and toxicity in a laboratory or industrial environment. Typical transition temperatures of tapes range from 100-115K. Sheng and Hermann noted there is a large variability of the transition temperature. This could be attributed to the resulting inhomogeneity which arises from thallium diffusion into the precursor material or to the sensitivity of thallium superconducting compounds to processing conditions.

A different tape fabrication approach was undertaken in this research. Instead of thallium diffusing into the precursor, it was believed a solid state

reaction of thallium with other precursors during sintering may lead to greater tape homogeneity and possibly improved properties and reproducibility.

Binder burnoff rate had a considerable influence on tape uniformity, presumably because of thallium/binder interactions. As stated in the experimental procedure, tapes were burned off at 550°C. A TGA profile, shown in Figure 9, shows a long, smooth burnoff starting at 150°C until 550°C, where virtually all of the binder has vaporized. A previous study found thallium/binder interactions occur during burnout.[12] If the binder burn out rate is too rapid, approximately 3°C/min or greater, tapes were relatively strong but were distorted, bubbled, bowed, and nonuniform in color. Large density variations in the 12°C/min burn out tape are evident upon examination of the SEM photomicrographs displayed in Figure 10; whereas, the tape ramped at 2°C/min is relatively uniform. Presumably the density variation of rapidly burned out tapes is due to a highly exothermic thallium/binder reaction. Portions of the tape became red-hot during the reaction even though the furnace atmosphere was at 350°C.

It was thought that reducing the amount of binder would result in less thallium loss and consequently improve tape quality. However, lowering binder concentration from 35 to 28 weight percent (the lowest binder concentration which allows a tape to be cast) produced no significant improvement of tape quality.

Tapes maintained their strength when the burnoff rate was reduced from 12°C/min to 3°C/min However, tapes burned off at 3°C/min were still slightly distorted, bubbled, and showed color nonuniformity. Reducing the burnoff rate to 2°C/min yielded tapes which were completely free from distortion and were uniformly black, yet these tapes were more fragile than tapes burned off at 3°C/min. Figure 11 shows a resistance versus temperature curve for a tape with a binder burnoff rate of 5°C/min and one of 3°C/min. The tape with a slower burnoff rate exhibited transition temperature of 100K while the tape with a rapid burnoff did not superconduct .

Tapes which were presintered at 840°C and had a relatively coarse grain size before sintering (powder passed through 60 mesh before adding binder) did not exhibit zero resistance down to liquid nitrogen temperature (approximately 77K), as seen in Figure 12. In fact, sintering for only 30 minutes produced semiconducting behavior throughout the temperature range studied. As

evident in Figure 13, tapes which had finer grain size before sintering (powder passed through 400 mesh before adding binder) displayed significantly better properties: transition temperatures rose from nonsuperconducting at liquid nitrogen temperatures to 97.3K for 120 minute soak time. Microstructure of tapes fired at 890°C for 30 minutes is shown in Figure 14. The tape of the powder which was passed through 400 mesh shows a much finer, more uniform microstructure than the tape which had powder passed through 60 mesh.

Presintering at 890°C showed a similar dependence on grain size. Figures 15 and 16 show that tapes with smaller initial grain size yielded higher transition temperatures. The smallest grain size tape with the longest soak time resulted in a transition temperature of 106.5K. The SEM photomicrograph shown in Figure 17 shows microstructure found in the 106.5K sample consists of long rectangular grains. This is indicative of the presence of the Tl-2212 phase in the sample--for reference, a more acicular morphology is indicative of the higher transition Tl-2223 phase.

III.E Low Sintering Temperature of Superconducting Tapes

Many studies have found it is desirable to add small amounts of silver or silver oxide to the $YBa_2Cu_3O_{7-\delta}$ and Bi-Sr-Ca-Cu-O superconducting systems because silver does not react with the superconductor[22] but drastically reduces sintering temperature,[23] enhances resistance to chemical degradation,[23] and increases critical current densities.[24,25] Some of these improvements stem from easy oxygen diffusion in silver and silver oxide[26,27,28] Because of this effect, tapes were wrapped in thin silver foil, rather than expensive and commonly used gold foil before sintering (silver foil allows oxygen to permeate to the tape from the oxygen rich furnace atmosphere while containing thallium vapors). However unlike other high temperature superconductor systems, silver reacts with thallium superconductors close to the "normal" sintering temperature range of 870-920°C and drastically reduces the superconducting transition temperature. Therefore, it was not surprising that Tl-tapes wrapped in silver foil envelopes often adhered to the foil and areas of the tapes were found to be nonsuperconducting.

In order to circumvent the difficulties associated with silver-thallium reactivity, a low temperature, long soak sintering schedule was examined. While the schedule is uncommon, a previous study has found partial melting of

the ceramic upon sintering is not needed to form appreciable amounts of the high temperature $Tl_2Ba_2Ca_2Cu_3O_{10}$ phase if sintered at 720-800°C for 24 hours.[29] It was believed sintering at low temperatures could enhance reproducibility (since partial melting and substantial thallium loss would no occur) while allowing the less expensive silver wrap to be used.

Figure 18 shows transition temperature curves for thallium tapes fired at 745°C for times between 12 to 48 hours. It is evident that an increase in soak time increases transition temperatures. Figures 19 and 20 show a similar trend for sintering temperatures of 760°C and 775°C. Also, increasing the sintering temperature increases the superconducting transition temperature. However when sintered at 800°C, transition temperatures decreased with increasing soak time, as illustrated in Figure 21. The relationship of longer soak time enhancing transition temperature and an optimized sintering temperature is in accordance with the previously cited study of low temperature thallium superconductor sintering, except the optimized temperature was found to be close to 775°C instead of 760°C in the other study. The highest transition temperature found for tapes sintered at low temperatures was 101K.

It is interesting to note the difference in properties of tapes burned out at 2°C/min and 3°C/min. Figure 22 shows the transition temperature of tapes burned at 2°C/min and 3°C/min when processed at 775°C and a 48 hour soaks. In the figure, the transition of the 3°C/min tape has a significantly higher transition temperature. The highest superconducting transition temperature of a tape was found to be approximately 110K for a 3°C/min burned out tape. To compare the best results to date of a Tl-superconducting tape to a ceramic pellet, a transition temperature curve of a bulk pellet, T_c=117.8K, is illustrated in Figure 23. It is typical for thallium superconducting pellets to exhibit much higher transition temperatures than tapes. Therefore it should not be surprising tape transition temperatures are more than 10°C below ceramic pellet transitions. In fact, transition temperatures of tape cast superconductors found in this study are comparable to the transition temperatures reported in the literature.[6,21]

Slowly burned off tapes were extremely fragile compared to tapes burned out at 3°C/min. Density measurements showed tapes processed under a slow burn out rate had a low density of 3.42 g/cm^3 (determined by Archimedes method); while quickly burned out tapes had densities of 4.03g/cm^3. Tape

densities probably became higher during the red-hot heating of an exothermic reaction during rapid binder burnoff.[12] Since sintering of the tapes was done at a much lower temperature than the melting point, ceramic consolidation is not as effective when sintered at 775°C and tapes do not acquire much strength. Another, important consideration is the quickly burned out tapes probably had less thallium than slowly burned off tapes due volatilization of thallium during the exothermic reaction. Some studies of bulk materials have found that a greater amount of $Tl_2Ba_2Ca_2Cu_3O_{10}$ can be formed when batched to a deficient thallium concentration.[8] It is uncertain if increased transition temperatures will occur in tapes batched with deficient thallium concentrations. A future study will examine thallium concentration effects.

Critical current densities, at liquid nitrogen temperatures, are very low for slowly burned off tapes. Depending on the cooling rate to liquid nitrogen temperature, the critical current densities varied from 0.35A/cm^2 to 1.2A/cm^2, for rapidly and slowly cooled tapes. A variety of factors influence J_c of a sample. However, the fragility of the tapes and the microcracking which occurs upon cooling the sample (indicated by an audible click of the sample and an accompanying change in resistance) suggest poor grain connectivity and superconductor/silver electrical contact integrity. Contacts can be easily pulled from the samples especially after taking a temperature/resistance measurements. Thallium volatility or reactions between thallium and silver/glass frit in the conductive paste could give rise to poor contacts. An assortment of conductive pastes, from a gold paste to high-and low-temperature silver pastes and mixtures of the two, were applied. It appears the best contacts occur with a low-fire silver paste, cured at 550°C for 10 minutes. However, these contacts are still not adequate. It is believed further improvements in contacts and a change in the sintering schedule will be needed to obtain satisfactory critical current densities.

III.F. Thallium Superconductor Grounding Link Fabrication

Thallium tapes were encapsulated in a resin binder similar to the method of Haertling, Buckley, and Hsi.[30] It is known that thermal expansion of 123, Bi-, and Tl-superconductors exhibit similar thermal expansion, approximately $7x10^{-6}K^{-}$ as determined by x-ray diffraction.[31] It was anticipated that since 123 and Tl-superconductors exhibit similar thermal expansion, fabrication of Tl-

superconductor grounding straps could be accomplished by the same method of encapsulation. In addition, the low thermal expansion of the tapes relative to thermal expansion of the resin, approximately $50x10^{-6}K^{-}$, would create a compressive stress on the tapes resulting in enhanced structural integrity and mechanical shock resistance.[30]

Since the tapes were fragile and were easily broken, a great deal of care was taken when removing the tapes from the silver encapsulation and soldering the contacts to connecting pins. However once encapsulated, the superconducting straps seemed to show greatly improved structural integrity. A encapsulated grounding link is pictured in Figure 24. To date, finished grounding links with lengths up to 3.5 inches have been fabricated.

Figure 25 shows two superconducting transition curves for thallium parts. As expected the transition temperatures, about 95K, were slightly lower than 'bare' tapes due to a temperature gradient in the grounding link when the measurement was taken.

IV. Summary

IV. A Bulk Ceramic Studies

•Below 6.7 mole percent substitutions, lithium oxide enhanced the superconducting transition temperature.

•Manganese substitutions for copper reduced the transitition temperature for all manganese concentration investigated.

•Coprecipitation produced nonsuperconducting pellets under the sintering conditions studied. Lower sintering temperatures will be studied in the future.

•In this study, the highest superconducting transition temperature of a bulk ceramic was found to be 117.8K.

IV. B Thallium Tapes

Tape cast superconducting thallium tapes have been made by a solid state reaction technique. Most of the critical processing influences which affect the superconducting properties are related to thallium reactivity and volatility and are listed below.

•A prereaction step is needed to form appreciable amounts of the superconducting phase prior to tape casting. Failure to react thallic oxide to form a more stable phase with respect to elevated temperatures will cause thallium to leave the system during binder burnout.

•A slow binder burnout rate, approximately 2°C/min or less is required for producing straight, uniform tapes.

•If silver foil is used to encapsulate the tape while sintering, low sintering temperatures with long soak times, approximately 775°C with a soak of 24 hours, is needed to prevent thallium/silver reactions.

•In this study, the tape highest transition temperature was found to be approximately 110K.

While the investigated method appears to yield reproducible results, improvements in grain connectivity (possibly a very brief high temperature final firing) and improvements in superconductor/electrode contacts must be made to create satisfactory, high temperature thallium grounding straps.

VI. References

1. C. C. Torardi, M. A. Subramian, J. C. Calabrese, J. Gopalakrishnan, K. J. Morrissey, T. R. Askew, R. B. Flippen, U. Chowdry, and A. W. Sleight, "Crystal Structure of the High-Temperature Superconductor $Tl_2Ba_2Ca_2Cu_3O_{10}$," *Science* **240**, 631-634 (1988).

2. K. L. Keester, R. M. Housley, and D. B. Marshall, "Growth and Characterization of Large $YBa_2Cu_3O_{7-\delta}$ Single Crystals," *J. Cryst. Growth* **91**, 295-301 (1988).

3. J. J. Ratto, J. P. Porter, R. M. Housley, and P. E. D. Morgan, "Monitoring Sintering/Densification and Crystallization/Grain-Growth in Tl-Based High Temperature Superconductors by Electrical Conductivity Measurements," *Japan. J. Appl. Phys.* **29**, 244-251 (1990).

4. J. R. Thompson, J. Brynestad, D. M. Kroeger, Y. C. Kim, S. T. Sekula, D. K. Christen, and E. D. Specht, "Superconductivity, Intergrain, and Intragrain Critical Current Densities of $Tl_2Ba_2Ca_2Cu_3O_{10+x}$ and $Tl_2CaBa_2Cu_2O_{8+x}$," *Phys. Rev. B* **39**, 6652-6658 (1989).

5. D. S. Ginley, E. L. Venturini, J. F. Kwak, B. J. Baughman, M. J. Carr, P. F. Hlava, J. E. Schirber, and B. Morosin, "A 120K Bulk Superconductor," *Physica C* **152**, 217-222 (1988).

6. J. D. Smith, Q. A. Shams, M. J. Saeed, D. Marsh, F. Arammash, J. Bennett, Z. Z. Sheng, and A. M. Hermann, "Formation of Tl-Ca-Ba-Cu-O Superconducting Thick Films by Vapor Evaporation of Tl_2O_3 in Rolled $Ba_2Ca_2Cu_3O_7$," *Appl. Phys. Commun.* **9**, 129-144 (1989).

7. A. W. Sleight, "Synthesis of Oxide Superconductors," *Physics Today* **44**, 24-30 (1991).

8. R. M. Iyer, G, M. Phatak, K. Gagadharan, M. D. Sastry, R. M. Kadam, P. V. P. S. S. Sastry, and J. V. Yakhmi, "Superconducting Transition Temperature of Single-Phase Tl-2223; Crucial Role of Ca-Vacancies and Tl-Content," *Physica C* **160**, 155-160 (1989).

9. B. Morosin, R. J. Baughman, D. S. Ginley, J. E. Schriber, and E. L. Venturini, "Structure Studies on Tl-Ba-Ca-Cu-O Superconductors; Effects of Cation Disorder and Oxygen Vacancies," *Physica C* **161**, 115-124 (1990).

10. M. Kikuchi, T. Kajitani, T. Suziki, S. Nakajima, K. Hiraga, N. Kobayashi, H. Iwasaki, Y. Syono, and Y. Muto, "Preparation and Chemical Composition of Superconducting Oxide $Tl_2Ba_2Ca_nCu_{n+1}Cu_3O_{10}$ with n=1, 2, and 3," *Japan. J. Appl. Phys.* **28**, L382-Ll385 (1989).

11. C. Martin, A. Maignan, J. Provost, C. Michel, M. Hervieu, R. Tournier, and B. Raveau, "Thallium Cuprates: The Critical Temperature is Mainly Governed by the Oxygen Nonstoichiometry," *Physica C* **168**, 8-22 (1990).

12. G. Haertling and P. Gilmour, "Development of High T_c (>110K) Bi, Tl, and Y-Based Materials as Superconducting Circuit Elements. Part II Development of Tl-Based Materials," NASA Annual Report, Contract No. NAG-1-1108, June 28, 1991.

13. Z. Z. Sheng, L. Sheng, H. M. Su, and A. M. Hermann, "Tl_2O_3 Vapor Process of Making Tl-Ba-Ca-Cu-O Superconductors," *Appl. Phys. Lett.* **53**, 2686-2688 (1988).

14. R. W. Rice, "Fabrication of Dense MgO," NRL Report 7334, Naval Research Laboratory, Washington D. C. Nov. 16, 1971.

15. "A Pressing Way to Better Transducers," *Industrial Research* **32**, 63 (1972).

16. R. E. Newnham, "Structure-Property Relations," 66-67 (Springer Verlag, NY 1975).

17. P. C. Gilmour, "The Effect of Manganese Additions on the Stoichiometry and Resistivity of a Lead-Iron-Niobate Ceramic," M.S. Thesis, The Pennsylvania State University, 1987.

18. P. Strobel, C. Paulson, and J. L. Tholence, "Superconducting Properties of Substituted $YBa_2Cu_{3(1-x)}Mn_{3x}O_{7-\delta}$," *Solid State. Commun.* **65**, 585-589 (1988).

19. Y. Ying-Chang, Z. Yuan-Bo, Y. Wei-Chun, Y. Ji-Lian, Z. Bui-Sheng, Z. Hui-Ming, D. Yong-Fan, J. Lan, and Y. Chun-Tang, "Substitution Effects and Neutron Diffraction Study of $YBa_2(Cu_{0.95}Mn_{0.05})_3O_{7-\delta}$," *Acta Phys. Sin.* **39**, 111-118 (1990).

20. Z. Z. Sheng, L. Sheng, H. M. Su, and A. M. Hermann, "Tl_2O_3 Vapor Process of Making Tl-Ba-Ca-Cu-O Superconductors," *Appl. Phys. Lett.* **53**, 2686-2688 (1988).

21. R. Sugise, M. Hirabayashi, N. Terada, M. Jo, F. Kawashima, and H. Ihara, "Preparation of $Tl_2Ba_2Ca_2Cu_3O_{10}$ Thick Films from Ba-Ca-Cu-O Films," *Japan. J. Appl. Phys.* **27**, L2314-L2316 (1988).

22. C. Laubschat, M. Domke, M. Prietsh, T. Mandel, M. Bodenvach, G. Kaindl, H. J. Eikenbush, R. Schoellhorn, R. Miranda, E. Noran, F. Garcia, and M. A. Alario, "Interface Formation Between $MBa_2Cu_3O_{7-\delta}$ (M=Y,Sm and the Monovalent Metals Ag, and Rb)," *Europhysics Lett.* **6**, 555-560 (1988).

23. A. Goyal, S. J. Burns, and P. D. Funenbusch, "Effect of Ag/AgO Additions on the Resistive Behavior of Preformed $YBa_2Cu_3O_{7-\delta}$ Compacts in the Low Temperature Sintering Regime," *Physica C* **168**, 405-416 (1990).

24. D. Pavuna, H. Berger, M. Affronte, J. Van der Maas, J. J. Cappon, M. Guillot, P. Lovejay, and J. L. Tholence, "Electronic Properties and Critical Current Densities of Superconducting $(Y_1Ba_2Cu_3O_{6.9})_{1-x}Ag_x$ Compounds," *Solid St. Commun.* **68**, 535-538 (1988).

25. M. K. Malik, V. D. Nair, A. R. Biswas, R. V. Raghavan, P. Chaddah, P. K. Mishra, G. R. Kumar, and B. A. Dasannacharya, "Texture Formation and Enhanced Critical Currents in $YBa_2Cu_3O_7$," *Applied Phys. Lett.* **52**, 1515-1527 (1988).

26. W. Eichenauer and G. Müller, "Diffusion und Löslichkeit von Sauerstoff in Silber," *Z. Metallk.* **53**, 321-324 (1962).

27. H. Rickert and R Steiner, "Elektochemische Messung der Sauerstoffdiffusion in Metullen bei Höheren Temperaturen," *Z. Physik. Chem.* **49**, 127-137 (1966).

28. J. S. Hirschhorn and J. G. Berglund, "Effect of Oxygen on the Sintering Rate of Silver Compacts," *Scr. Met.* **2**, 319-322 (1968).

29. S. Adachi, K. Mizuno, K. Setsune, and K. Wasa, " Synthesis of Tl-Ba-Ca-Cu-O Ceramics Showing Meissner Effect Over 125K," *Physica C* **171**, 543-546 (1990).

30. G. Haertling and D. Hsi, "Development and Evaluation of Superconducting Circuit Elements," NASA Annual Report, Contract No. NAG-1-820, October 31, (1990).

31. E. Braun, W. Schnell, H. Broicher, J. Harnischmacher, D. Wohlleben, C. Allegeier, W. Reith, J. S. Schiling, J. Bock, E. Preisler, and G. J. Vogt, "Specific Heat and Thermal Expansion of the Bi and Tl High Temperature Superconductors Near T_c," *Z. Phys. B* **84**, 333-341 (1991).

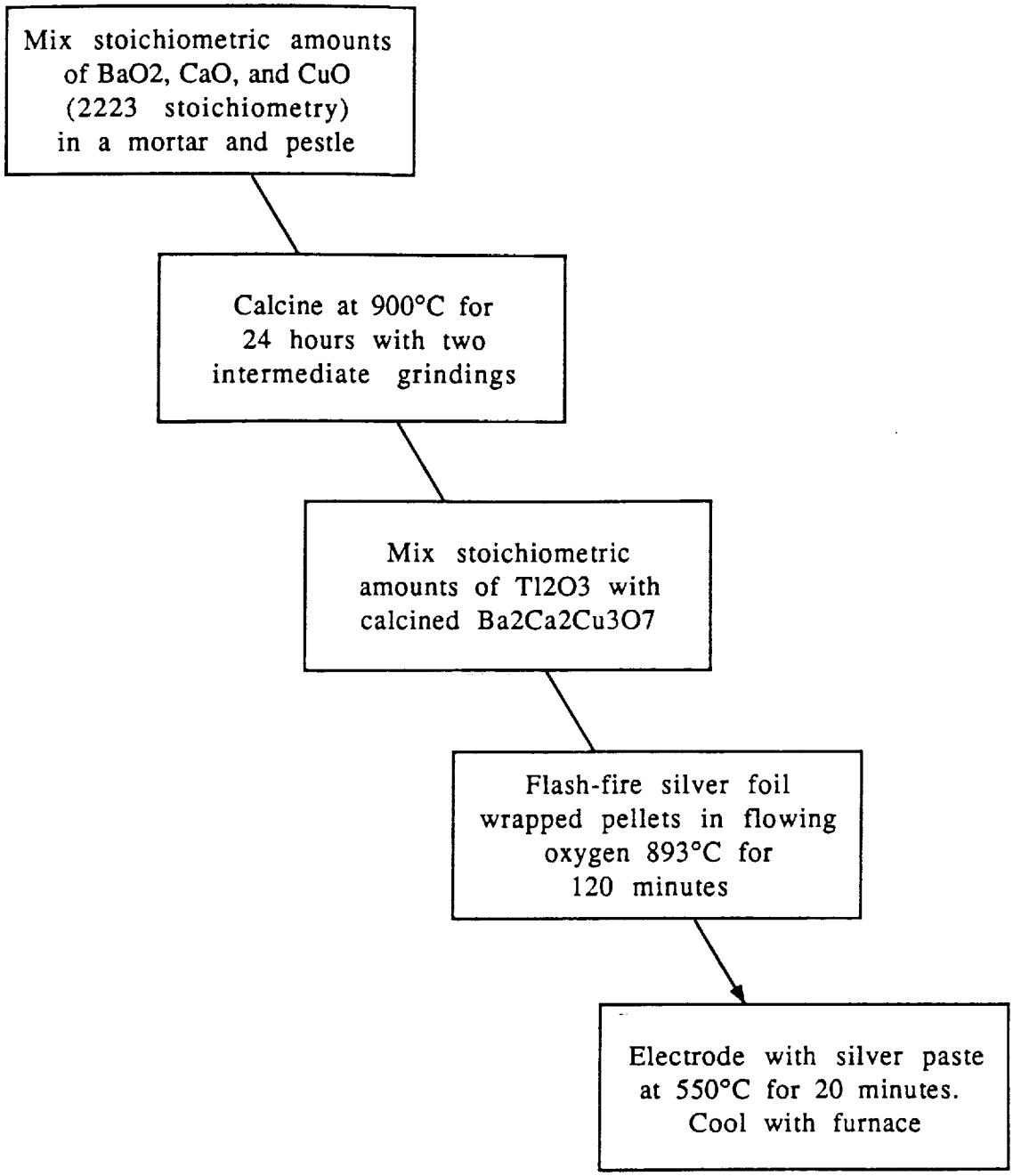

Figure 1

Schematic of the Oxide Precursor Process
Used to Make Thallium Superconductors

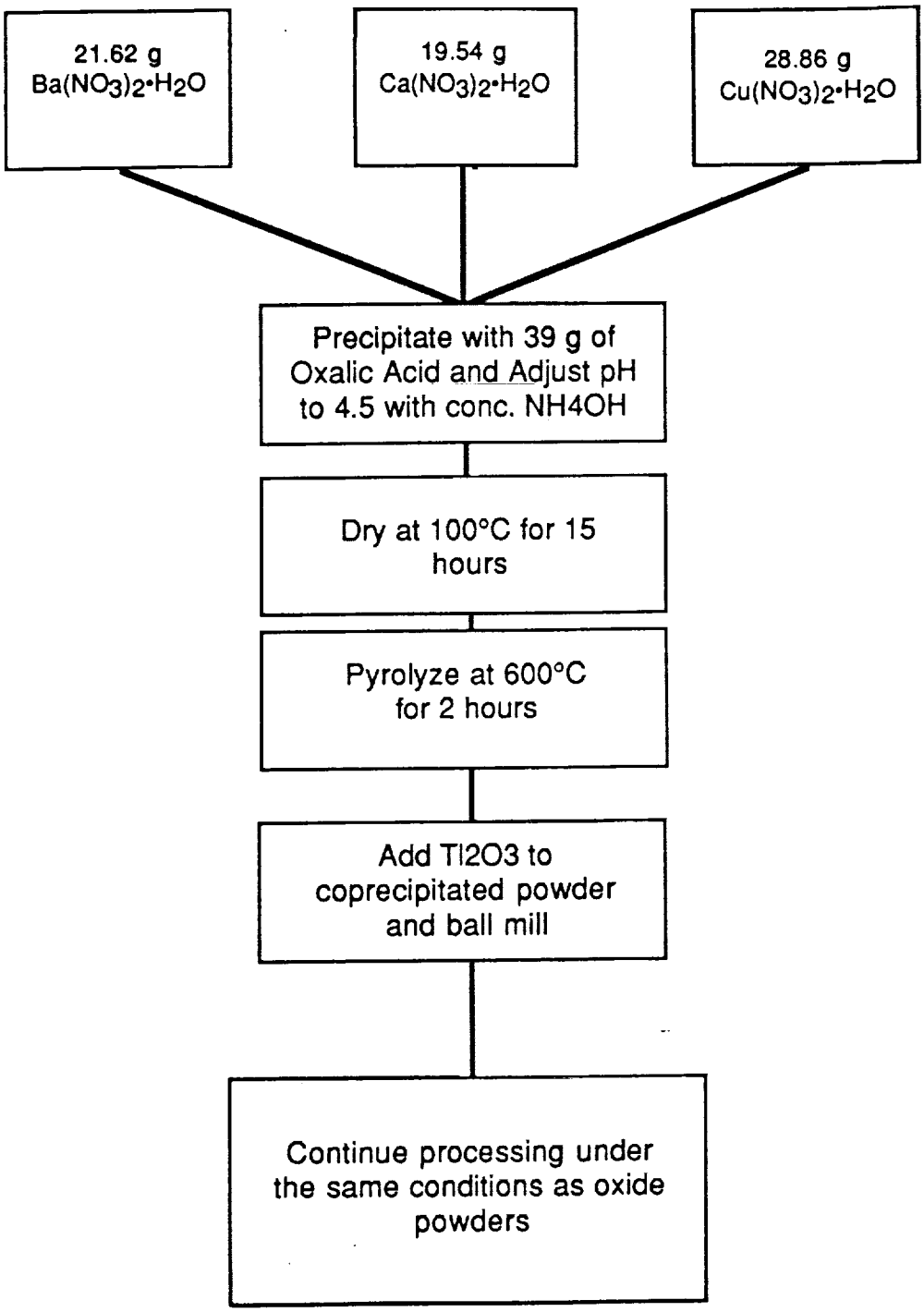

Figure 2
Schematic of the Oxalate Coprecipitation Process
Used to Make Thallium Superconductors

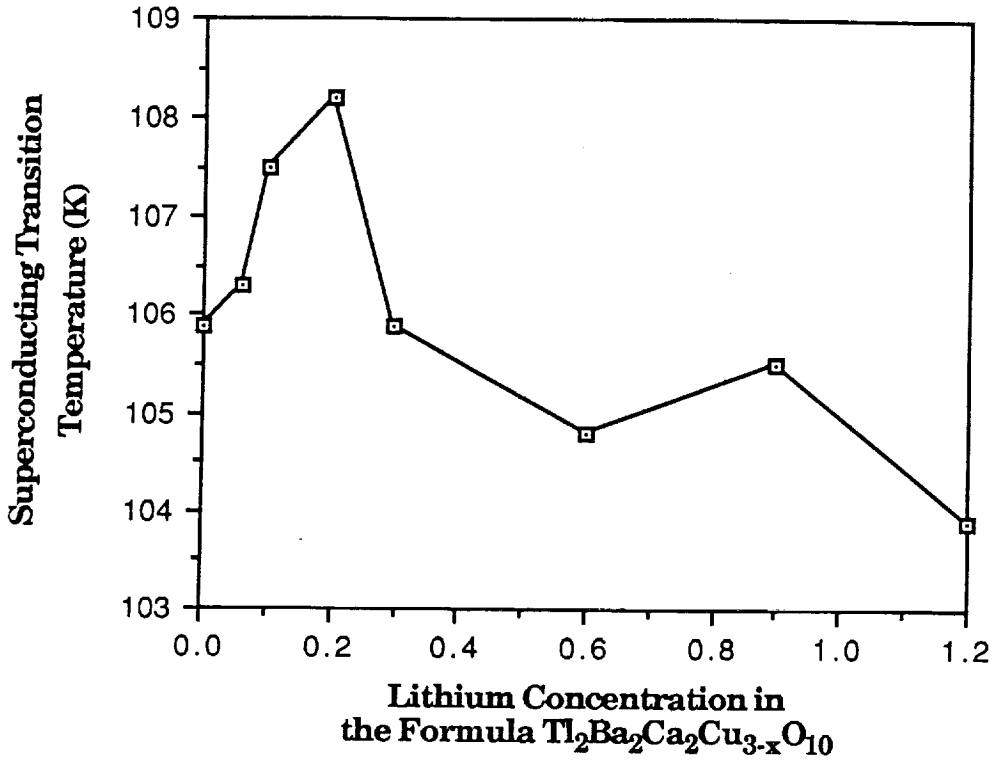

Figure 3

Superconducting Transition Temperatures of Ceramic Pellets Containing Lithium Substitutions for Copper

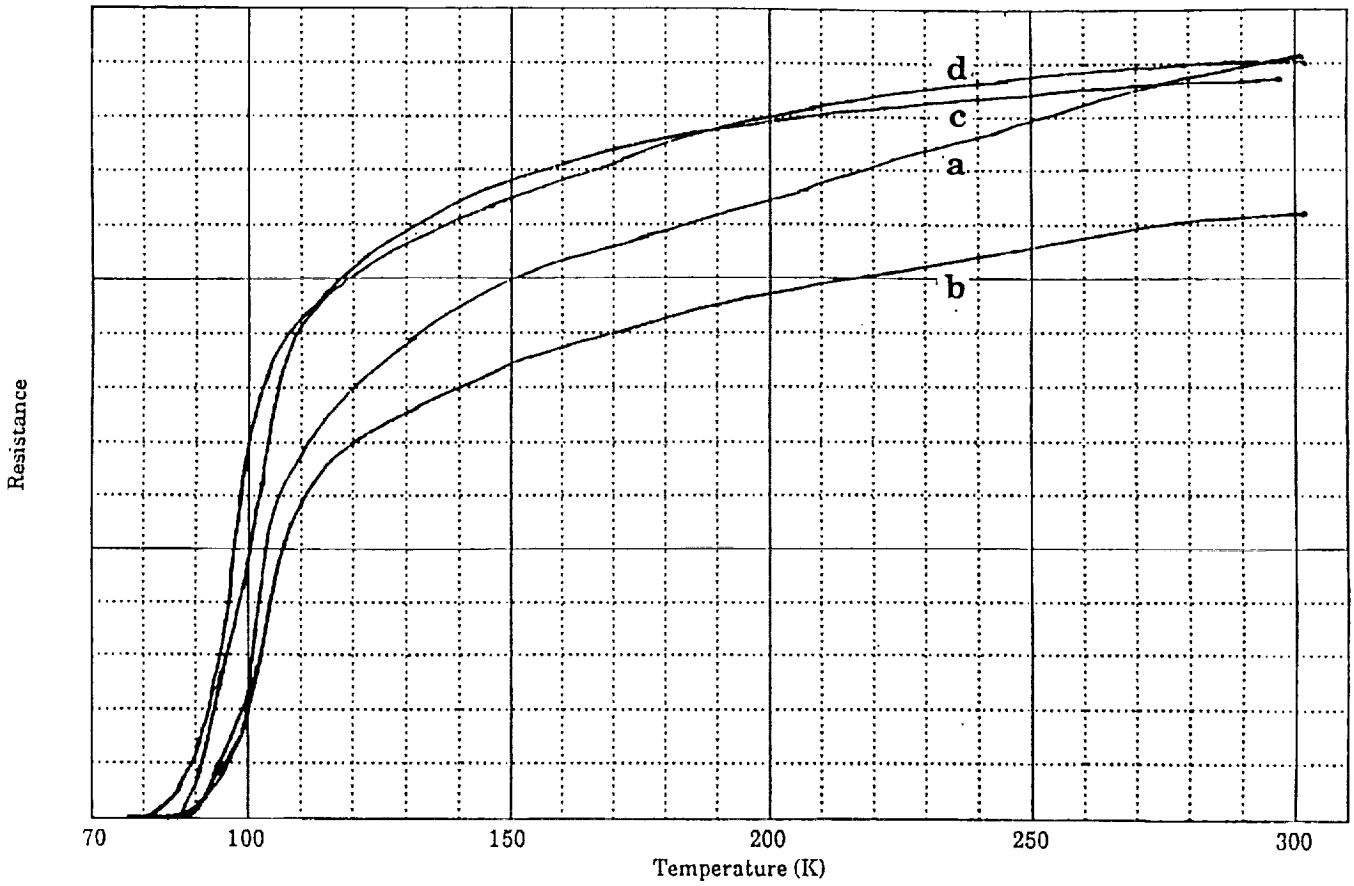

Figure 4

Superconducting Transition Curves of Ceramic Pellets with Various Manganese Substitutions. Flash-Fired at 885°C for 30 Minutes

a) 0 mole percent Mn for Cu (T_c=88.7K)

b) 0.47 mole percent Mn for Cu (T_c=86.3K)

c) 0.93mole percent Mn for Cu (T_c=87.3K)

d) 1.87 mole percent Mn for Cu (T_c=81.6K)

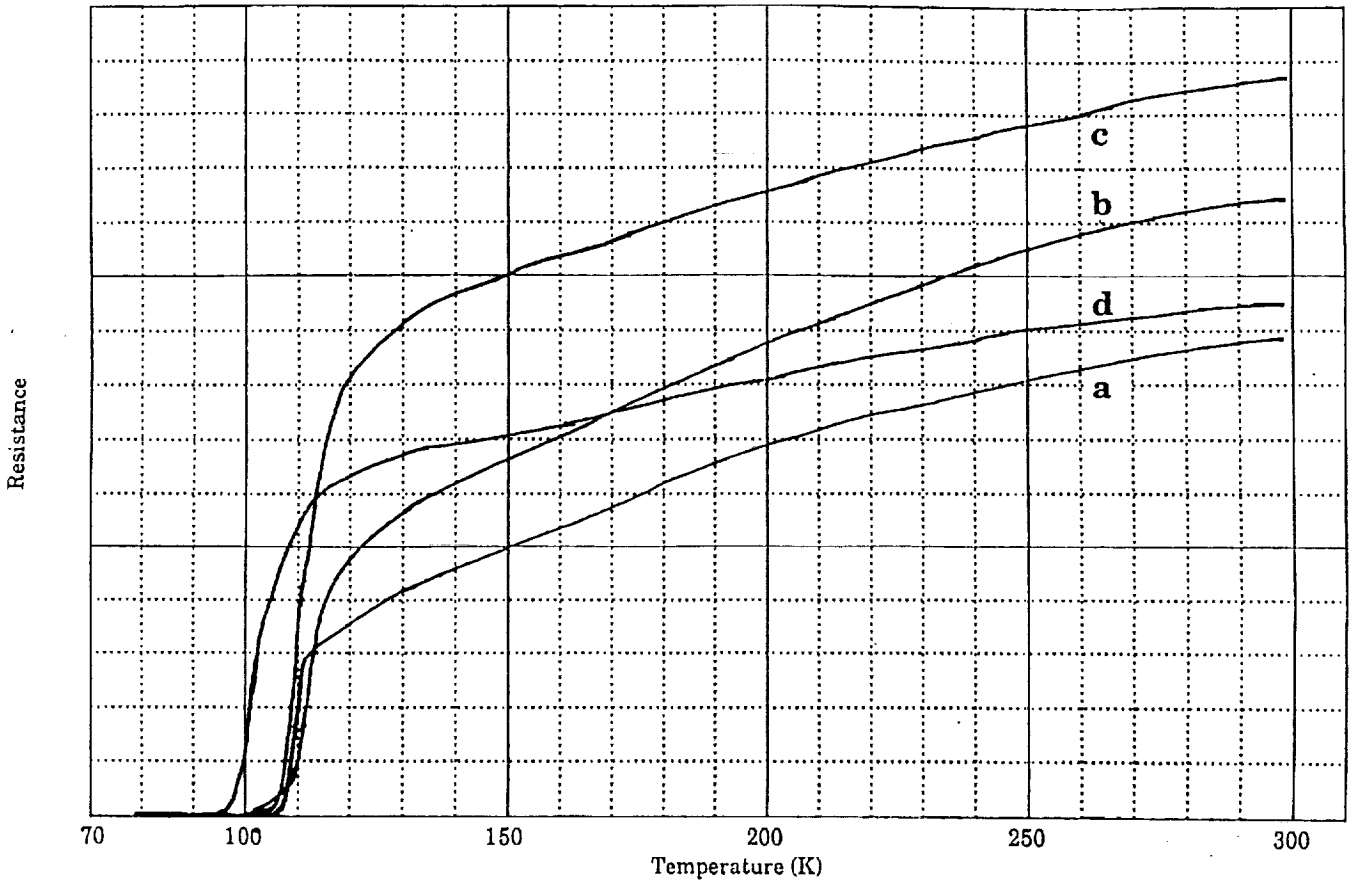

Figure 5

Superconducting Transition Curves of Ceramic Pellets with Various Manganese Substitutions. Flash-Fired at 885°C for 120 Minutes

a) 0 mole percent Mn for Cu (T_c=108.0K)

b) 0.47 mole percent Mn for Cu (T_c=101.3K)

c) 0.93mole percent Mn for Cu (T_c=105.7K)

d) 1.87 mole percent Mn for Cu (T_c=97.4K)

a

b

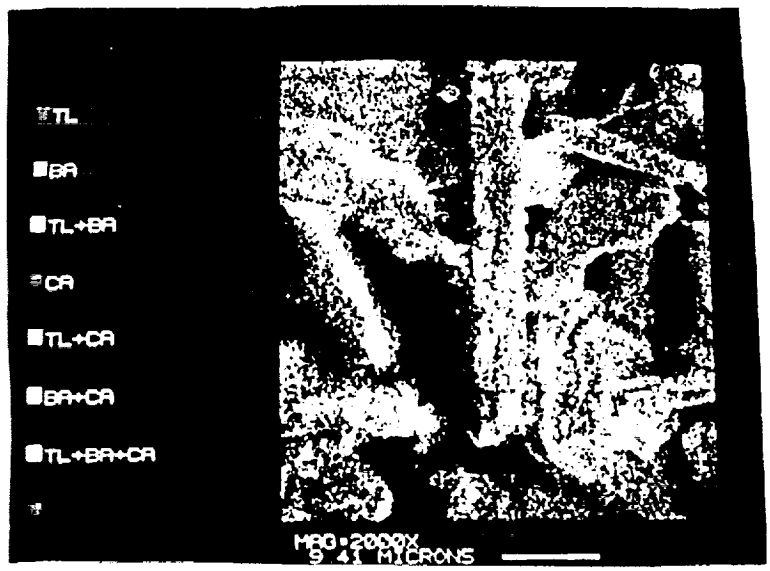

c

Figure 6

Scanning Electron Micrographs and Energy Dispersive X-Ray Analysis Mappings of As-Fired Surface of a Thallium Superconductor Pellet Sintered at 893°C for Two Hours--Oxide Precursors
Final Magnification after Copying--1000X
a) SEM Photomicrograph
b) SEM Photomicrograph and EDX Mappings of Tl, Ba, and Cu
c) SEM Photomicrograph and EDX Mappings of Tl, Ba, and Ca

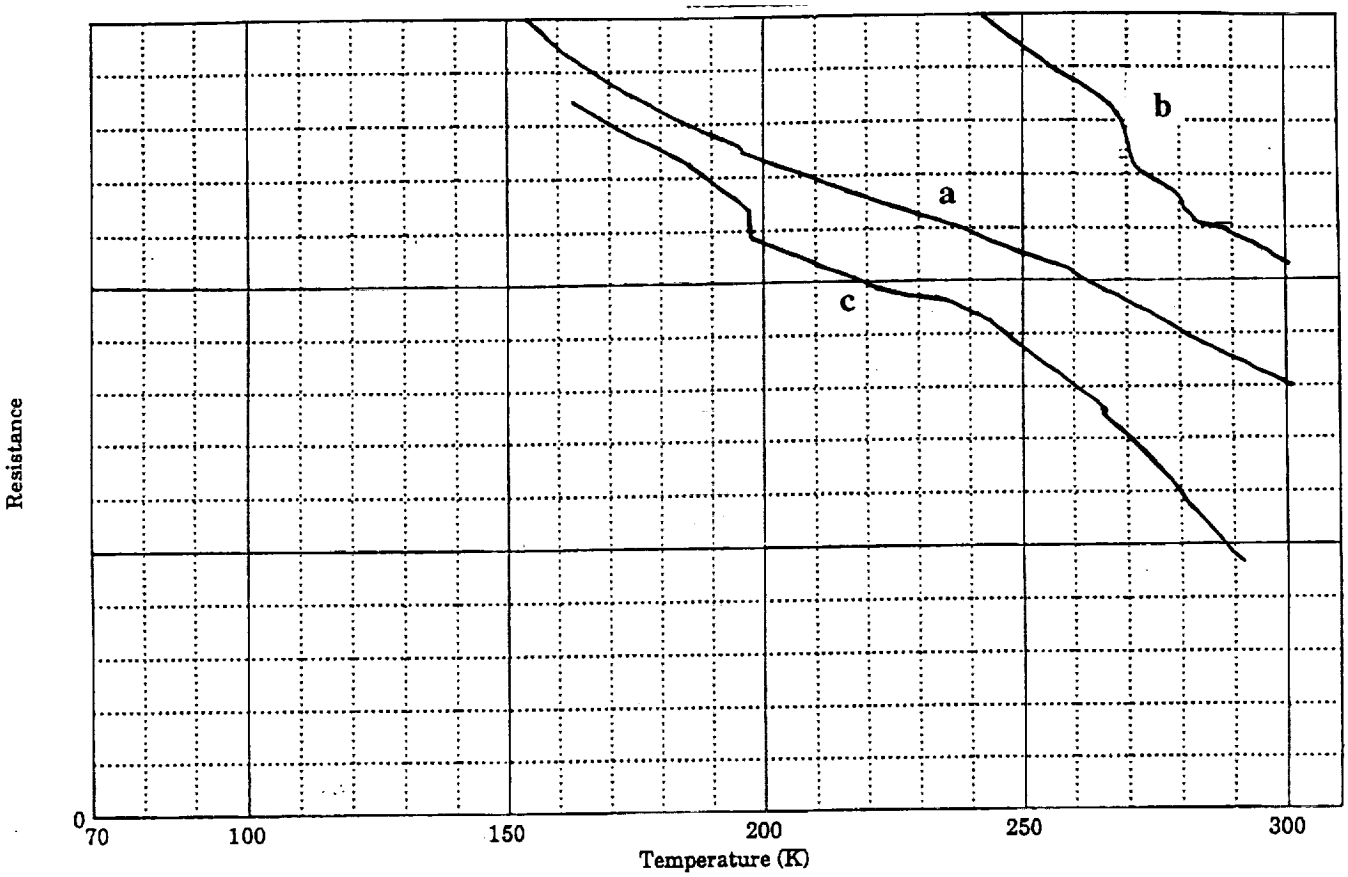

Figure 7

Resistance as a Function of Temperature for Ceramic Pellets Made with Coprecipitated Powder
Nominal Composition of the Powder: $Tl_2Ba_2Ca_2Cu_3O_{10}$
a) 30 Minute Soak at 893°C (Nonsuperconducting at 77K)
b) 60 Minute Soak at 893°C (Nonsuperconducting at 77K)
c) 120 Minute Soak at 893°C (Nonsuperconducting at 77K)

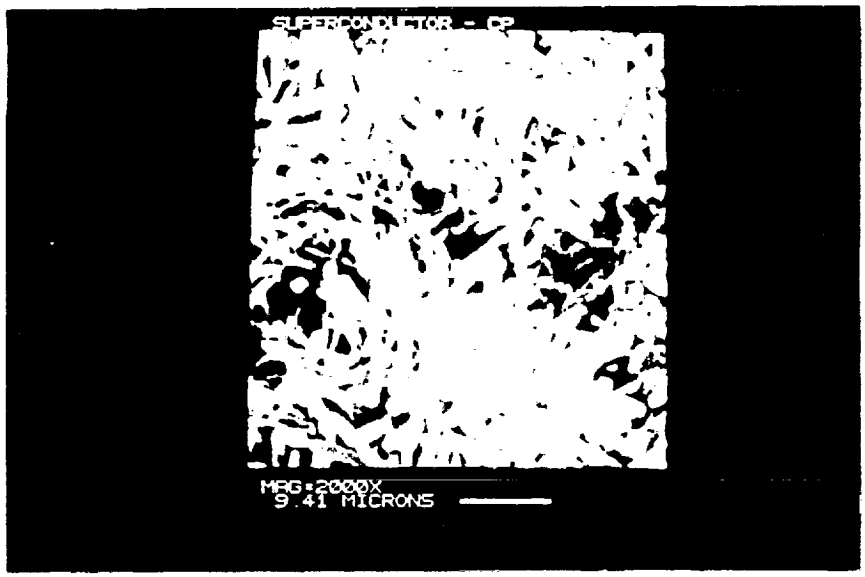

a

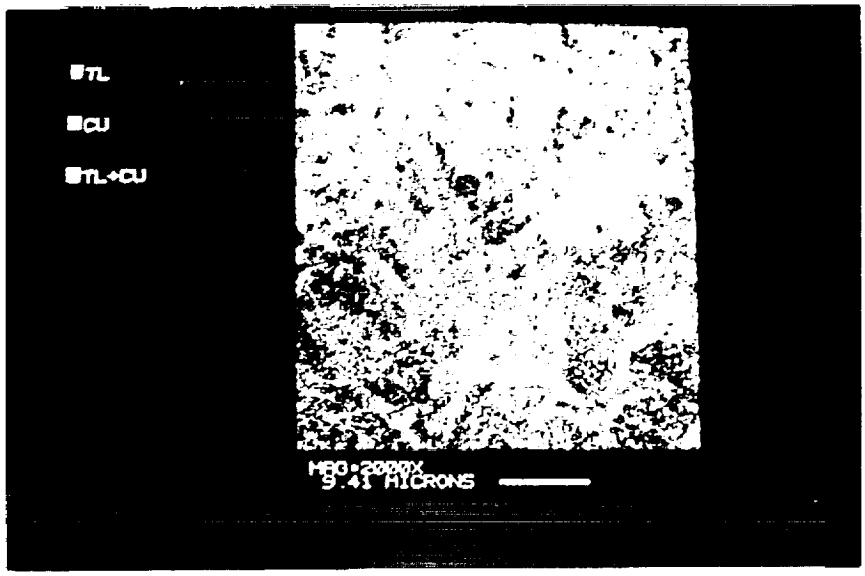

b

Figure 8

Scanning Electron Micrographs and Energy Dispersive X-Ray Analysis Mappings of As-Fired Surface of a Thallium Superconductor Pellet Sintered at 893°C for Two Hours--Coprecipitated Precursors
Final Magnification after Copying--1000X
a) SEM Photomicrograph
b) SEM Photomicrograph and EDX Mappings of Tl and Cu
(Ba and Ca are not present in the area shown)

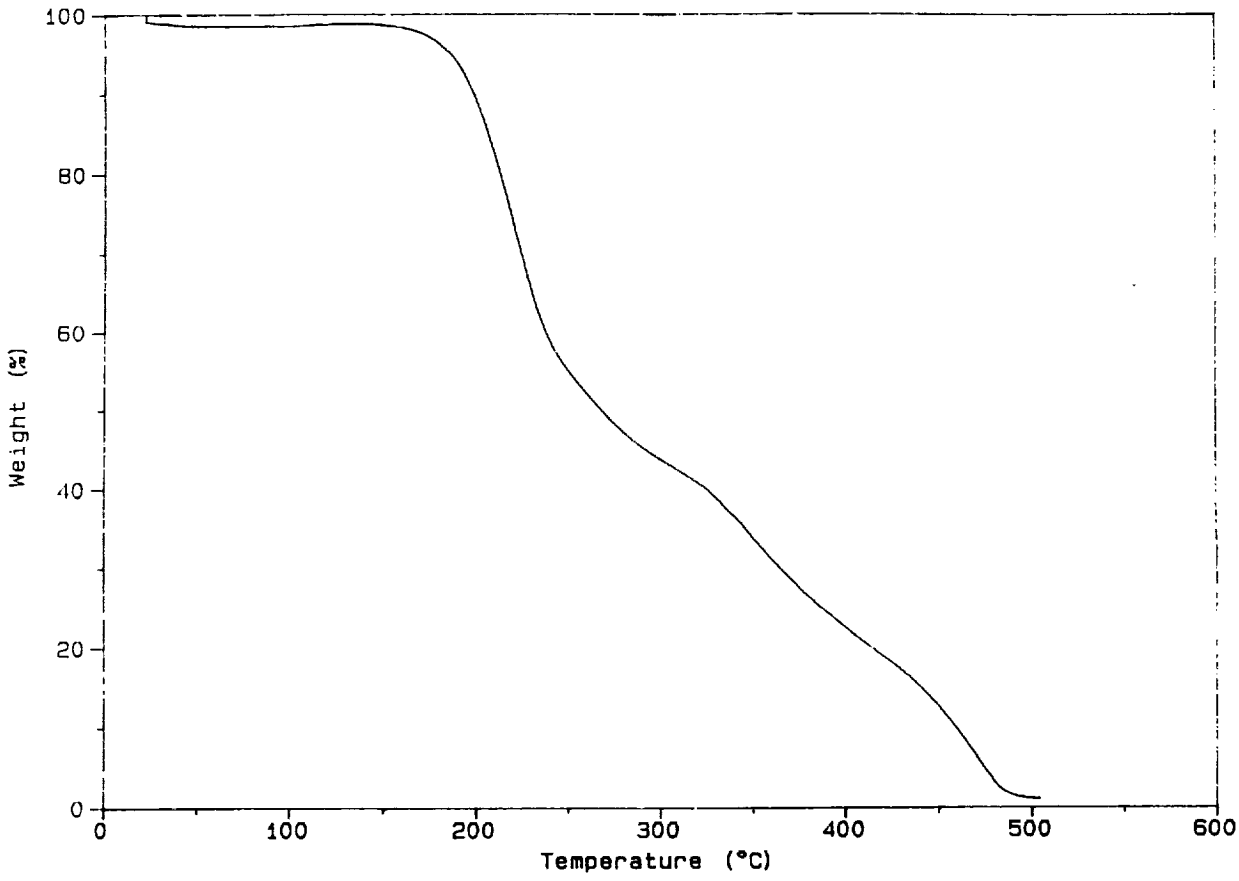

Figure 9

Thermogravimatric Analysis of Binder Used for Tape Casting.
Air Purged-Rate 1°C/min.

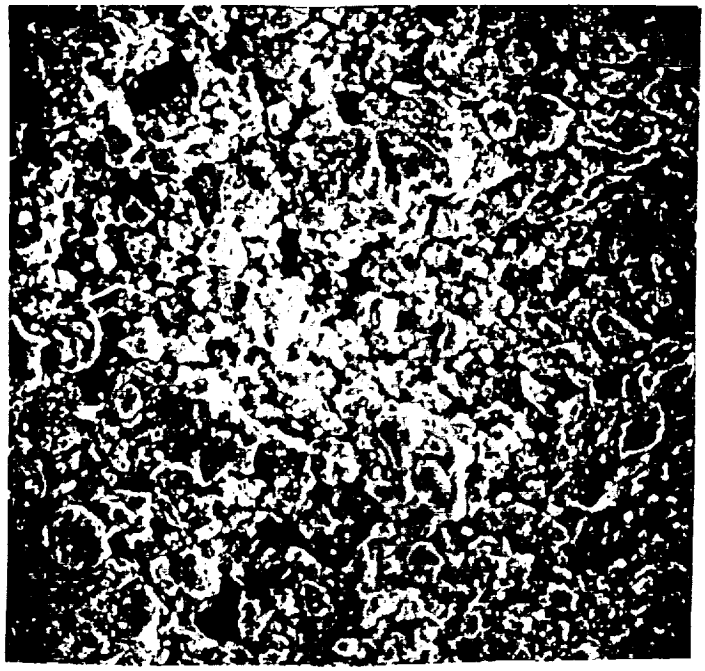

a) Ramp 2°C/min to 550°C. Soak for Two Hours.

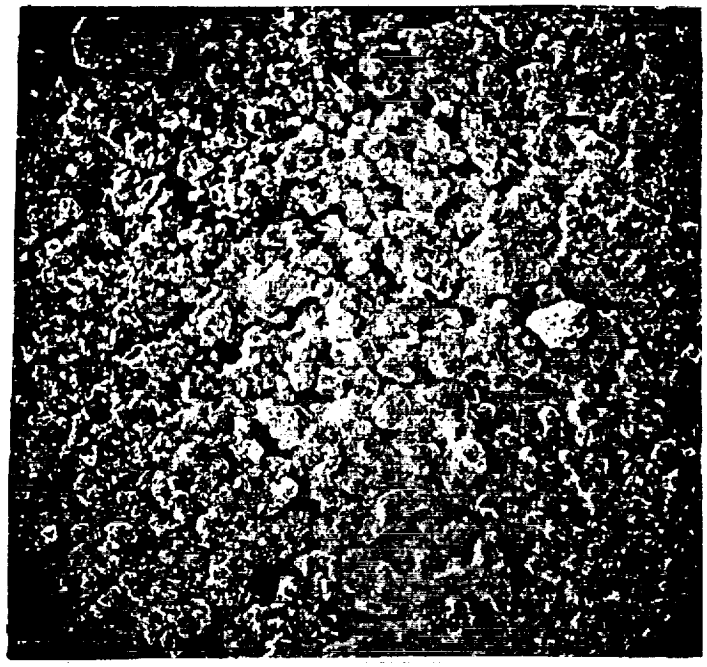

b) Ramp 12°C/min to 550°C. Soak for Two Hours.

Figure 10

SEM Photomicrographs of Post-Binder Burnout Tapes.
Nominal Composition of Precursor Powder $Tl_2Ba_2Ca_2Cu_3O_{10}$.

200X

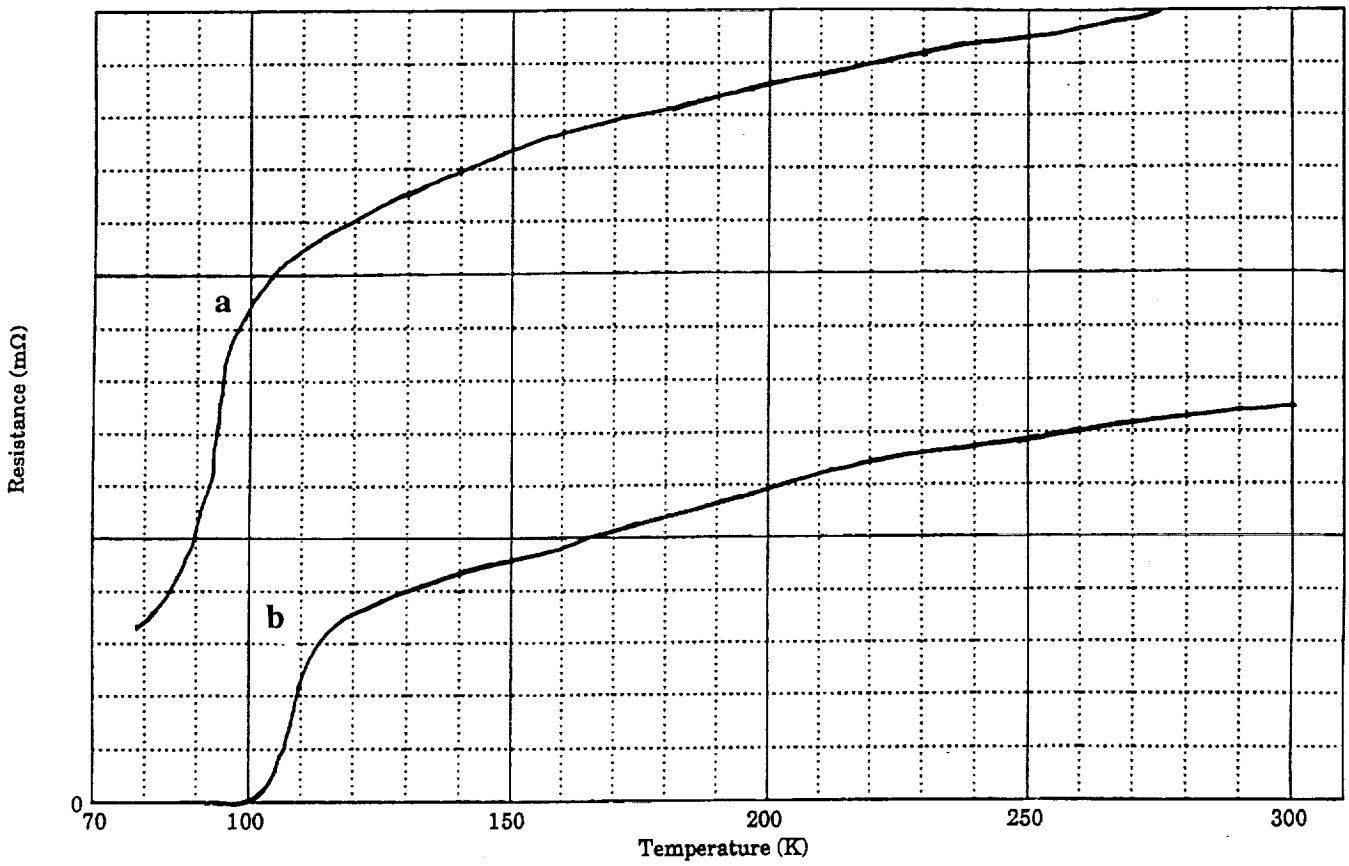

Figure 11

Resistance as a Function of Temperature for Ceramic Tapes.
Nominal Composition of the Powder: $Tl_2Ba_2Ca_2Cu_3O_{10}$

a) 5°C/min Binder Burnout Rate--893°C, 60 Minute Soak

b) 3°C/min Binder Burnout Rate--893°C, 60 Minute Soak

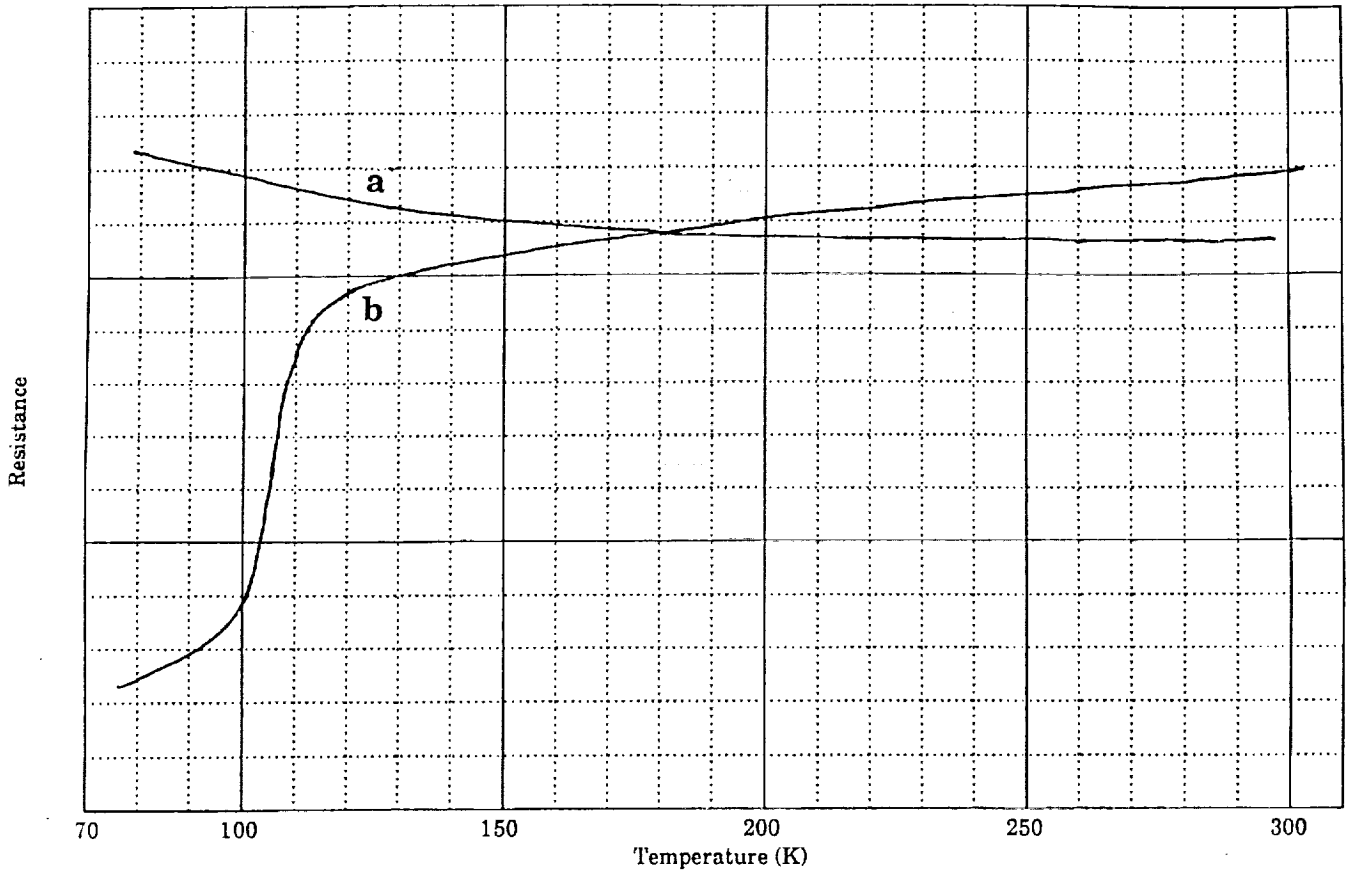

Figure 12

Superconducting Transition Curves of Ceramic Tapes.
Nominal Composition of Precursor Powder $Tl_2Ba_2Ca_2Cu_3O_{10}$.
840°C Presinter--Sieved through 60 mesh.
a) 30 Minute Soak at 890°C (Nonsuperconducting at 77.7K)
b) 60 Minute Soak at 890°C (Nonsuperconducting at 77.7K)

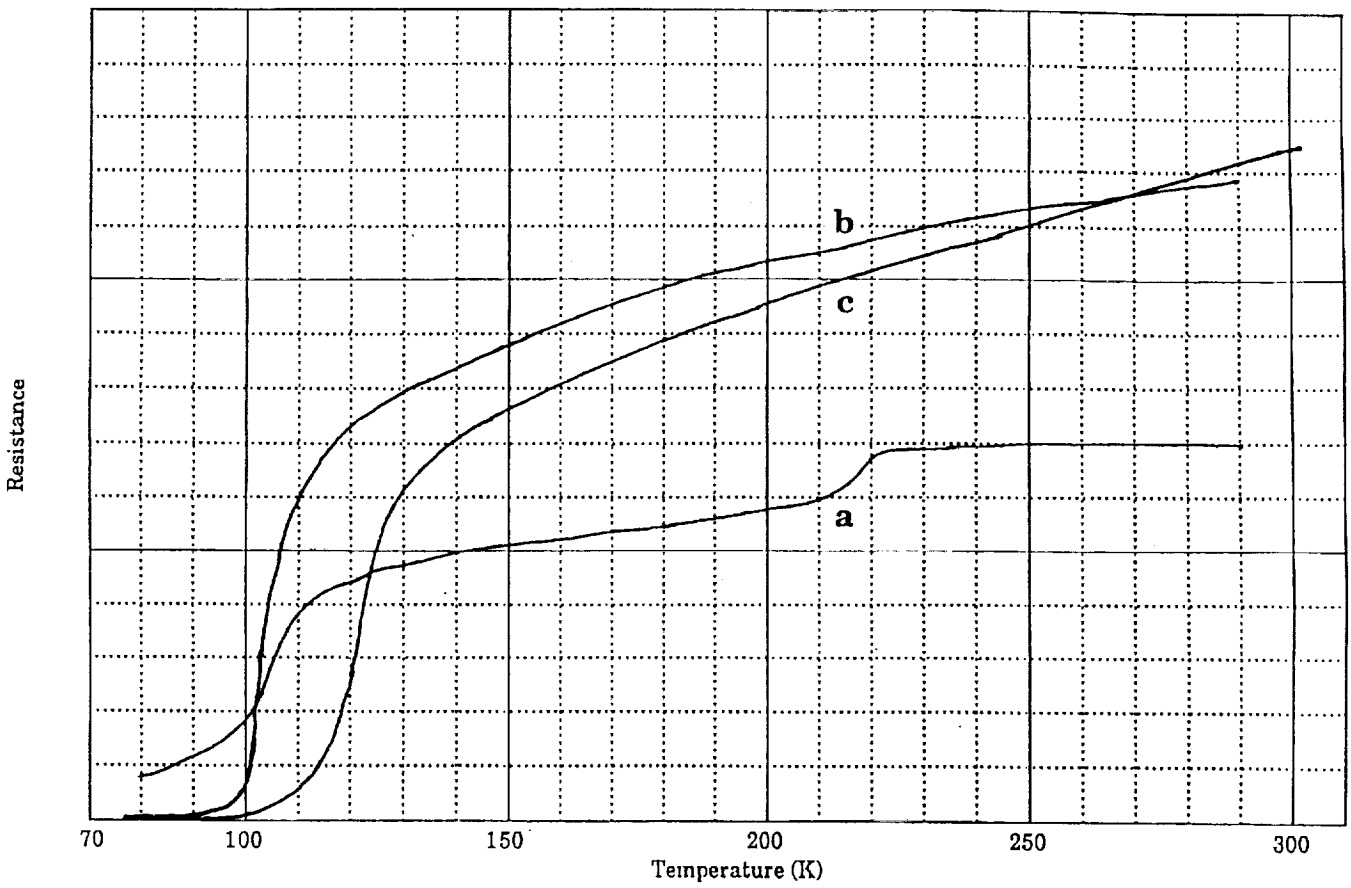

Figure 13

Superconducting Transition Curves of Ceramic Tapes.
Nominal Composition of Precursor Powder $Tl_2Ba_2Ca_2Cu_3O_{10}$.
840°C Presinter--Sieved through 400 mesh.
a) 30 Minute Soak at 890°C (Nonsuperconducting at 77.7K)
b) 60 Minute Soak at 890°C (Nonsuperconducting at 77.7K)
c) 120 Minute Soak at 890°C (T_c=97.3 at 1 mA)

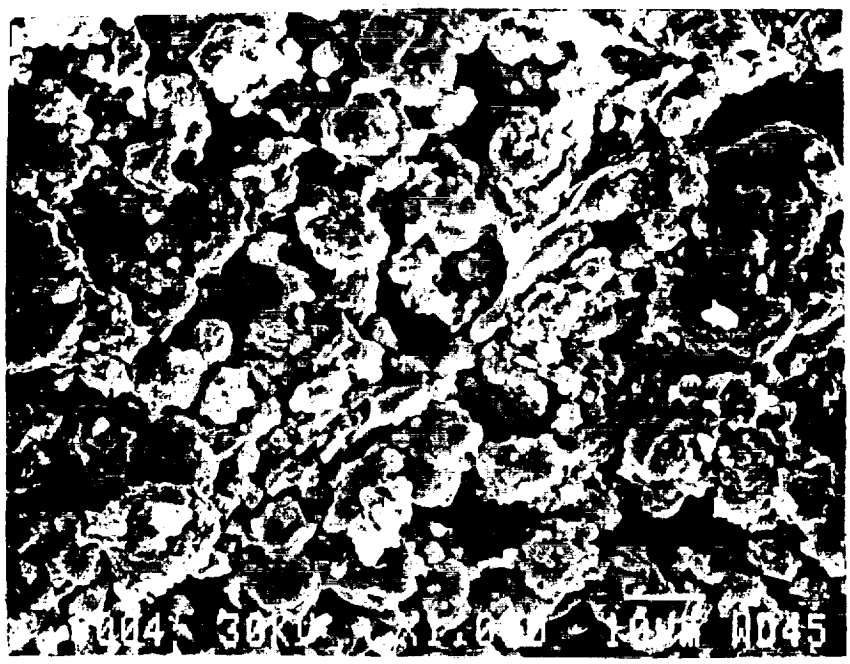

a) Precursor Powder Sieved Through 60 Mesh

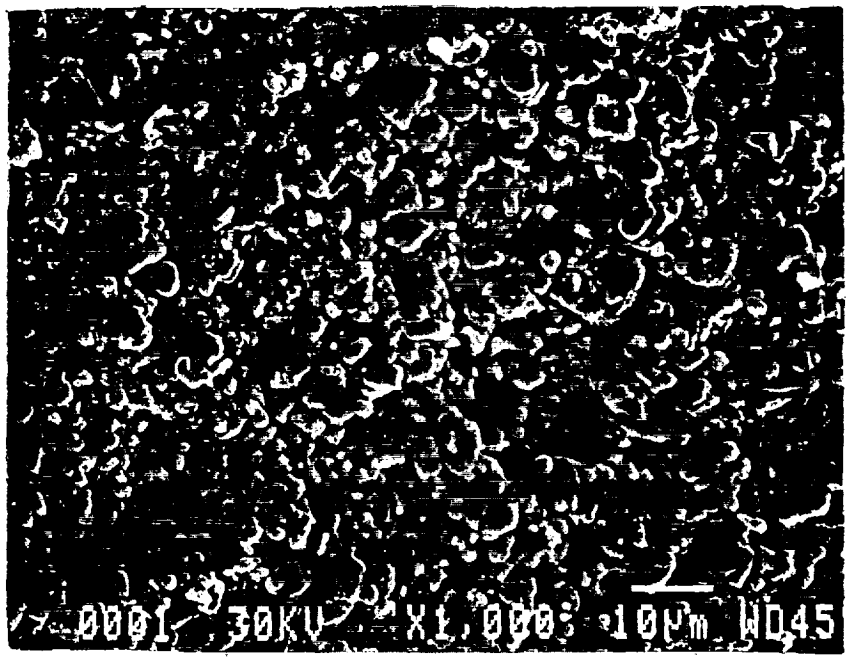

b) Precursor Powder Sieved Through 400 Mesh.

Figure 14

SEM Photomicrographs of the As-Fired Surface of Ceramic Tapes
Flash Fired at 890°C for 30 Minutes.
Nominal Composition of Precursor Powder $Tl_2Ba_2Ca_2Cu_3O_{10}$.
1000X

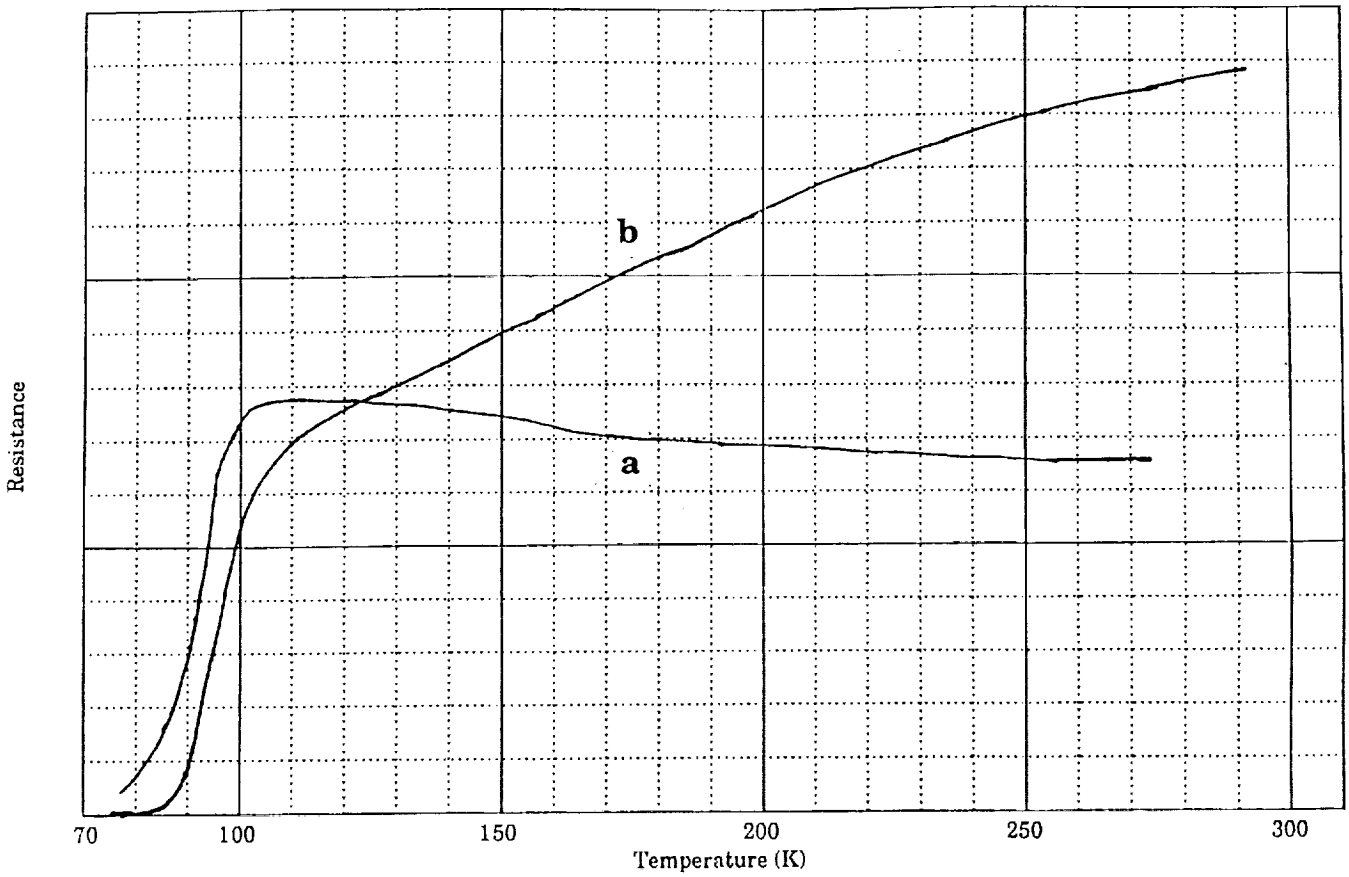

Figure 15

Superconducting Transition Curves of Ceramic Tapes.
Nominal Composition of Precursor Powder $Tl_2Ba_2Ca_2Cu_3O_{10}$.
890°C Presinter--Sieved through 60 mesh.
a) 30 Minute Soak at 890°C (Nonsuperconducting at 77.7K)
b) 60 Minute Soak at 890°C (T_c=90.7K at 100 mA)

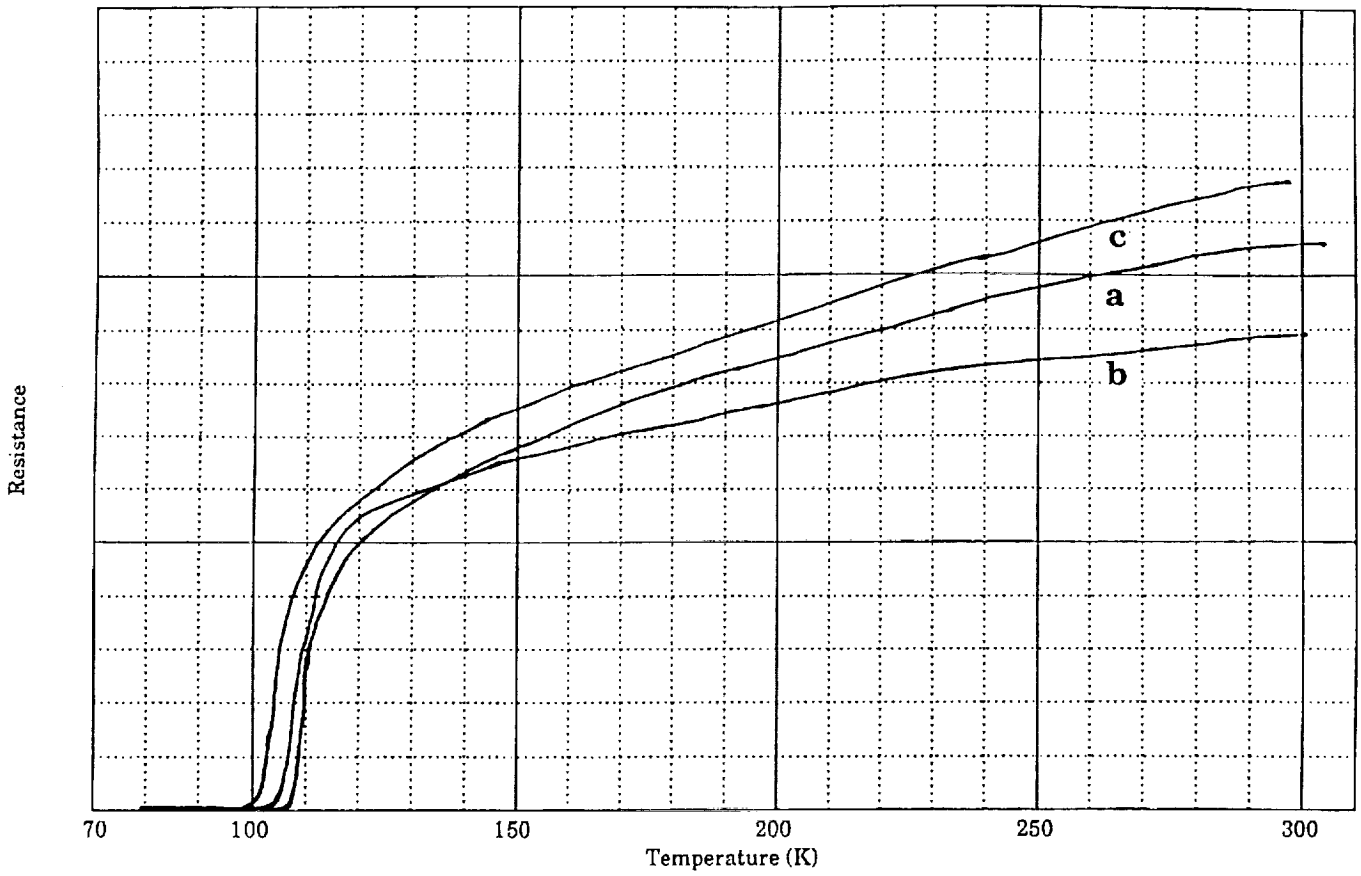

Figure 16

Superconducting Transition Curves of Ceramic Tapes.
Nominal Composition of Precursor Powder $Tl_2Ba_2Ca_2Cu_3O_{10}$.
890°C Presinter--Sieved through 400 mesh.
a) 30 Minute Soak at 890°C (T_c=96.4K at 100 mA)
b) 60 Minute Soak at 890°C (T_c=104.6K at 100 mA)
c) 120 Minute Soak at 890°C (T_c=106.5K at 100 mA)

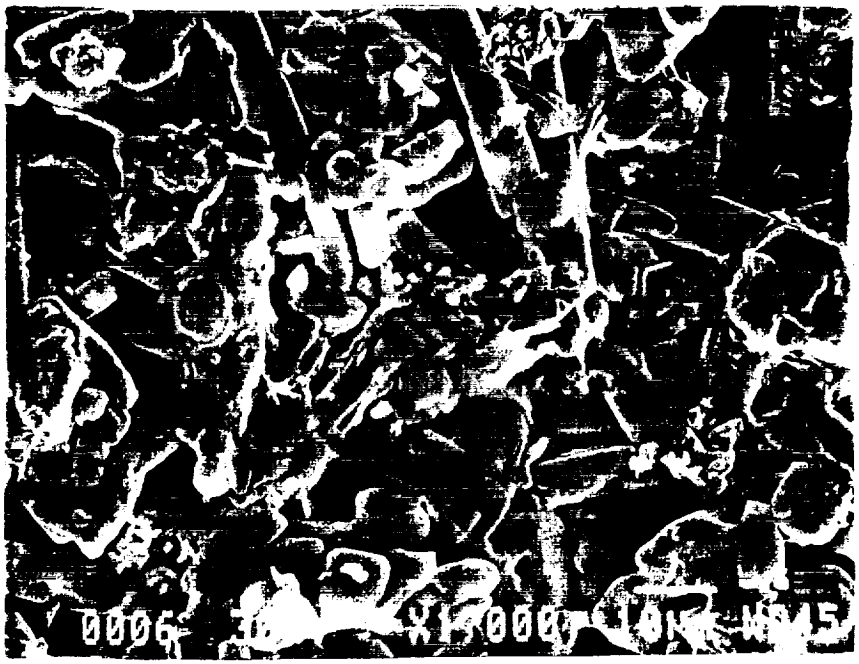

Figure 17

SEM Photomicrograph of the As-Fired Surface of a Ceramic Tape.
Nominal Composition of Precursor Powder $Tl_2Ba_2Ca_2Cu_3O_{10}$.
Presintered at 890°C for 60 Minutes
Passed through 400 mesh.
Flashed-Fired at 890°C for 120 Minutes
1000X

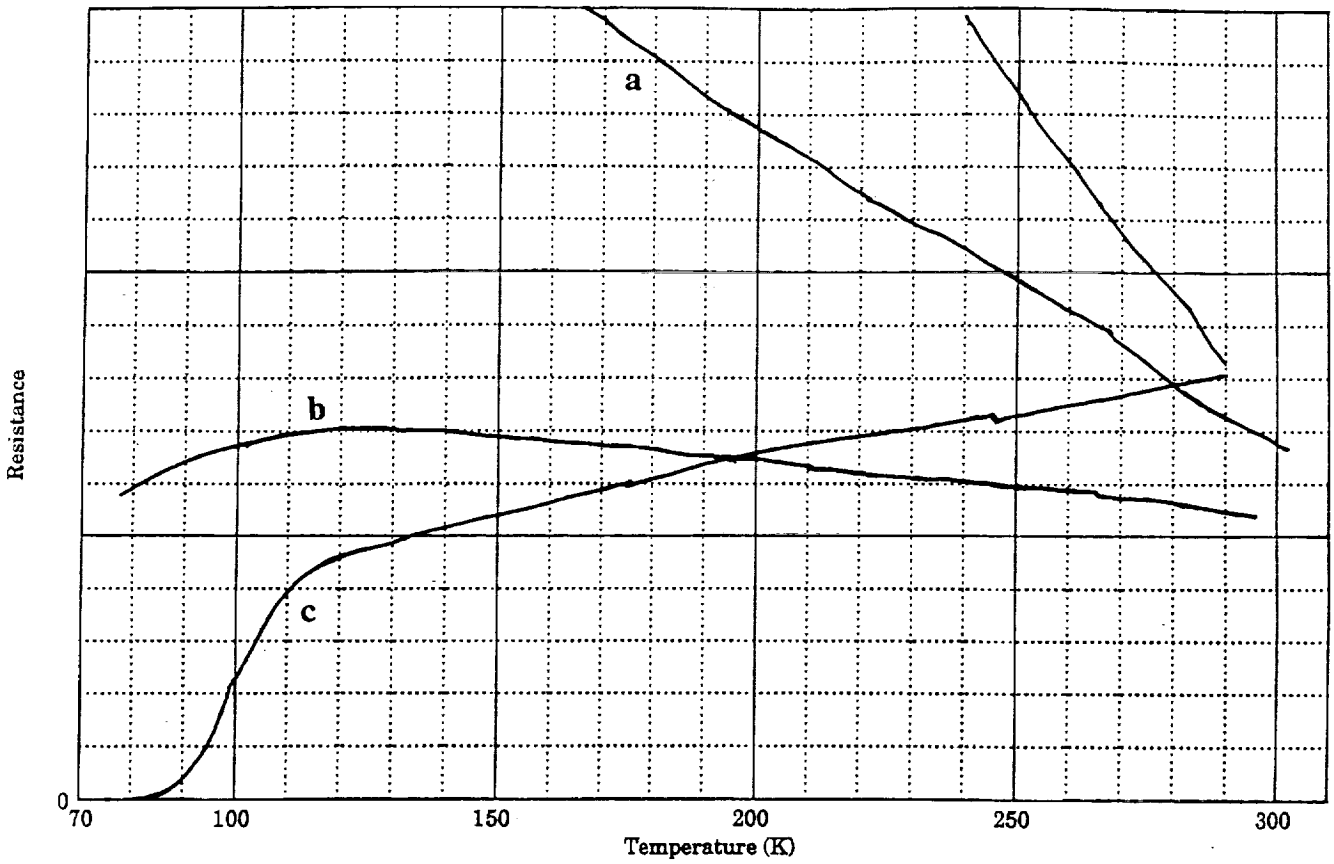

Figure 18

Superconducting Transition Temperature Curves of Ceramic Tapes.
Nominal Composition of Precursor Powder $Tl_2Ba_2Ca_2Cu_3O_{10}$.

a) 2°C/min Binder Burnout Rate--745°C, 12 Hour Soak

b) 2°C/min Binder Burnout Rate--745°C, 24 Hour Soak

c) 2°C/min Binder Burnout Rate--745°C, 48 Hour Soak

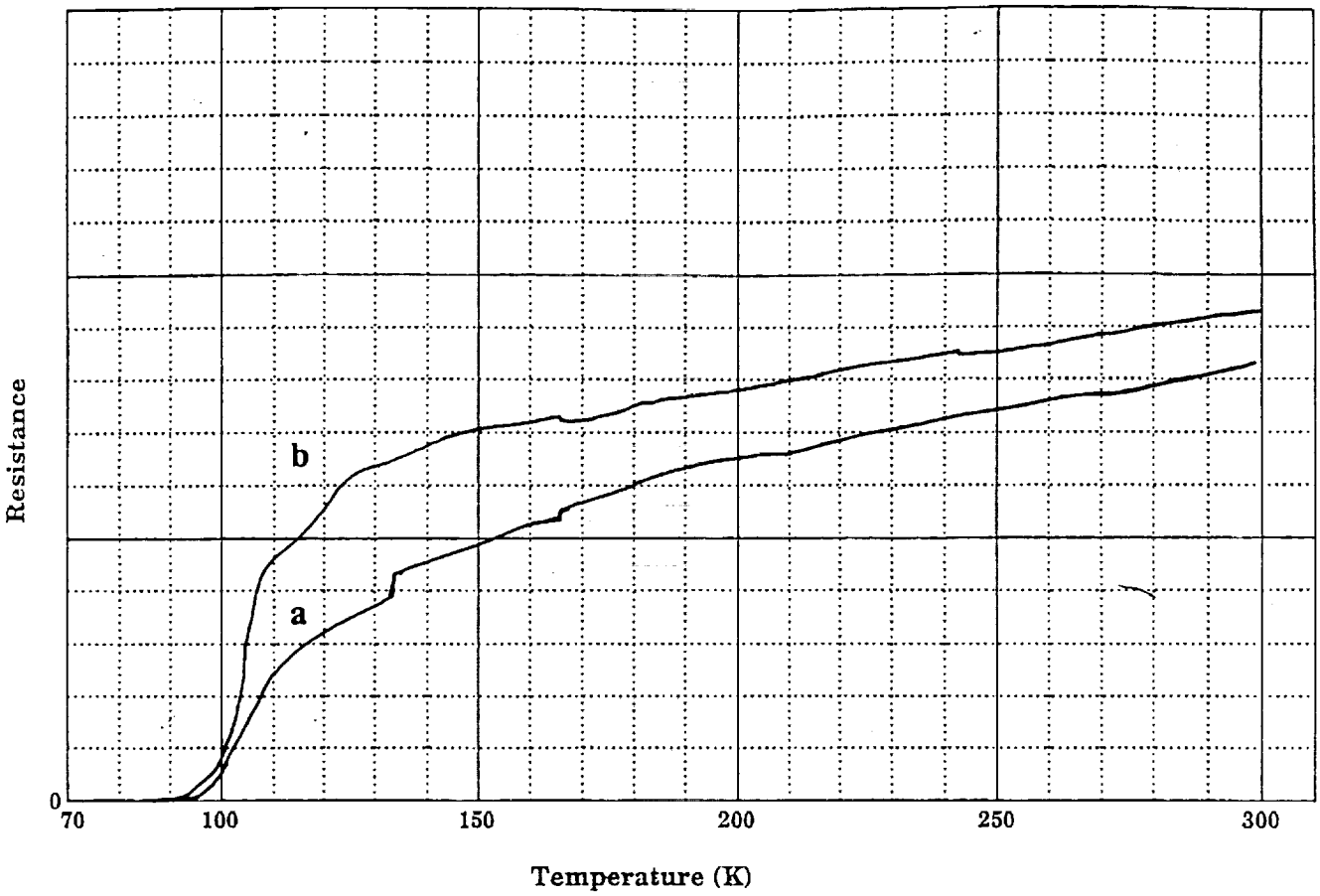

Figure 19

Superconducting Transition Temperature Curves of Ceramic Tapes.
Nominal Composition of Precursor Powder $Tl_2Ba_2Ca_2Cu_3O_{10}$.

a) 2°C/min Binder Burnout Rate--760°C, 24 Hour Soak

b) 2°C/min Binder Burnout Rate--760°C, 48 Hour Soak

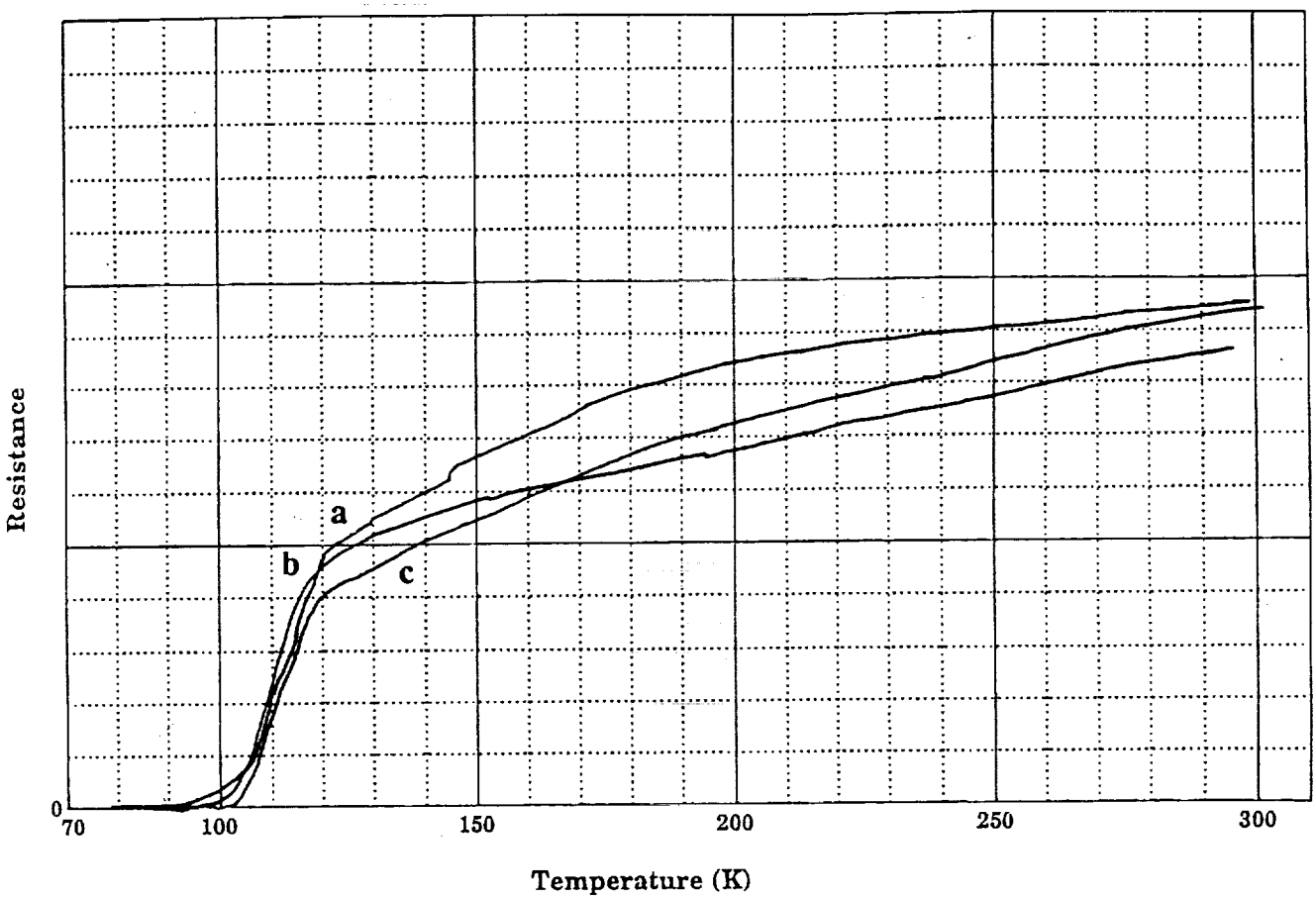

Figure 20

Superconducting Transition Temperature Curves of Ceramic Tapes. Nominal Composition of Precursor Powder $Tl_2Ba_2Ca_2Cu_3O_{10}$.

a) 2°C/min Binder Burnout Rate--775°C, 12 Hour Soak

b) 2°C/min Binder Burnout Rate--775°C, 24 Hour Soak

c) 2°C/min Binder Burnout Rate--775°C, 48 Hour Soak

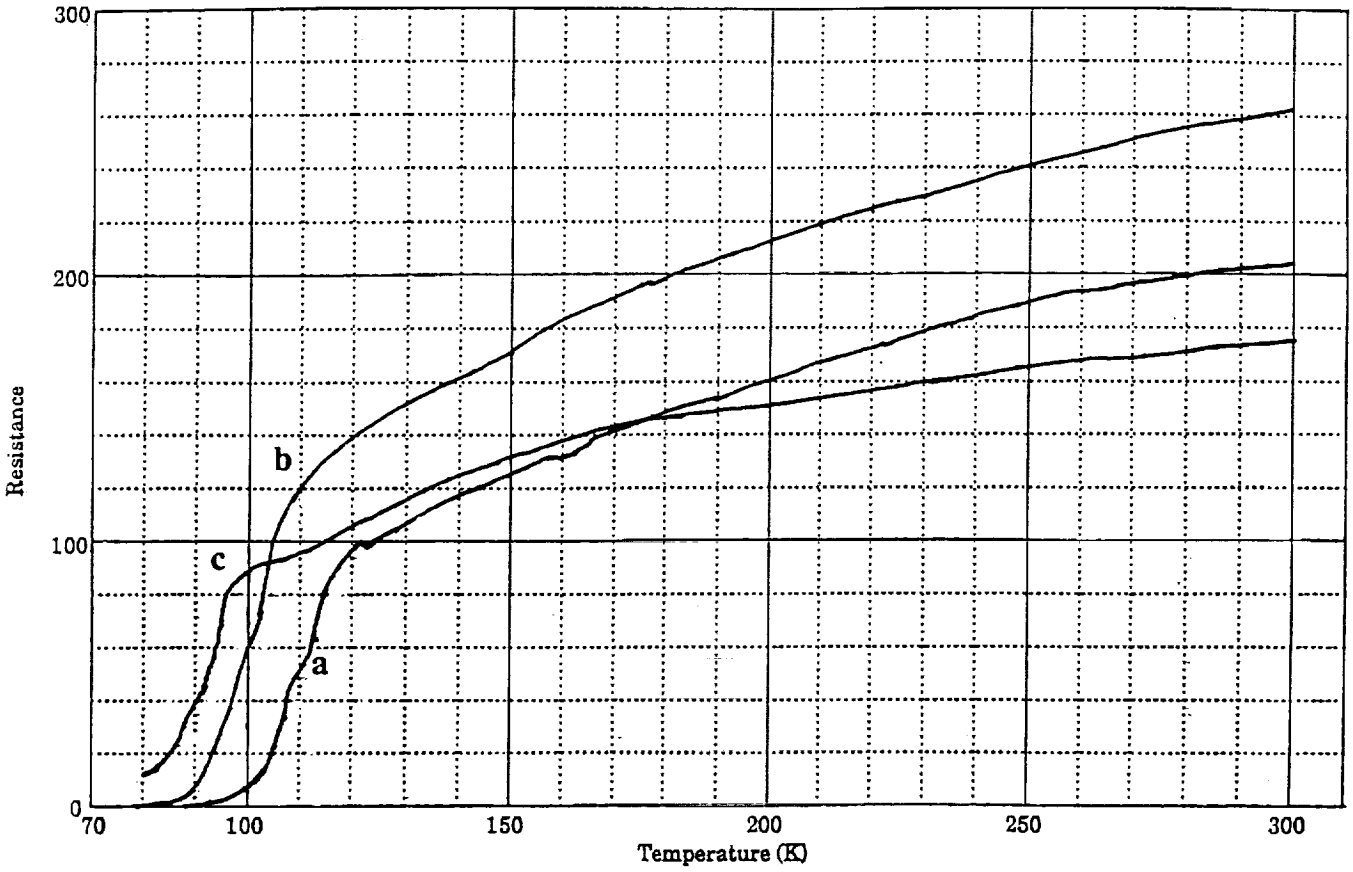

Figure 21

Superconducting Transition Temperature Curves of Ceramic Tapes.
Nominal Composition of Precursor Powder $Tl_2Ba_2Ca_2Cu_3O_{10}$.

a) 2°C/min Binder Burnout Rate--800°C, 12 Hour Soak

b) 2°C/min Binder Burnout Rate--800°C, 24 Hour Soak

c) 2°C/min Binder Burnout Rate--800°C, 48 Hour Soak

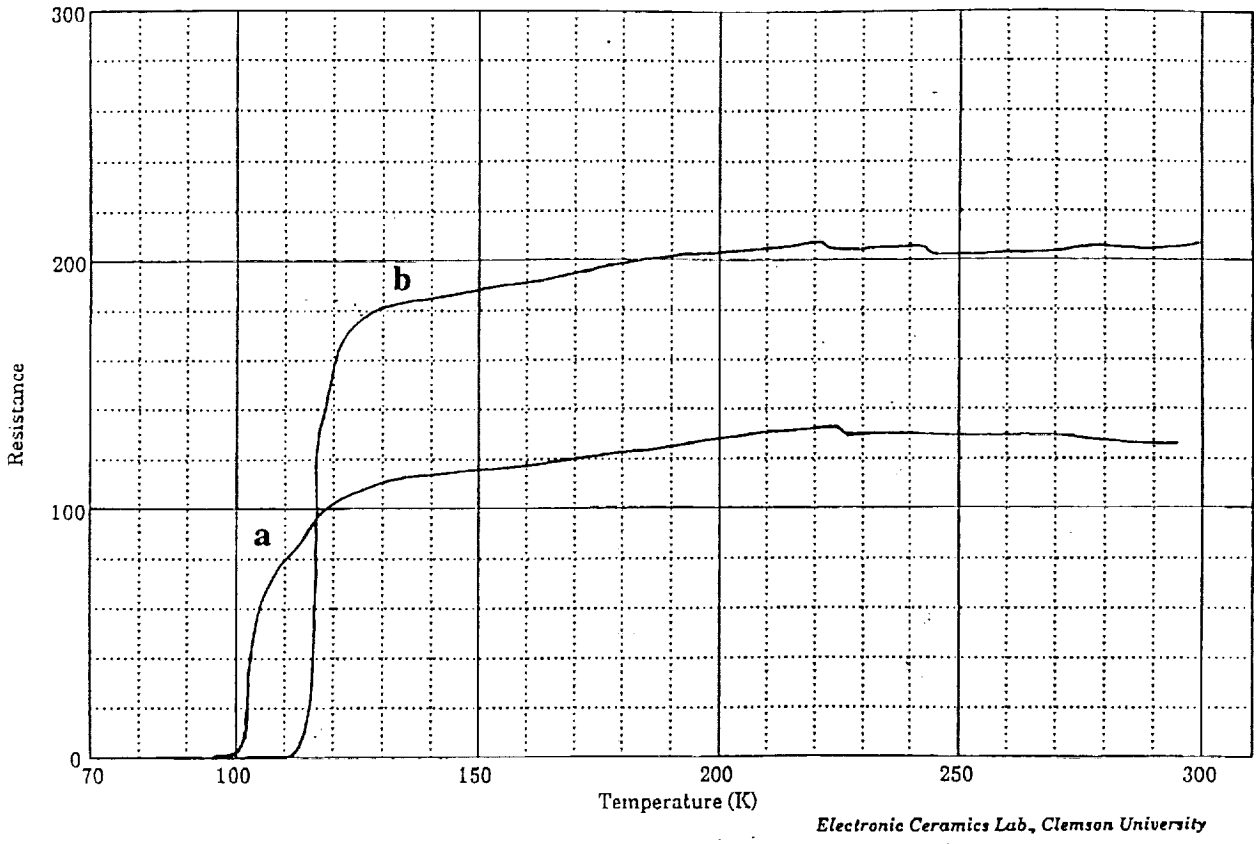

Figure 22

Superconducting Transition Temperature Curves of Ceramic Tapes.
Nominal Composition of Precursor Powder $Tl_2Ba_2Ca_2Cu_3O_{10}$.

a) 2°C/min Binder Burnout Rate--775°C, 48 Hour Soak

b) 3°C/min Binder Burnout Rate--775°C, 48 Hour Soak

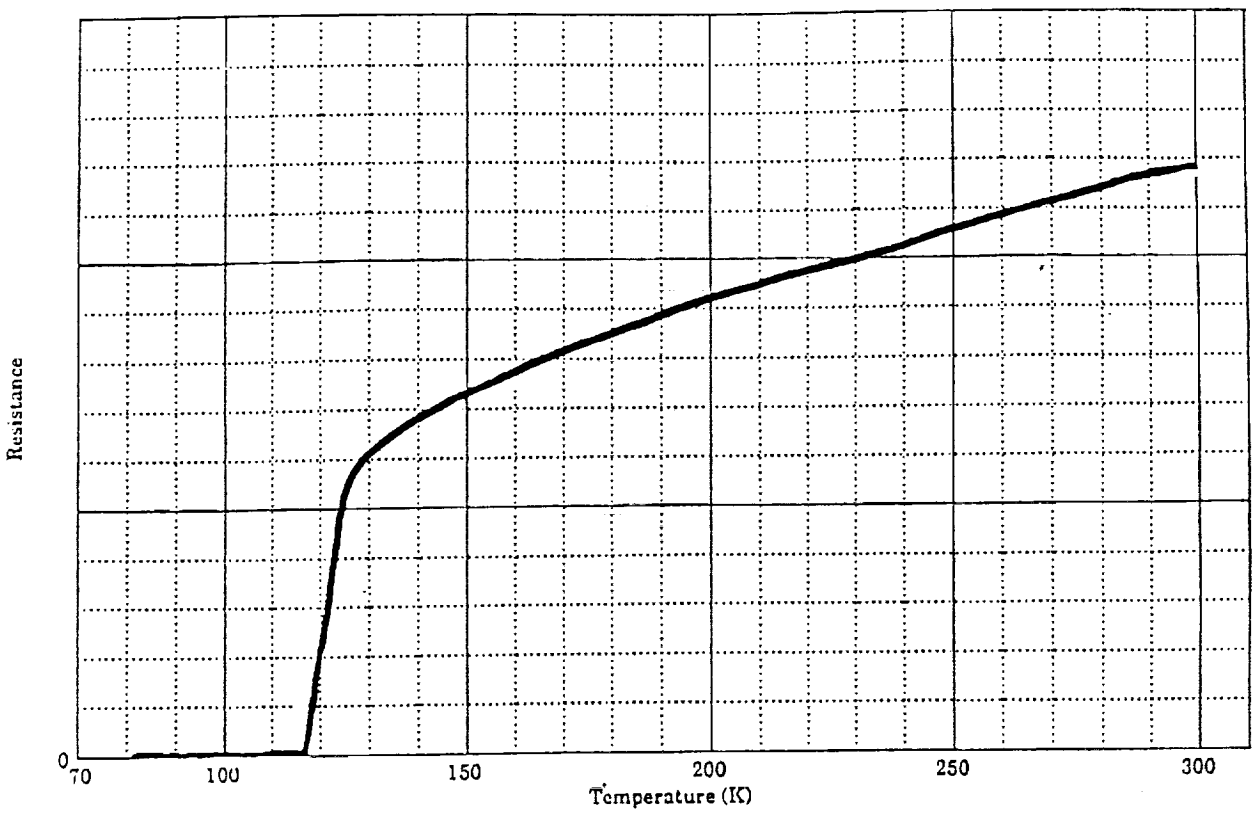

Figure 23

Superconducting Transition Temperature Curve of a Ceramic Pellet.
Nominal Composition of Precursor Powder $Tl_2Ba_2Ca_2Cu_3O_{10}$.
840°C Presinter--Sieved through 400 mesh.
180 Minute Soak at 893°C (T_c=117.8K)

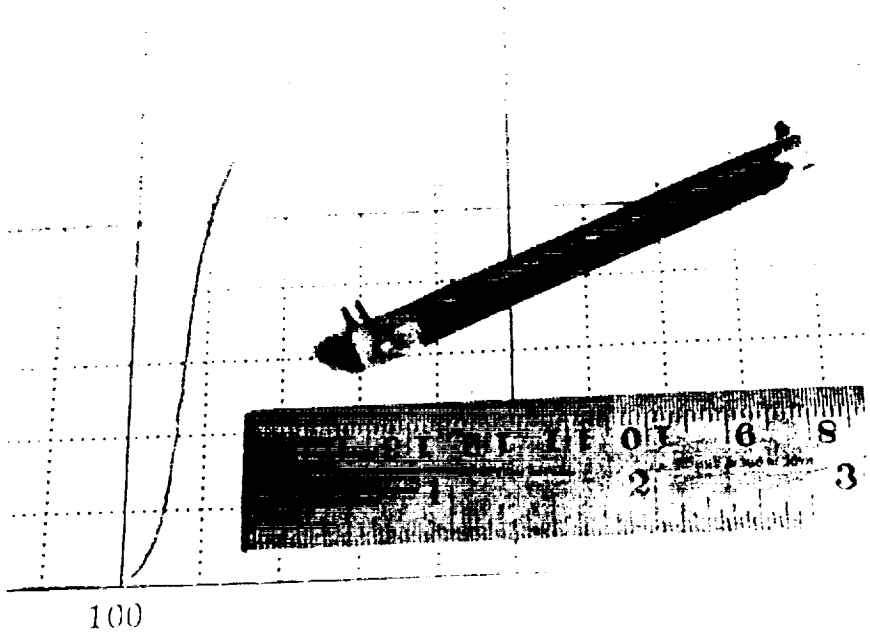

Figure 24

Photograph of Thallium Superconductor Grounding Links.
Nominal Composition of Precursor Powder $Tl_2Ba_2Ca_2Cu_3O_{10}$.
840°C Presinter--Sieved through 400 mesh.
2°C/min Binder Burnout Rate--775°C, 48 Hour Soak

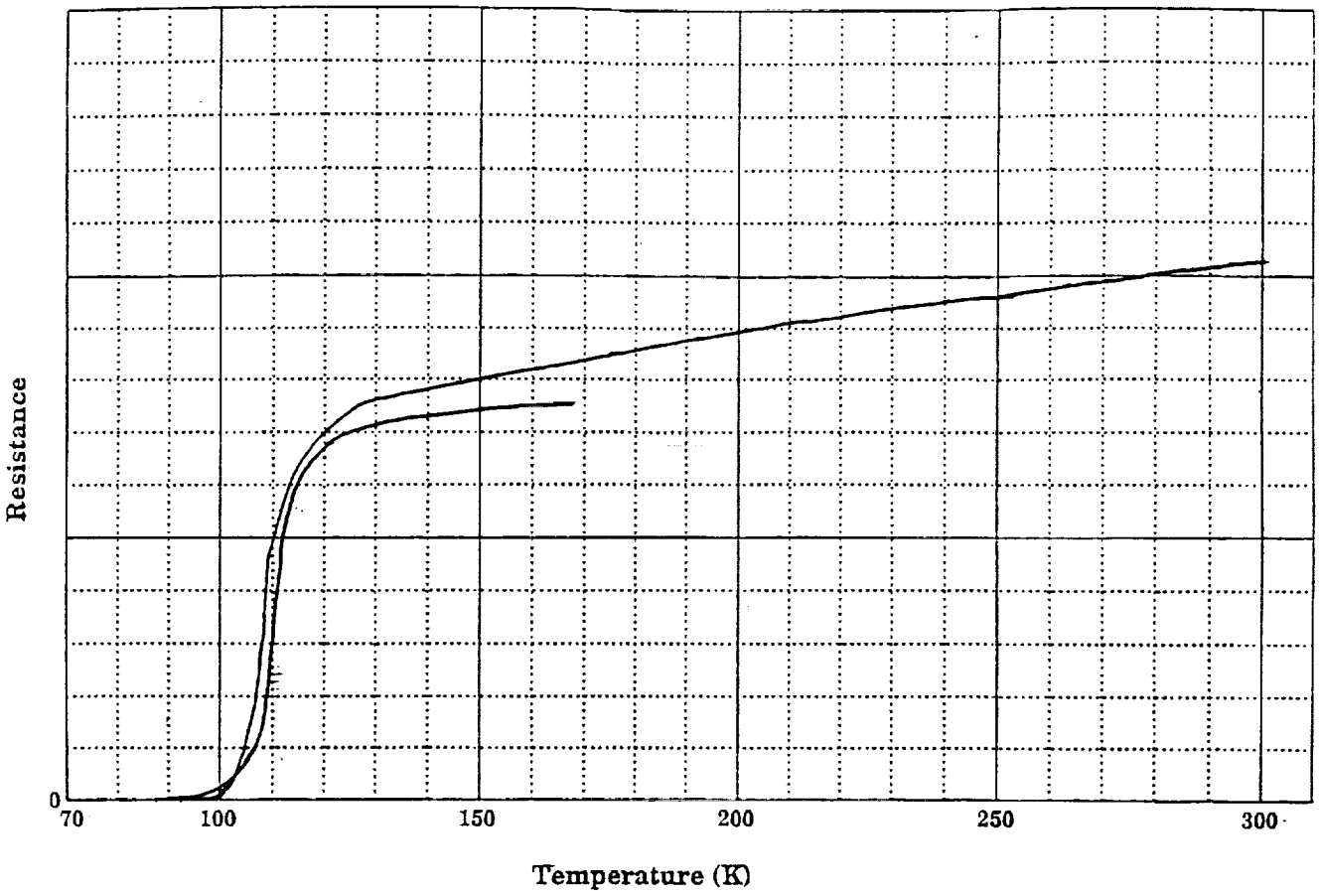

Figure 25

Superconducting Transition Temperature Curves of Grounding Links.
Nominal Composition of Precursor Powder $Tl_2Ba_2Ca_2Cu_3O_{10}$.
840°C Presinter--Sieved through 400 mesh.
2°C/min Binder Burnout Rate--775°C, 48 Hour Soak